2018

Ampa Receptor Dysregulation And Therapeutic Interventions In A Mouse Model Of Cdkl5 Deficiency Disorder

Madhumita Yennawar
University of Pennsylvania, madhu.yennawar@gmail.com

Ampa Receptor Dysregulation And Therapeutic Interventions In A Mouse Model Of Cdkl5 Deficiency Disorder

Abstract
CDKL5 Deficiency Disorder (CDD) is a rare disease that presents as a set of neurological deficits including early-life epilepsy, intellectual disability, and autistic-like behaviors. It results from pathogenic mutations in the gene for cyclin-dependent kinase-like 5 (CDKL5), a protein that is highly expressed in brain. There is no cure for CDD and seizures in this disorder are typically resistant to traditional anti-epileptic drugs, although some patients respond well to cannabidiol. However, underlying mechanisms of what causes hyperexcitability and neurological deficits in CDD is poorly understood. We investigated the novel Cdkl5R59X mouse (R59X), and observed that mutant mice have social interaction and memory deficits, and decreased latency to seizure after administration of pentylenetetrazol. Given the observed behavioral alterations and hyperexcitability in R59X mice, we hypothesized that mutant mice would exhibit underlying molecular and functional alterations in proteins involved in regulating the E:I balance. Indeed, we observed a specific decrease in membrane-bound AMPA receptor (AMPAR) subunit GluA2 as well as decreased GluA2:GluA1 in the hippocampus of R59X mice, suggesting an increase in hippocampal GluA2-lacking AMPARs, which are calcium permeable and have significant roles in regulating neuronal plasticity and excitability. Indeed, decreased hippocampal GluA2 was accompanied by inward rectification of AMPAR currents in whole-cell patch recordings from hippocampal CA1 neurons, indicative of an increased population of functional GluA2-lacking AMPARs, and elevated early-phase long-term potentiation at Schaffer collateral-CA1 synapses. Finally, we evaluated the therapeutic potential of GluA2-lacking AMPAR blocker IEM-1460 as well as cannabidiol to observe 1) whether blocking increased hippocampal GluA2-lacking AMPARs would attenuate behavioral alterations and hyperexcitability in R59X mice and 2) whether cannabidiol shows therapeutic efficacy in R59X mice similar to human CDD patients, thus validating R59X mice as a relevant model to test potential therapeutics in CDD. Indeed, IEM-1460 significantly rescued deficits in social behavior, short-term memory, and latency to seizure while cannabidiol significantly rescued deficits in short and long-term memory and latency to seizure. These results verify that blocking increased GluA2-lacking AMPARs may be a successful therapeutic strategy in CDD, and that both IEM-1460 and cannabidiol may attenuate hyperexcitability as well as autistic-like behaviors and memory deficits in CDD.

Degree Type
Dissertation

Degree Name
Doctor of Philosophy (PhD)

Graduate Group
Pharmacology

First Advisor
Frances E. Jensen

Keywords
AMPA, autism, CDKL5, therapeutic

Subject Categories
Neuroscience and Neurobiology

AMPA RECEPTOR DYSREGULATION AND THERAPEUTIC INTERVENTIONS IN A MOUSE MODEL OF CDKL5 DEFICIENCY DISORDER

Madhumita Yennawar

A DISSERTATION

in

Pharmacology

Presented to the Faculties of the University of Pennsylvania

in

Partial Fulfillment of the Requirements for the

Degree of Doctor of Philosophy

2018

Supervisor of Dissertation

_____

Dr. Frances E. Jensen

Chair, Department of Neurology

Graduate Group Chairperson

_____

Dr. Julie Blendy

Professor of Pharmacology

Dissertation Committee
Dr. Marc A. Dichter, Emeritus Professor of Neurology
Dr. Eric Marsh, Associate Professor of Neurology
Dr. Zhaolan Zhou, Associate Professor of Genetics
Dr. Edward Brodkin, Associate Professor of Psychiatry

AMPA RECEPTOR DYSREGULATION AND THERAPEUTIC INTERVENTIONS IN A MOUSE MODEL OF CDKL5 DEFICIENCY DISORDER
COPYRIGHT

ACKNOWLEDGMENT

I would first like to thank Penny, Dustin and Harper Howard, who raised the initial funds to start this project. Thank you for sharing your stories with me and showing me how important CDKL5 research is for you and families like yours.

I would also like to thank my advisor, Frances Jensen, for the opportunity to join her lab and work on this exciting and fulfilling project. Frances has been a great mentor, and not only taught me about epilepsy and neurodevelopment, but how to think critically, ask the right questions, and demand more of myself. I would also like to acknowledge Marc Dichter, my committee chair, and the rest of my thesis committee for their ideas, guidance, and encouragement.

To the Jensen lab members, you have been the most supportive, fun, and helpful colleagues I could have asked for. In particular, thank you to Yeri Song for sharing puppy videos, always having a solution to my problems, and being an amazing friend.

Thank you Jen Chan and Christie Ojiaku for being the most wonderful, supportive, and loving friends from day one of graduate school.

Finally, I would like to thank my amazing parents, Neela and Hemant, my superstar sister Sneha, and my incredible partner Chris for their endless love and encouragement. Thank you for reading over my documents, listening to my practice talks, and telling me that you believe in me when I needed it most.

ABSTRACT

AMPA RECEPTOR DYSREGULATION AND THERAPEUTIC INTERVENTIONS IN A MOUSE MODEL OF CDKL5 DEFICIENCY DISORDER

Madhumita Yennawar

Frances E. Jensen

CDKL5 Deficiency Disorder (CDD) is a rare disease that presents as a set of neurological deficits including early-life epilepsy, intellectual disability, and autistic-like behaviors. It results from pathogenic mutations in the gene for cyclin-dependent kinase-like 5 (CDKL5), a protein that is highly expressed in brain. There is no cure for CDD and seizures in this disorder are typically resistant to traditional anti-epileptic drugs, although some patients respond well to cannabidiol. However, underlying mechanisms of what causes hyperexcitability and neurological deficits in CDD is poorly understood. We investigated the novel *Cdkl5*^{R59X} mouse (R59X), and observed that mutant mice have social interaction and memory deficits, and decreased latency to seizure after administration of pentylenetetrazol. Given the observed behavioral alterations and hyperexcitability in R59X mice, we hypothesized that mutant mice would exhibit underlying molecular and functional alterations in proteins involved in regulating the E:I balance. Indeed, we observed a specific decrease in membrane-bound AMPA receptor (AMPAR) subunit GluA2 as well as decreased GluA2:GluA1 in the hippocampus of R59X mice, suggesting an increase in hippocampal GluA2-lacking AMPARs, which are calcium permeable and have significant roles in regulating neuronal plasticity and excitability. Indeed, decreased hippocampal GluA2 was accompanied by inward

rectification of AMPAR currents in whole-cell patch recordings from hippocampal CA1 neurons, indicative of an increased population of functional GluA2-lacking AMPARs, and elevated early-phase long-term potentiation at Schaffer collateral-CA1 synapses. Finally, we evaluated the therapeutic potential of GluA2-lacking AMPAR blocker IEM-1460 as well as cannabidiol to observe 1) whether blocking increased hippocampal GluA2-lacking AMPARs would attenuate behavioral alterations and hyperexcitability in R59X mice and 2) whether cannabidiol shows therapeutic efficacy in R59X mice similar to human CDD patients, thus validating R59X mice as a relevant model to test potential therapeutics in CDD. Indeed, IEM-1460 significantly rescued deficits in social behavior, short-term memory, and latency to seizure while cannabidiol significantly rescued deficits in short and long-term memory and latency to seizure. These results verify that blocking increased GluA2-lacking AMPARs may be a successful therapeutic strategy in CDD, and that both IEM-1460 and cannabidiol may attenuate hyperexcitability as well as autistic-like behaviors and memory deficits in CDD.

TABLE OF CONTENTS

ACKNOWLEDGMENT ..... **III**
ABSTRACT ..... **IV**
LIST OF TABLES ..... **X**
LIST OF ILLUSTRATIONS ..... **XI**
CHAPTER 1- INTRODUCTION **1**
Overview **1**
I. CDKL5 Deficiency Disorder **2**
Regulation of CDKL5 subcellular distribution and activity 5
Role of CDKL5 in synapse stability 6
Role of CDKL5 in synaptic function 8
Role of CDKL5 in neuronal migration and axon growth 9
Role of CDKL5 in dendrites 9
Nuclear substrates of CDKL5 10
Cytoplasmic substrates of CDKL5 11
Models of CDD 13
II. Excitatory:inhibitory (E:I) balance in development and disease **16**
Developmental regulation of neurotransmitter receptors 16
The role of GluA2-lacking AMPARs in synaptic development and function 19
GluA2-lacking AMPARs in epilepsy, autism, and ID 20
III. Novel therapeutic strategies for treatment-resistant early-life epilepsy **21**
Therapeutic potential of GluA2-lacking AMPAR blockers 21
Cannabidiol for use in treatment-resistant epilepsy 22
CHAPTER 2 – BEHAVIORAL PHENOTYPING OF CDKL5 R59X MICE **24**
Introduction **24**
Results **27**
R59X mice do not express CDKL5 protein 28
R59X mice demonstrate hyperactivity and deficits in motor function 28
R59X mice exhibit social interaction deficits 29
R59X mice have learning and memory impairments 30

R59X mice show decreased latency to seizure activity following administration of the chemoconvulsant pentylenetetrazol 31
Discussion 32
Materials and Methods 35
Animals 35
Western blotting 36
Animal Behavior 36
Experimental design and statistical analysis 39
Figures 41
Figure 2-1 41
Figure 2-2 42
CHAPTER 3 – GLUTAMATE RECEPTOR AND CHLORIDE CHANNEL ANALYSIS IN R59X MICE AND TWO HUMAN CASES OF CDD 45
Introduction 45
Results 47
Decreased membrane-bound GluA2:GluA1 protein in R59X hippocampus 47
Levels of NMDAR subunits and chloride transporters are not altered in the hippocampus or cortex in R59X mice 48
Fraction of synapses containing GluA2 is significantly decreased in CA1 and dentate gyrus hilus 49
Expression and whole cell levels of GluA1 and GluA2 are not altered in R59X hippocampus 50
Investigation of GluA2 trafficking proteins in R59X hippocampus 50
Exploring human tissue to validate neurotransmitter receptor expression changes in postmortem hippocampal tissue from CDD patients 51
Discussion 51
Materials and Methods 55
Western Blotting 55
Immunohistochemistry 56
RT-qPCR 57
Experimental design and statistical analysis 57
Figures 59

Figure 3-1 59
Figure 3-2 61
Figure 3-3 63
Figure 3-4 65
Figure 3-5 66
Figure 3-6 67
Figure 3-7 68
Figure 3-8 69
Tables 70
Table 3-1 70
Table 3-2 71
CHAPTER 4 – FUNCTIONAL ANALYSIS IN HIPPOCAMPAL SLICES 72
Introduction 72
Results 74
Extracellular recordings reveal normal I-O function, PPR, and LTD, but elevated LTP in R59X mice 74
Whole-cell patch clamp recordings show inward rectification of AMPAR-mediated currents 75
Discussion 75
Materials and Methods 79
Hippocampal slice preparation 79
Extracellular field recordings 79
Whole-cell patch-clamp 80
Experimental design and statistical analysis 81
Figures 82
Figure 4-1 82
Figure 4-2 83
CHAPTER 5 – THERAPEUTIC EFFECTS OF GLUA2-LACKING AMPAR BLOCKER IEM-1460 IN R59X MICE 84
Introduction 84
Results 85

IEM-1460 rescues social behavior deficits and working memory in R59X mice 85
IEM-1460 rescues latency to behavioral seizures after PTZ administration in R59X mice 86
Discussion 87
Materials and Methods 89
Effect of IEM-1460 on memory and social interaction 89
Effect of IEM-1460 on seizure threshold 89
Experimental design and statistical analysis 89
Figures 90
Figure 5-1 90
CHAPTER 6 – THERAPEUTIC EFFECTS OF CANNABIDIOL IN R59X MICE. 92
Introduction 92
Results 93
CBD attenuates memory and hyperexcitability deficits in R59X mice 93
Expression of GPR55, a target of CBD, is not altered in R59X mice or in CDD patient samples 94
Discussion 95
Materials and Methods 97
Effect of CBD on memory and social interaction 97
Effect of CBD on seizure threshold 97
Experimental design and statistical analysis 97
Figures 98
Figure 6-1 98
Figure 6-2 100
CHAPTER 7 – DISCUSSION 101
BIBLIOGRAPHY 107

LIST OF TABLES

Table 3-1: Normalized mRNA and protein levels of GluA1, GluA2 and associated trafficking proteins in whole cell hippocampal lysate……..70

Table 3-2: Temporal and hippocampal tissue from two human CDD cases ……71

LIST OF ILLUSTRATIONS

Figure 2-1: Western blot showing absence of CDKL5 protein in R59X whole brain lysates. 41

Figure 2-2: R59X mice display behavioral deficits consistent with mouse models of autism and intellectual disability, and lowered seizure threshold. 42

Figure 3-1. AMPAR subunit GluA2 and ratio of subunits GluA2:GluA1 are significantly decreased at developmental time points P30, P50 and P125 in R59X hippocampus. 60

Figure 3-2: No alterations in NMDAR subunit levels in R59X cortex and hippocampus over development. 61

Figure 3-3: No alterations in chloride transporters NKCC1 or KCC2 levels in R59X cortex or hippocampus over development. 63

Figure 3-4: Fraction of GluA2-containing synapses is significantly decreased in CA1. 65

Figure 3-5: Fraction of synapses containing GluA2 is significantly decreased in DG. 66

Figure 3-6: No change in fraction of synapses containing GluA2 or GluA1 in CA3. 67

Figure 3-7: No change in fraction of synapses containing GluA2 or GluA1 in cortex layer II/III. 68

Figure 3-8. Western blot analysis in post-mortem hippocampal tissue from patients with CDD. 69

Figure 1. Extracellular recordings in R59X mice show no change in IO function, paired-pulse ratio, or LTD but elevated early-phase LTP. 82

Figure 5-1. Effect of GluA2-lacking AMPAR-specific blocker IEM-1460 on behavioral deficits in R59X mice. 90

Figure 6-1. Effect of experimental therapeutic CBD on behavioral deficits in R59X mice. 98

Figure 6-2: Developmental expression of GPR55 in R59X and WT mice and human CDD and neurotypical cases. 100

CHAPTER 1- Introduction

Overview

CDKL5 Deficiency Disorder (CDD) is a rare disease that is marked by a constellation of neurological deficits including early-life epilepsy, severe intellectual disability, and autistic behaviors. It is caused by pathogenic mutations in the gene for cyclin-dependent kinase-like 5 (CDKL5), a serine-threonine kinase that is highly expressed in the brain (Kilstrup-Nielsen et al., 2012; Zhou et al., 2017). CDKL5 is reported to interact with several nuclear and cytoplasmic proteins that modulate cellular processes ranging from gene regulation (Mari et al., 2005; Kameshita et al., 2008) to synaptic stability (Ricciardi et al., 2012) and microtubule dynamics (Baltussen et al., 2018; Munoz et al., 2018). Animal models of CDD have learning and memory impairments and autistic-like behavioral deficits, yet they exhibit inconsistencies in some behavioral phenotypes, dendritic spine abnormalities, and signaling pathways. However, as CDKL5 has repeatedly been found to localize to dendrites and loss of CDKL5 affects synaptic function, it is possible that it regulates proteins involved in the excitatory:inhibitory balance. Indeed, alterations neurotransmitter receptors and signaling are frequently observed in other neurodevelopmental disorders involving intellectual disability, autism, and epilepsy.

Here we investigated a novel model of CDD, the *Cdkl5*^{R59X} (R59X) mouse. We hypothesized that R59X mice would display autistic-like behaviors, learning and memory impairments, and increased seizure susceptibility consistent with features of the human disease. Furthermore, we predicted that R59X mice would exhibit underlying alterations

in membrane-bound glutamate receptor subunits, and that pharmacologically targeting the alterations would reduce seizure susceptibility and other behavioral deficits in these mice. R59X mice display key phenotypes reflective of the human disorder, including deficits in social interaction, impaired short-term and long-term memory, and subtle hyperexcitability that manifests as decreased latency to behavioral seizures (Chapter 2). We also found evidence of increased GluA2-lacking AMPA receptors in the adult R59X hippocampus (Chapter 3) that was accompanied with functional changes in hippocampal slice recordings (Chapter 4). Finally, we assessed the therapeutic efficacy of GluA2-lacking AMPA receptor blocker IEM-1460 (Chapter 5) and the experimental therapeutic cannabidiol (CBD; Chapter 6) in attenuating behavioral deficits in R59X mice.

I. CDKL5 Deficiency Disorder

CDKL5 Deficiency Disorder (CDD) results from pathogenic mutations in the X-linked gene for cyclin-dependent kinase-like 5 (CDKL5), a serine-threonine kinase that is highly expressed in the brain, particularly in neurons (Montini et al., 1998; Lin et al., 2005; Rusconi et al., 2008; Chen et al., 2010). CDD was first characterized in early 2000s when two unrelated female patients presented with identical phenotypes, consisting of early-onset severe infantile spasms, developmental arrest, hypsarrhythmia, and mental retardation and were subsequently found to possess mutations in *CDKL5,* initially termed *STK9* for serine-threonine kinase 9 (Kalscheuer et al., 2003). Although the gene for CDKL5 is on the X chromosome, CDD affects both males and females (Kilstrup-Nielsen et al., 2012). Originally the disorder was thought to be a variant of Rett Syndrome (RTT), but studies soon supported the conclusion that it is a separate

neurodevelopmental disease with a distinct clinical profile, consisting mainly of seizure onset before 3 months of age, severely impaired language and gross motor skills, rather than the developmental regression commonly observed in RTT (Kalscheuer et al., 2003; Weaving et al., 2004; Fehr et al., 2015).

Seizures are an early presentation in patients with CDD and typically can be described as progressing through three stages. Stage I, early epilepsy, is characterized by brief but frequent seizures, typically infantile spasms, that occur daily and often greater than five times a day (Bahi-Buisson et al., 2008). At this stage patients are typically treated by the conventional antiepileptic drugs (AEDs) valproate or vigabatrin alone or in combination. While treatment is often effective initially, most patients experience relapse of seizures after a honeymoon period that lasts anywhere from 3-30 months. Stage II of seizures is marked by epileptic encephalopathy, which is an “epileptic condition characterized by epileptiform abnormalities associated with progressive cerebral dysfunction” (Khan and Baradie, 2012), but in CDD consists of infantile spasms, tonic seizures and hypsarrhythmia. Infantile spasms occur as clusters of contractions of the muscles in the neck, trunk, arms, and legs, and are often treated with corticosteroids with varied success (Pavone et al., 2013). Stage III manifests as late multifocal and myoclonic epilepsy, in which seizure types can vary from tonic seizures to spasms, myoclonia and absence seizures. (Bahi-Buisson et al., 2008)

As above, seizures in CDD are often refractory to traditional anti-epileptic drugs and are extremely difficult to manage for patients with CDD and their families. Because of this, many have recently turned to alternatives such as the experimental therapeutic

cannabidiol (CBD) for its purported therapeutic effects in children with early-life epilepsy (Porter et al., 2013). This has resulted in the first double-blind study where CBD was found to be effective as an add-on therapy in reducing monthly seizure frequency in CDD and other neurodevelopmental disorders with early-life epilepsy such as Doose syndrome and Dravet syndrome (Devinsky et al., 2018a., 2018b.). Additionally, the FDA has recently approved Epidiolex, purified CBD, to treat Lennox-Gastaut Syndrome and Dravet Syndrome (Corroon et al., 2018).

In addition to seizures being a major component of the disorder in most cases, children with CDD also exhibit severe neurodevelopmental delay. Gross motor hypotonia and poor eye contact are observed as early as a few months of age, and within 2-3 years patients exhibit severe intellectual disability, hypotonia (Bahi-Buisson et al., 2008). Additionally, many patients display poor social interaction, avoidance of eye contact and poor eye fixation, and stereotyped hand movements which are considered autistic features (Bahi-Buisson et al, 2008). According to the CDKL5 Forum, over 1,600 patients with CDKL5 mutations have been documented worldwide to date (https://www.cdkl5forum.org/). Pathogenic mutations occur anywhere along the gene and symptoms can range in severity (Kilstrup-Nielsen et al., 2012).

Although the number of patients identified with CDD is growing, how pathogenic mutations in CDKL5 result in CDD is still relatively unclear. Normally, CDKL5 is particularly enriched in the hippocampus and cerebral cortex (Rusconi et al., 2008; Wang et al., 2012; Schroeder et al., 2018), brain regions that are critical for learning and memory and higher cognitive functions (Brown and Aggleton, 2001). In rodents,

expression of CDKL5 is low during embryonic time points, but is upregulated significantly soon after birth and remains steady throughout adulthood (Rusconi et al., 2008; Chen et al., 2010; Nawaz et al., 2016; Schroeder et al., 2018). Several isoforms of CDKL5 have been reported, some of which are predominantly found in the human and mouse brain (Hector et al., 2016, 2017), but the importance of the splice isoforms remains unclear. Recent studies have probed into potential roles of CDKL5 in neuronal function, and the following sections discuss what is currently known about CDKL5, its activity in neurons, and its interacting partners.

Regulation of CDKL5 subcellular distribution and activity

Expression of CDKL5 is high in neurons and relatively low in glia (Rusconi et al., 2008; Chen et al., 2010). Although CDKL5 localizes to both cytoplasmic and nuclear compartments in neurons, it appears to be primarily cytoplasmic (Rusconi et al., 2008; Chen et al., 2010; Wang et al., 2012; Ricciardi et al., 2012). However, the relative proportion of CDKL5 that localizes to the nuclear compartment increases over brain development (Rusconi et al., 2008). In the nucleus, CDKL5 is reported to localize to nuclear speckles, which are centers of RNA splicing and processing (Ricciardi et al., 2009). In cell culture, CDKL5 is initially found in growth cones that mediate neurite outgrowth (Chen et al., 2010). As neurons mature, CDKL5 localizes to dendritic spines and is particularly enriched at the post-synaptic density (PSD) where it interacts with excitatory synaptic proteins (Ricciardi et al., 2012; Zhu et al., 2013; Schroeder et al., 2018). Recruitment of CDKL5 to the PSD is achieved through its interaction with post-synaptic density protein 95 (PSD-95), which anchors it at the synapse (Zhu et al., 2013).

Splice variants of CDKL5 could also play a role in localization, as some variants have distinct C-terminal regions that may result in targeting of the kinase to specific subcellular locations (Rusconi et al., 2008; Chen et al., 2010).

Phosphorylation of CDKL5 itself may also play a role in its activity and subcellular localization, as, CDKL5 can be phosphorylated at Ser308 by DYRK1A, which causes it to localize to the cytoplasm in Neuro2a cells (Oi et al., 2017), as well as at an unknown site by BDNF signaling (Chen et al., 2010). Finally, dephosphorylation of CDKL5 occurs through activity of protein phosphatase 1 (PP1) which induces proteasomal degradation of CDKL5 (La Montanara et al., 2015). Thus, activity, localization and stability of CDKL5 may be regulated through phosphorylation and dephosphorylation.

Role of CDKL5 in synapse stability

Synapses mediate excitatory and inhibitory neurotransmission between neurons and are stabilized by PSD proteins (Okabe, 2007), many of which are implicated in neurodevelopmental disorders (Kaizuka and Takumi, 2018). Indeed, abnormal dendritic morphology is observed in numerous neurodevelopmental disorders (Martínez-Cerdeño, 2017), including CDD. CDKL5 knock-out (KO) mice have a significant reduction in spine density and number of mature spines in cortex layer V pyramidal neurons, dentate gyrus granule cells, and hippocampal CA1 pyramidal neurons (Della Sala et al., 2016; Trazzi et al., 2018). Furthermore, in cell culture, CDKL5 downregulation by RNAi resulted in decreased excitatory synaptic markers such as PSD-95, as well as decreased frequency of miniature EPSCs, suggesting an overall reduction in excitatory synapses (Ricciardi et al., 2012; Zhu et al., 2013). In contrast,

however, conditional KO of CDKL5 in excitatory neurons in the cortex and hippocampus results in significantly increased PSD-95 (Schroeder et al., 2018) and a trend toward increased spine density and volume (Tang et al., 2017), perhaps due to selective gene deletion from excitatory neurons in the hippocampus and cortex rather than constitutively ablating CDKL5 in all cell types and brain regions. These results suggest that while CDKL5 likely plays a role in individual synapse stability, neuronal excitability and function in CDD are also modulated by circuit-level changes in connectivity or neuronal wiring.

As mentioned previously, CDKL5 is anchored at the PSD through interaction with PSD-95 (Zhu et al., 2013), a critical scaffolding protein at excitatory synapses involved with regulating the organization of neurotransmitter receptors and other molecules that modulate synaptic activity (Chen et al., 2011, 2015). The CDKL5-PSD-95 interaction enables CDKL5 to interact with downstream effector molecules, such as netrin-G1 ligand (NGL-1) (Ricciardi et al., 2012), a synaptic adhesion protein that is also implicated in neurodevelopmental disorders (Maussion et al., 2017). CDKL5 phosphorylates NGL-1 and promotes its interaction with PSD-95, which supports dendritic spine stability (Ricciardi et al., 2012). Additionally, the CDKL5-PSD-95 interaction is regulated by activity-dependent post-translational palmitoylation of PSD-95 (Zhu et al., 2013; El-Husseini et al., 2002), and is thought to facilitate neurotransmitter receptor clustering at the synapse (Saneyoshi and Hayashi, 2014; Chen et al., 2015). This suggests that CDKL5 has a critical role in synaptic function and plasticity.

Role of CDKL5 in synaptic function

CDKL5 deficiency results in functional changes at the neuronal level. *Cdkl5* knockdown in primary hippocampal neurons significantly reduced frequency and amplitude of mini excitatory post-synaptic potentials (mEPSCs; Ricciardi et al, 2012), which are spontaneous events that result from quantal release of neurotransmitters from the presynaptic neuron (Pinheiro and Mulle, 2008). The frequency of mEPSCs are dependent on presynaptic release of neurotransmitters from vesicles whereas the amplitude of mEPSCs depends on activation of post-synaptic receptors (Pinheiro and Mulle, 2008). Thus, a change in both frequency and amplitude of mEPSCs suggests that loss of CDKL5 results in alterations in both presynaptic and postsynaptic function. A decrease in amplitude of mEPSCs was also observed in neurons after shRNA knock-down of CDKL5 (Tramarin et al., 2018), supporting postsynaptic alterations. However, in CDKL5 KO mice, mEPSC amplitude was not altered in layer V pyramidal cells although mEPSC frequency was significantly decreased (Della Sala et al., 2016), suggesting a presynaptic deficit. Furthermore, loss of CDKL5 in excitatory forebrain neurons in the hippocampus and cortex resulted in increased frequency of mEPSCs without a change in amplitude in hippocampus CA1 (Tang et al., 2017), suggesting an increase in presynaptic function.

Studies investigating synaptic plasticity in mouse models of CDD have been limited. One group found that CDKL5 KO mice exhibit impaired long-term potentiation in the cortex layer II/III (Della Sala et al., 2016) while another showed elevated LTP in CDKL5 KO hippocampus (Okuda et al., 2017). The contrasting results from mEPSC and LTP

recordings are difficult to reconcile, but they may be due to region-specific effects of loss of function of CDKL5.

Role of CDKL5 in neuronal migration and axon growth

RNAi of CDKL5 in neural progenitor cells causes abnormal migration of layer II-III pyramidal neurons in the rodent brain (Chen et al., 2010; Ricciardi et al., 2012), potentially due to impaired microtubule dynamics. CDKL5 is reported to interact with IQGAP1, a molecule that regulates cell migration and polarity, and promote association of IQGAP with Rac1, a small GTPase that is part of a family of proteins that are involved with cell morphology and actin dynamics, and CLIP170, a microtubule-associated protein (Barbiero et al., 2017). In cultured neurons, CDKL5 is found to modulate axon development by phosphorylating Shootin1, a regulator of axon outgrowth that co-localizes with CDKL5 in growth cones during early neuronal development (Nawaz et al., 2016). Silencing or overexpressing CDKL5 results in neurons with multiple axons, which authors attributed to dysregulation of Shootin1 phosphorylation. However, loss of function of CDKL5 does not affect axon formation (Chen et al., 2010; Nawaz et al., 2016), suggesting that CDKL5, though important for normal axon development, is likely not critical for axon formation.

Role of CDKL5 in dendrites

Dendritic abnormalities have been observed in numerous developmental disorders such as Fragile X Syndrome, Tuberous Sclerosis, epilepsy, and autism (Martínez-Cerdeño, 2017). Neurite growth and dendritic arborization are severely compromised in cell culture after CDKL5 downregulation by RNAi (Chen et al., 2010). Dendritic abnormalities are

also observed *in vivo,* where in utero electroporation-induced silencing of CDKL5 causes reduced dendritic arborization (Chen et al., 2010), and in CDKL5 KO mice where total length of apical dendrites is reduced in the cortex and hippocampus (Amendola et al., 2014) and in dentate gyrus (Fuchs et al., 2014). Reduced dendritic complexity is also observed in a conditional KO mouse where CDKL5 is absent in forebrain excitatory neurons (Tang et al., 2017). Interestingly, overexpression of CDKL5 in neuronal culture results in increased dendritic length (Chen et al., 2010), suggesting that CDKL5 regulates and is sufficient for dendritic growth.

Although the exact mechanism by which CDKL5 modulates dendritic growth is unknown, the kinase does form a protein complex with Rac1, a small GTPase that regulates actin dynamics. Furthermore, CDKL5 plays a key role in activation of Rac1 by brain-derived neurotrophic factor (BDNF)—downregulation of CDKL5 decreases Rac1 activation through BDNF and BDNF treatment causes an increased phosphorylation of CDKL5 that occurs before Rac1 activation. Thus, CDKL5 may be an upstream regulator of Rac1 signaling, although it is still unclear if Rac1 is a direct substrate of CDKL5. CDKL5 may induce Rac1 activation through other signaling pathways such as the AKT/mTOR pathway or AKT/GSK-3β, both of which are dysregulated in CDKL5 KO mice (Wang et al., 2012; Fuchs et al., 2014) and regulate neuronal morphogenesis (Kumar et al., 2005; Jin et al., 2012).

Nuclear substrates of CDKL5

There have been several reported nuclear substrates of CDKL5. *In vitro*, CDKL5 phosphorylates DNA methyltransferase 1 (Dnmt1) (Kameshita et al., 2008), a nuclear

protein involved in cytosine methylation, gene silencing, and neurocognitive development (Irwin et al., 2016). CDKL5 is also reported to weakly bind and phosphorylate Methyl-CpG-binding protein 2 (MeCP2) (Mari et al., 2005; Kameshita et al., 2008), a global transcriptional regulator implicated in Rett syndrome (Chahrour et al., 2008). Neither MeCP2 nor Dnmt1 phosphorylation by CDKL5 have been observed in the brain, and downstream effects of abnormal MeCP2 or Dnmt1 phosphorylation in CDD have not been elucidated. Therefore, further experiments are needed to investigate whether they are true endogenous substrates of CDKL5. More recently, HDAC4 was found to be a substrate of CDKL5 both *in vitro* in SH-SY5Y cells and *in vivo* in knockout mice (Trazzi et al., 2016). HDAC4 is another transcriptional regulator that represses genes that are important for synaptic function, and its deficiency in mice and flies impairs learning and memory (Sando et al., 2012). Translocation of HDAC4 from the cytoplasm to the nucleus is regulated by its activity-dependent phosphorylation (Chawla et al., 2003). Indeed, decreased phosphorylation of HDAC4 in neuronal precursor cells from CDKL5 KO mice caused abnormal cytoplasmic accumulation of HDAC4 (Trazzi et al., 2016).

Cytoplasmic substrates of CDKL5

Two cytoplasmic substrates of CDKL5 have been identified in *in vitro* assays: NGL-1 (Ricciardi et al., 2012) and Amphiphysin 1 (Amph1; Sekiguchi et al., 2013). NGL family proteins promote excitatory synapse development through interaction with PSD-95, cell adhesion molecules, and other proteins at the PSD (Kim et al., 2006; Woo et al., 2009). CDKL5 was found to phosphorylate NGL-1, promoting its interaction with PSD-95 and

consequently synaptic stability (Ricciardi et al., 2012). Amph1 is found at synapses, and is involved in clathrin-mediated endocytosis that is critical for actin polymerization (Yamada et al., 2007). Phosphorylation of NGL-1 and Amph1 by CDKL5 has not yet been verified in the brain.

Several additional cytoplasmic substrates of CDKL5 have recently been identified through a study utilizing an analog-specific (AS) form of CDKL5 (AS-CDKL5) that is able to accept bulky ATP analogs and subsequently thiophosphorylate targets for identification. Through this method, CDKL5 appears to thiophosphorylate Rho guanine nucleotide exchange factor 2 (ARHGEF1), microtubule-associated protein 1S (MAP1S) and microtubule-associated protein RP/EB family member 2 (MAPRE2/EB2) in mouse brain lysate. CDKL5 also phosphorylates all three substrates in *in vitro* kinase assays in a time- and CDKL5 concentration-dependent manner (Baltussen et al., 2018). ARHGEF1, MAP1S, and EB2 all contain an RPXS* consensus motif, where X is any amino acid and S* is the phosphorylated serine. MAP1S contains two such sites, and CDKL5 phosphorylates MAP1S at both sites *in vitro*. A reduction in both EB2 Ser222 and MAP1S Ser812 phosphorylation was observed in CDKL5 KO mouse cortex using validated phospho-specific antibodies. Decreases in ARHGEF2 Ser122 or MAP1S Ser786 phosphorylation were not able to be detected, perhaps due to decreased sensitivity of those antibodies. However, defects microtubule dynamics were observed in CDKL5 KO neurons that were attributed to abnormal MAP1S activity. Furthermore, CDKL5 phosphorylation of EB2 is inhibited by NMDAR activity, suggesting that it may play a role in activity-dependent circuit formation. Finally, although EB2 phosphorylation

was absent in CDD patient-derived neurons, abnormal phosphorylation of MAP1S and ARHGEF1 was not reported in these cells, calling into question whether these proteins are substrates of CDKL5 in humans.

An independent report, which was co-published with the AS-CDKL5 study, used quantitative phosphoproteomics to identify three substrates of CDKL5: MAP1S, CEP131, and DLG5 (Muñoz et al., 2018). These proteins are regulators of microtubule and centrosome function and all contain the same RPXS* consensus motif that the substrates from the AS-CDKL5 report contain. Although mechanistic studies were not performed to investigate the consequence of CDKL5 phosphorylation of MAP1S, CEP131, or DLG5, all three substrates were validated in cells using FLAG pull-down assays. Further experiments are necessary to determine the functional consequence of CDKL5 phosphorylation of these proteins, but the identification of MAP1S as a substrate of CDKL5 in two independent studies is promising. Indeed, growing evidence suggests that dysregulated microtubule-associated proteins can contribute to neurodevelopmental disorders including intellectual disability and autism (Lasser et al., 2018).

Models of CDD

Mouse models are excellent tool to study disease pathogenesis, molecular alterations, network function, plasticity, and circuit dynamics in CDD. Several constitutive and conditional knock-out (KO) models have been created to date that recapitulate core features of the human disease (Wang et al., 2012; Amendola et al., 2014; Tang et al., 2017; Okuda et al., 2018). Interestingly, no CDD model exhibits visible spontaneous

convulsive seizures, although seizures are a strong feature in the human syndrome (Bahi-Buisson et al., 2008a.).

Constitutive KO models

Several mouse models of CDD exist to date, most of which are whole-body knock out models and have been tested for behavioral abnormalities. Some discrepancies in behavioral results do exist between CDKL5 KO models. For example, hypoactivity in the open field test was observed in two models (Amendola et al., 2014; Okuda et al., 2017) whereas the other two CDKL5 KO models showed hyperactivity (Wang et al., 2012; Jhang et al., 2017) although different methods were used to characterized activity in these studies. Anxiety phenotypes have also been inconsistent between models, with one model showing increased anxiety (Okuda et al., 2018) and one showing decreased (Wang et al., 2012). The phenotypes that are consistently observed in all constitutive knock-out mouse models of CDD have been impaired motor coordination, social interaction, and learning and memory (Wang et al., 2012; Fuchs et al., 2014; Jhang et al., 2017; Okuda et al., 2018), highlighting the importance of normal CDKL5 function for these processes.

Conditional KO models

The Nex-cKO mouse is a conditional knock-out model where CDKL5 was removed from forebrain glutamatergic neurons, specifically those in the cortex and hippocampus (Tang et al., 2017). Interestingly, Nex-cKO mice do not exhibit alterations in activity, anxiety, motor coordination, or social behavior. They do, however, show deficits in hippocampal-dependent learning and memory (Tang et al., 2017), suggesting that CDKL5 function in

hippocampal glutamatergic neurons plays a key role in mechanisms of learning and memory.

Finally, two conditional KO mouse models of CDD were recently generated to investigate the effects of loss of function of CDKL5 in excitatory cortical neurons (CDKL5 Fl/Y CaMKIIα-cre mice) and in inhibitory neurons (CDKL5 Fl/Y +/− Gad2-IRES-Cre mice; Schroeder et al., 2018). No behavioral studies were conducted in these mice, however, loss of CDKL5 in excitatory and inhibitory neurons respectively was found to differentially dysregulate components of mTOR signaling (Schroeder et al., 2018), a critical pathway that integrates intracellular and extracellular cues to modulate gene expression, protein synthesis and neuronal growth (Lipton and Sahin, 2014). Further investigation must be performed to investigate the consequence of such disruption in terms of downstream alterations in cell signaling or metabolic pathways.

The Cdkl5^{R59X} model

The *Cdkl5*^{R59X} (R59X) mouse was developed in the laboratory of Dr. Zhaolan Zhou at the University of Pennsylvania based on a mutation found in a human patient with CDD known to have severe daily seizures that began shortly after birth (Castrén et al., 2011). Tonic flexion of her upper limbs was associated with sharp-wave discharges in EEG recordings and her seizures were only just controlled by multiple anti-epileptic drugs including valproic acid, oxcarbazepine, and vigabatrin. By six years of age, the patient exhibited severe intellectual disability, stereotyped behaviors and poor eye contact (Castrén et al., 2011). R59X mice are on a C57BL/6J genetic background and were produced with a targeting vector that was designed to insert a *frt*-flanked neomycin

resistance (neo) cassette downstream of exon 5 and a single nucleotide change of C to T, leading to a nonsense mutation at arginine 59 (R59X) of the cyclin-dependent kinase-like 5 (*CDKL5*) gene. To date no studies have been published evaluating behavioral, molecular, or functional alterations in R59X mice.

II. Excitatory:inhibitory (E:I) balance in development and disease

Synapses mediate excitatory and inhibitory neurotransmission in the brain, and synaptic activity modulates essential processes of normal neuronal function such as intracellular signaling, gene regulation, protein trafficking, and plasticity (Citri and Malenka, 2008; Okuno, 2011; Kaushik et al., 2014). Furthermore, synaptic activity is dynamically regulated during development through differential expression of neurotransmitter receptor subunits to facilitate a period of heightened experience-dependent synaptic plasticity (Rakhade and Jensen, 2009). It is therefore unsurprising that synaptic dysfunction underlies neurodevelopmental disorders such as autism, intellectual disability, and epilepsy, and is a convergence point of disease pathogenesis (Zoghbi and Bear, 2012; Keller et al, 2017).

Developmental regulation of neurotransmitter receptors

Glutamate and GABA are the main neurotransmitters in the brain and mediate excitatory and inhibitory neurotransmission respectively (Ben-Ari, 2002; Owens and Kriegstein, 2002; Willard and Koochekpour, 2013). When released from vesicles at the presynaptic membrane they travel across the synaptic cleft and bind glutamate or GABA receptors at the post-synaptic membrane. Neurotransmitter binding to ionotropic glutamate or GABA receptors induces a conformational change in the receptors, opening an ion channel

pore that allows the flow of small anions or cations (Owens and Kriegstein, 2002; Willard and Koochekpour, 2013). Glutamate binding causes positively charged sodium and calcium ions to enter the synapse, causing depolarization that can result in an action potential. In the adult brain, neurons become hyperpolarized and less likely to fire an action potential after GABA binding due to influx of negatively charged chloride ions. However, in the immature brain the chloride gradient at $GABA_A$ receptors is reversed due to the developmental regulation of chloride channels NKCC1 and KCC2. This causes GABA to be excitatory during early developmental periods, contributing to hyperexcitability and increased susceptibility to seizures (Ben-Ari, 2002).

Ionotropic glutamate receptors are tetrameric structures responsible for fast synaptic transmission in the brain. The predominant ionotropic glutamate receptors are N-methyl-D-aspartate receptors (NMDARs), α-amino-3-hydroxy-5-methyl-4-isoxazolepropionic acid receptors (AMPARs), and kainate receptors (Willard and Koochekpour, 2013). Changes in NMDAR and AMPAR levels are commonly associated with neurological deficits such as seizures, autism, and intellectual disability (Rakhade and Jensen, 2009; Rojas, 2014).

NMDARs are composed of two obligate GluN1 subunits along with two GluN2 subunits or GluN3 subunits, of which there are GluN2A, GluN2B, GluN2C, GluN2D, GluN3A and GluN3B subtypes (Paoletti et al., 2013). In the adult brain GluN2A and GluN2B are predominantly expressed (Watanabe et al., 1992) and play a significant role in synaptic function and plasticity (Paoletti et al., 2013). In the immature brain however, GluN2B, GluN2D, and GluN3A are all highly expressed to contribute to elevated excitability. All

NMDARs are permeable to Ca^{2+} and are sensitive to a voltage-dependent Mg^{2+} block, but subunit composition modulates receptor deactivation kinetics or sensitivity to Mg^{2+}. For example, during development, high levels of GluN2B extend the current decay times, and GluN2D and GluN3A decrease sensitivity to the magnesium block. Additionally, there are more total NMDARs present during early development, contributing to increased Ca^{2+} influx. These NMDAR receptor changes facilitate a period of rapid synapse formation and circuit development, but they also cause the brain to be more susceptible to seizures (Rakhade and Jensen, 2009).

AMPARs are composed of GluA1, GluA2, GluA3, GluA4 and are predominantly found in combinations of GluA1/2 or GluA2/3 at adulthood (Wenthold et al., 1996; Mansour et al., 2001), although GluA2-lacking AMPARs do exist and are present particularly during early-postnatal development (Monyer et al., 1991). AMPARs, unlike NMDARs, are predominantly impermeable to Ca^{2+} due to inclusion of the GluA2 subunit. GluA2 mRNA undergoes post-transcriptional editing that changes a glutamine residue in the channel pore to arginine. The positively charged arginine residue prevents both the passage of Ca^{2+} ions and block by endogenous intracellular polyamines at high voltages, and also reduces single channel conductance (Verdoorn et al., 1991; Jonas et al., 1994; Jonas and Neuron, 1995; Swanson et al., 1997). Thus, GluA2-lacking AMPARs are Ca^{2+}-permeable and they also exhibit inward rectification in the AMPAR current-voltage plot due to the intracellular spermine block (Burnashev et al., 1992). Ca^{2+} not only contributes to neuronal excitation, but also is a critical secondary intracellular messenger, so even small changes in the levels of GluA2-lacking AMPARs can have

profound and long-lasting effects on excitability, plasticity, and intracellular signaling (Isaac et al., 2007).

The role of GluA2-lacking AMPARs in synaptic development and function

During development, GluA2-lacking AMPARs are upregulated to facilitate a period of activity-dependent synaptic plasticity (Kumar et al., 2002; Pandey et al., 2015), but they are also present in high levels at adulthood in cortical GABAergic interneuron subtypes (Jonas et al., 1994) and are important at glutamatergic synapses for mechanisms of synaptic plasticity (Plant et al., 2006; Isaac et al., 2007; Sanderson et al., 2016). Transient incorporation of GluA2-lacking AMPARs at the synapse is necessary for NMDAR-dependent long-term depression (LTD), and blocking GluA2-lacking AMPARs impaired expression of LTD (Sanderson et al., 2016). Similarly, GluA2-lacking AMPARs are recruited to the synapse during the induction phase of long-term potentiation (LTP), before being removed and replaced by GluA2-containing AMPARs during the consolidation phase (Plant et al., 2006). Another study shows that GluA2-lacking AMPARs are delivered to peri-synaptic sites before expression of LTP (Yang et al., 2008), and that GluA2-lacking AMPARs are essential for LTP and enable activity-dependent synaptic enlargement (Yang et al., 2010). Interestingly, it appears that the anchoring and regulatory proteins that interact with GluA2-lacking AMPARs to the synapse play a large role in which form of plasticity is expressed (Guire et al., 2008; Park et al., 2016; Sanderson et al., 2016). Nevertheless, recruitment of GluA2-lacking AMPARs to the synapse is essential for several forms of plasticity, and disruptions in the

GluA2 subunit can have profound effects on synaptic scaling and plasticity throughout the lifetime.

GluA2-lacking AMPARs in epilepsy, autism, and ID

GluA2-lacking AMPARs are unique in that they are the only AMPAR subtype to allow Ca^{2+} influx. As a result, changes in GluA2 subunit levels can contribute to disease pathogenesis due to significant effects on synaptic scaling (Man, 2011), plasticity (Jia et al., 1996; Rakhade et al., 2008; Lippman-Bell et al., 2016), and downstream signaling pathways (Rosenberg et al., 2018). Dysregulation in GluA2-lacking AMPARs and associated regulatory proteins have been increasingly observed in several neurodevelopmental disorders. Decreased GluA2 is observed in neural progenitor cells from patients with Fragile X Syndrome, and results in increased Ca^{2+} influx and inward rectification in the current-voltage plot (Achuta et al., 2018). Downregulation of the intellectual disability protein RAB39B in hippocampal neurons causes synaptic GluA2 deficits due to disrupted trafficking of the GluA2 subunit (Mignogna et al., 2015). Finally, the Jensen lab has observed that early-life hypoxic seizures (HS) cause GluA2 dysregulation 48 hours post-HS (Lippman-Bell et al., 2016) and premature “unsilencing” of NMDAR-only synapses (Sun et al., 2018). GluA2 dysregulation post-HS results in immediate downstream mTOR pathway upregulation and MeCP2 phosphorylation (Talos et al., 2012; Rosenberg et al., 2018), and later-life autistic-like behavioral deficits and long-term epilepsy (Talos et al., 2012; Lippman-Bell et al., 2013). The Jensen lab also showed that blocking AMPARs immediately post-HS prevented the immediate mTOR upregulation (Talos et al., 2012) as well as later-life alterations in autistic-like

social deficits (Lippman-Bell., 2013), and occlusion of long-term plasticity (Zhou et al., 2011), suggesting that blocking CP-AMPARs may have significant long-term therapeutic effects in epilepsy and autism.

III. Novel therapeutic strategies for treatment-resistant early-life epilepsy

The neonatal brain presents numerous challenges for therapeutics in part due to the differential expression of receptors that mediate the E:I balance (Rakhade et al., 2012). Traditional anti-epileptic drugs typically target the inhibitory system by increasing GABA activity or excitatory system by blocking glutamate receptors, sodium channels, voltage gated calcium channels, and potassium channels (Lee, 2014). Newer anti-epileptic drugs on the whole do not show increasing levels of efficacy compared to older treatments, supporting the need for novel therapeutics with varying mechanisms of action. We centered our therapeutic investigation in CDD on a GluA2-lacking AMPAR blocker and the experimental therapeutic cannabidiol.

Therapeutic potential of GluA2-lacking AMPAR blockers

AMPAR antagonists have strong anti-seizure activity in preclinical models of epilepsy, and recently the general noncompetitive AMPAR antagonist perampanel was the first AMPAR blocker approved for epilepsy in patients over 12 years of age **[cite**]. However, to date no GluA2-lacking AMPAR blockers have been implemented in either children or adults with epilepsy. IEM-1460 is a GluA2-lacking open channel blocker that has shown efficacy in delaying onset of PTZ-induced seizures immature rats (Szczurowska et al., 2014). Furthermore, our lab has found that IEM-1460 treatment prevents downstream signaling alterations due to increased GluA2-lacking AMPARs after hypoxic seizures

(Rosenberg et al., 2018). Given the already increased population of GluA2-lacking AMPARs early in development, selectively blocking these receptors in patients with early-life epilepsy where the ratio of GluA2 to other subunits is even lower may show efficacy in seizure reduction or severity. In a recent study in Asian pediatric neurology clinics, perampanel was effective in reducing seizure frequency and was in general well-tolerated as an add-on treatment for children and adolescents with epilepsy (Lin et al., 2018). However, there are currently no FDA approved drugs that selectively target GluA2-lacking AMPARs.

Cannabidiol for use in treatment-resistant epilepsy

Cannabidiol (CBD) is a cannabis-derived compound increasingly being used in treatment-resistant early-life epilepsies. CBD is the major non-psychoactive component of cannabis and recently has shown numerous anti-excitatory and immunomodulatory effects (Pisanti et al., 2017), and is reported to act at a multitude of cellular targets. Relevant to its anti-excitatory effects, CBD has poor activity at the endogenous cannabinoid receptors CB1 and CB2, but may indirectly affect the endocannabinoid system through its effects on other targets. CBD appears to block G-protein coupled receptor 55 (GPR55), a protein involved in regulating intracellular Ca^{2+} (Lauckner et al., 2008). It also has activity activating transient receptor potential of vanilloid type-1 (TRPV1; Bisogno et al., 2001), blocking T-type Ca^{2+} channels (Ross et al., 2008), and can target mutant sodium channels (Patel et al., 2016) Additionally, it has the ability to modulate adenosine receptors, voltage-dependent anion selective channel protein (VDAC1), and tumor necrosis factor alpha (TNFα) release (Devinsky et al., 2014).

CBD has exhibited anti-seizure properties in preclinical models of epilepsy (Do Val-da Silva et al., 2017; Kaplan et al., 2017), and rising off-label use of CBD in children with drug-resistant epilepsy recently led to the first double-blind placebo controlled clinical trials for CBD (commercial name Epidiolex) in several early-life epilepsies, including CDD, where it significantly reduced seizure frequency (Devinsky et al., 2018a, 2018b). Interestingly, CBD has also been reported by parents and some medical practitioners to have beneficial effects on autistic-like behaviors in children (Rosenberg et al., 2017). CBD treatment does attenuate social interaction deficits in a mouse model of Dravet syndrome, and prevents development of social recognition memory deficits in a transgenic mouse model of Alzheimer's disease (Cheng 2014). However, further investigation is necessary to validate and expand upon these results.

CHAPTER 2 – Behavioral phenotyping of CDKL5 R59X mice

Introduction

Mouse models of neurodevelopmental disorders are an excellent method of investigating circuit and regional alterations in the brain, and many display characteristics at the whole animal level that are parallel to symptoms found in human patients. For example, Fmr1 KO mice, a model of Fragile X Syndrome (FXS), displays increased seizure susceptibility to audiogenic seizures and also has been shown to exhibit elevated anxiety, autistic-like social deficits, and impairments in learning and memory (Musumeci et al., 2007; Kazdoba et al., 2014). The MeCP2 KO mouse, a model of Rett Syndrome (RTT), has similarly shown behavioral impairments that mirror characteristics of the human disease (Guy et al., 2001; Moretti et al., 2005). Although it is clearly not possible to perfectly replicate a complex neurodevelopmental human disorder in a mouse, these models have been valuable in furthering understanding of disease pathophysiology and in testing pharmacological interventions both at the circuit and whole animal levels. We chose to examine behavioral phenotypes in a novel mouse model of CDKL5 Deficiency Disorder (CDD), the CDKL5^{R59X} mouse (R59X), to validate it as a relevant model to investigate potential molecular and functional alterations in CDD.

Behavioral tests assessing home-cage activity, motor coordination and function, repetitive behaviors, sociability, and learning and memory are typically utilized to study mouse models of autism and other neurodevelopmental disorders. Here we chose to test R59X mice in a battery of behavioral assays that were of high relevance to

behaviors observed in patients with CDKL5 Deficiency Disorder (CDD), such as motor dysfunction, low sociability, and cognitive impairment.

Hyperactivity and motor function deficits are often observed in cases of autism and intellectual disability (Zingerevich et al., 2009; McClain et al., 2017), and in mouse models are typically assessed by the open field and rotarod assays. In the open field test, mice are placed in a home-cage like environment and allowed to roam freely to assess habituation and activity levels. The amount of time spent in the periphery vs the center of the arena is used as measure of anxiety-like behavior (Siebenhener 2015). Indeed, the amygdala, a brain region involved in anxiety-related behavior, is reported to be involved in open field activity along with the hippocampus (Daenen et al., 2001). The rotarod performance test, in contrast, measures motor coordination and motor learning, and is mainly related to cerebellar function (Goodlett et al., 1991). Mice are placed on an accelerating rotarod and latency to fall off the rod is measured over 3 trials per day for 4 days. Motor learning is assessed by how well mice learn to stay on the rod over repeated trials whereas latency to fall is a measure of motor coordination. Hyperactivity and impaired motor coordination in the open field and rotarod assays have been observed in several mouse models of autism (Paylor et al., 1999; Kazdoba et al., 2014).

Impaired sociability is another hallmark feature of autism, and can be investigated in mice using the three-chambered social choice test. Mice are placed into a three-chambered arena with a social cue (a novel mouse) and non-social cue (inanimate object) in either end chamber. Time spent sniffing and investigating each cue is measured; mice will normally spend significantly more time investigating the novel

mouse than the object. Mouse models of neurodevelopmental disorders on the other hand, consistently exhibit decreased social interaction (Moretti et al., 2005; Kazdoba et al., 2014), which is thought to be mainly hypothalamus and amygdala-dependent (Young, 2002) although the hippocampus may also be involved in discriminating social and non-social stimuli (Raam et al., 2017).

The Y maze and context-dependent fear conditioning paradigm are often utilized to test short and long-term hippocampal-dependent learning and memory respectively. For short-term memory, mice are placed in a Y shaped maze and allowed to explore the arms freely. Mice are naturally exploratory and normally will alternate the arms they explore so that spontaneous alternation behavior (SAB) is typically around 60%. However, mice with impaired short-term memory repeatedly enter the same arms causing SAB to be less than 50%. Long-term memory is assessed with the context-dependent fear conditioning paradigm, which measures how well mice remember a foot shock after 24 hrs. Mouse models of FXS and RTT display significantly impaired fear memory (Stearns et al., 2007; Kazdoba et al., 2014)

Although several mouse models of CDD have been developed that reflect core features of the human disease, including decreased motor coordination, social interaction deficits, and impaired learning and memory (Tang et al., 2017; Wang et al., 2012; Amendola et al., 2014; Fuchs et al., 2015; Okuda et al., 2017, 2018), no mouse model to date has exhibited visible spontaneous seizures or abnormal EEG patterns. Furthermore, provocation of seizures using kainic acid does not reveal a difference in latency to epileptiform activity bursts (Amendola et al., 2014) or seizure severity (Okuda et al.,

2017) in CDKL5 KO mice, though CDKL5 KO mice exposed to NMDA have increased seizure severity compared to WT littermates (Okuda et al., 2017). These data suggest that loss of CDKL5 does cause subtle hyperexcitability phenotypes in mice, but the variability between studies highlights the need for further investigation of seizure susceptibility in mouse models of CDD.

The CDKL5^{R59X} mouse is a novel model of CDD, developed after a mutation found in a human patient with severe seizures. The R59X mutation causes truncation of the kinase and a complete functional knock-out of the CDKL5 protein, which is comparable to constitutive knock-out models. However, demonstrating replicability and robustness of behavioral phenotypes and molecular alterations between mouse models is beneficial to our understanding of disease pathology.

Results

We show that whole brain lysates from R59X mice do not contain CDKL5 protein. Our behavioral analysis indicates that R59X mice display increased locomotion, social interaction deficits, and impaired working and long term memory. Additionally, they exhibit decreased latency to seizure behavior after a single low dose of pentylenetetrazol, suggesting that the mice have underlying hyperexcitability. These results verify that the R59X mouse is a relevant model to study the effects of loss of function of CDKL5 as well as investigate preclinical efficacy for potential therapeutics in CDD.

R59X mice do not express CDKL5 protein

We used male R59X mice for all of our studies to avoid the confounding effects of X inactivation. To produce R59X mice, a targeting vector was designed to insert a *frt*-flanked neomycin resistance (neo) cassette downstream of exon 5 and a single nucleotide change of C to T, leading to a nonsense mutation at arginine 59 (R59X) of the cyclin-dependent kinase-like 5 (*CDKL5*) gene. The construct was electroporated into C57BL/6N embryonic stem (ES) cells. Correctly targeted ES cells were injected into BALB/c blastocysts and resulting chimeric mice were bred with B6.Cg-Tg(ACTFLPe)9205Dym/J to remove the neo cassette. Resulting offspring were bred to C57BL/6J mice for at least 10 generations to establish a colony of R59X mice. To confirm that CDKL5 is not present in the brain of R59X mice, whole-brain lysates from R59X mice and WT littermates were probed for CDKL5. No CDKL5 is present in the R59X brain (Fig. 2-1).

R59X mice demonstrate hyperactivity and deficits in motor function

We aimed to determine whether R59X mice exhibited alterations in activity and motor coordination because hyperactivity and motor deficits are frequently observed in patients with ASD and in ASD murine models (Crawley, 2004, 2007; Brodkin, 2007; Moy et al., 2008; Wang et al., 2012). In the open field assay, R59X mice exhibited greater motor activity by increased number of beam breaks over time compared to WT controls (Fig. 2-2a. Two-way ANOVA, $F_{9, 280}$= 15.86, interaction $p<0.0001$). Additionally, mutant mice spent more time in the periphery of the arena (Fig. 2-2b. Unpaired t test, R59X: 69.04 ± 2.307 vs WT: 58.72 ± 2.900, $p=0.0095$), suggesting an elevated anxiety-like phenotype.

In the rotarod assay, R59X mice displayed decreased latency to fall, demonstrating impaired motor coordination (Fig. 2-2c. Two-way ANOVA, $F_{1, 336}$ = 30.13, main effect of genotype p<0.0001). Despite this impairment, latency to fall in mutant mice increased similarly across trials to WT, suggesting that the rate of motor learning was not altered. Finally, R59X mice had a significantly greater hindlimb clasping score than littermate controls (Fig. 2-2d. Unpaired t test, R59X: 2.200 ± 0.1447 vs WT: 0.6667 ± 0.1869, p<0.0001), a phenotype observed in other mouse models of autism and CDD that is interpreted as impaired motor function (Guy et al., 2001; Wang et al., 2012). These data show that R59X mice are hyperactive and have motor coordination and function deficits, phenotypes commonly observed in autism (Dewey et al., 2007).

R59X mice exhibit social interaction deficits

We next investigated sociability in R59X mice in the three-chambered social approach test, given the hallmark social interaction deficits in CDD and ASD (Bahi-Buisson et al., 2008b; Fehr et al., 2015). As expected, neither WT nor R59X mice showed a chamber preference during the initial habituation phase. However, upon introduction of a novel mouse, R59X mice spent significantly less time interacting with the novel mouse compared to WT littermates (Fig. 2-2e. Two-way ANOVA, $F_{1, 47}$= 115.6, interaction p<0.0001, Sidak's multiple comparisons test R59X: 16.653 ± 2.536 vs WT: 61.903 ± 3.3737, p<0.0001). Furthermore, during the five-minute direct interaction period R59X mice spent significantly less time sniffing and interacting with the novel mouse than WT littermates (Fig. 2-2f. Unpaired t test, R59X: 26.43 ± 5.493 vs WT: 64.85 ± 5.002, p<0.0001). The deficit in social interaction in R59X mice was not due to impaired

olfactory function, given there were no differences in time spent sniffing neutral, vanilla, and social scents between mutant mice and controls in the olfactory test (Fig. 2-2g).

R59X mice have learning and memory impairments

We tested whether R59X mice also have deficits in working and long-term memory, given that intellectual disability is another core feature of CDD (Fehr et al., 2016). The Y maze assay was used to test hippocampal-dependent working memory (Murray and Ridley, 1999), where mice were allowed to freely explore a maze with three arms. The number of alternation events was measured, where one alternation event was when the mouse entered all three arms without repeating one. We found that R59X mice had significantly decreased percent spontaneous alternation behavior (% SAB) compared to WT littermates, indicating a deficit in working memory (Fig. 2-2h. Unpaired t test, R59X: 44.03 ± 2.061 vs WT: 57.49 ± 1.329, $p<0.0001$). We then performed context-dependent fear conditioning to examine potential changes in hippocampal-dependent long-term memory (Phillips and LeDoux, 1992). Fear conditioning was performed over two days, a training day (day 1) and testing day (day 2). On day 1, both R59X mice and WT littermates showed similar levels of exploratory behavior during the habituation phase as well as comparable levels of freezing after the foot shock in the acquisition phase, indicating similar sensitivity to the foot shock. However, when placed back inside the shock-box 24 hours later (day 2) to test for long-term fear memory the R59X mice froze significantly less than WT littermates (Fig. 2-2i. Two-way ANOVA, $F_{2, 84} = 3.624$, interaction $p<0.0309$, Sidak's multiple comparisons test, R59X: 40.05 ± 4.865 vs WT 61.936 ± 4.114, $p<0.001$). Taken together, these data demonstrate impaired

hippocampal-dependent short- and long-term memory in the R59X mice compared to WT littermates.

R59X mice show decreased latency to seizure activity following administration of the chemoconvulsant pentylenetetrazol

Epilepsy has high prevalence in CDD patients, and many patients are refractory to conventional anti-epileptic drugs (Bahi-Buisson et al., 2008). There were no observed spontaneous seizures during both behavioral testing and routine animal husbandry interactions with R59X mice, consistent with other CDD mouse models to date (Wang et al., 2012; Amendola et al., 2014; Okuda et al., 2017; et al., 2017). Given the lack of evidence of a severe spontaneous seizure phenotype, we next aimed to determine whether R59X mice had elevated network hyperexcitability by evaluating seizure susceptibility. We therefore tested sensitivity to a single dose of pentylenetetrazol (PTZ, 40 mg/kg), a $GABA_A$ antagonist (Squires et al., 1984), which is well tolerated and causes mild seizure phenotypes (Racine stages 1-3) in WT mice. Mice were videotaped for 2 hours following PTZ administration and videos were scored for latency to onset of seizure activity. R59X mice exhibited significantly decreased latency to Racine stage 1 compared to WT mice (Fig. 2-1j. Unpaired t test, R59X: 79.00 ± 6.869 vs WT: 123.9 ± 14.46, p=0.0117). Seizure activity lasted on average 30 min post-injection for both R59X and WT mice, and no significant changes were found in total duration or overall severity of seizures (data not shown). Increased sensitivity to a sub-convulsive dose of PTZ suggests that although R59X mice do not exhibit spontaneous seizures, they do possess underlying hyperexcitability that may be contributing to their behavioral alterations.

Discussion

We show that the novel R59X mouse model displays reproducible, autistic-like behaviors and hyperexcitability that are core to the disease. Based on the lab's prior work (Lippman-Bell et al., 2013), this is plausible evidence for contributing molecular alterations that may be novel therapeutic targets in CDD. R59X mice display hyperlocomotion, decreased motor coordination, social interaction deficits, and impairments in spatial working memory as well as long-term hippocampal-dependent fear memory. Furthermore, R59X mice display decreased latency to seizure, indicating underlying hyperexcitability even in the absence of visible spontaneous seizures. Our results show that R59X mice replicate core clinical features of CDD. Importantly, R59X mice displayed increased susceptibility to seizure upon administration of a sub-convulsive dose of PTZ, indicating subtle hyperexcitability in the brain. This novel finding has not been observed in other mouse models of CDD. While spontaneous seizures or abnormal EEGs have not been observed in any rodent model of CDD to date (Wang et al., 2012; Amendola et al., 2014; Okuda et al., 2017), increased seizure severity has recently been shown in CDKL5 KO mice in response to NMDA, although the sample size in the study was quite small (Okuda et al., 2017). The same study reported that kainic acid had no effect on seizure score, although a prior report indicated that kainic acid *decreased* the total number of seizure events in CDKL5 KO mice but had no effect on latency or duration (Amendola et al., 2014). The variations in observed results may be due to the distinct pharmacology and doses of chemoconvulsants used, ages of mice at testing, and other environmental factors such as stress.

Increased seizure susceptibility is an indicator of altered excitatory:inhibitory (E:I) balance, which is mediated by excitatory and inhibitory receptors as well as ion transporters that regulate the electrochemical gradient in the brain (Eichler and Meier, 2008). In particular, excitatory glutamate receptor dysregulation is often observed in both autism and early-life epilepsy (Rakhade et al., 2012; Barker-Haliski and White, 2015; Fung and Hardan, 2015; Lippman-Bell et al., 2013, 2016) and will be discussed in the context of R59X mice in the next chapter.

The results shown here are similar to studies performed in constitutive knock-out mouse models of CDD where mutant mice exhibited hyperlocomotion (Wang et al., 2012; Okuda et al., 2018), decreased motor coordination (Wang et al., 2012), social interaction deficits (Wang et al., 2012; Jhang et al., 2017; Okuda et al., 2018), and impaired working and long-term context-dependent fear memory (Wang et al., 2012; Fuchs et al., 2015; Okuda et al., 2018). The robust replicability of deficits in social behavior and learning and memory across multiple mouse models of CDD highlight that normal function of CDKL5 is critical for these processes.

The hippocampal-associated memory deficits observed in R59X mice suggest that CDKL5 is important for normal hippocampal function. Indeed, impairments in hippocampal short-term working memory and long-term contextual fear memory have been observed in several constitutive knock-out mouse models of CDD (Wang et al., 2012; Fuchs et al., 2015; Okuda et al., 2018). Furthermore, these memory deficits were also observed in a conditional knock-out mouse where CDKL5 was deleted from glutamatergic neurons in cortex and hippocampus (Tang et al., 2017), suggesting that

not only is CDKL5 critical for hippocampal function, but that it likely plays a significant role in excitatory neurons allowing for normal processes that contribute to learning and memory.

Although several behaviors observed in R59X mice have been observed previously in CDKL5 KO mice (Wang et al., 2012), phenotyping this novel model is nonetheless valuable in showing robustness and replicability of the effects of loss of function of CDKL5. Furthermore, we verify that loss of CDKL5 in mice does cause subtle hyperexcitability in the absence of visible spontaneous seizures.

Materials and Methods

Animals

All procedures were performed in accordance with the guidelines of the National Institutes of Health Guide for the Care and Use of Laboratory Animals and approval of Institution of Animal Care and Use Committee at the University of Pennsylvania (Philadelphia, PA). All studies were performed on R59X mice and age-matched WT littermates on a congenic sv129**:**C57BL/6 background, available at Jackson Labs, stock number 028856. Mice were originally produced in the laboratory of Dr. Zhaolan Zhou at the University of Pennsylvania. To produce R59X mice, a targeting vector was designed to insert a *frt*-flanked neomycin resistance (neo) cassette downstream of exon 5, and a single nucleotide change of C to T, leading to a nonsense mutation at arginine 59 (R59X) of the *Cdkl5* gene. The construct was electroporated into C57BL/6N embryonic stem (ES) cells. Correctly targeted ES cells were injected into BALB/c blastocysts and resulting chimeric mice were bred with B6.Cg-Tg(ACTFLPe)9205Dym/J to remove the neo cassette. Resulting offspring were bred to C57BL/6J mice for at least 10 generations to establish a colony of R59X mice.

Male mice were used for all experiments to avoid confounding effects of X-inactivation that would be present in heterozygous female mice. All efforts were made to minimize animal suffering and numbers. Mice were genotyped using a PCR protocol designed to detect the R59X mutation. The genotyping primers (5'-GCTGCTTACATTAGGAGAGACTGC-3' and 5'-GTCACATGACCAGCCAGCGT-3') give rise to a 204 bp product from WT mice and a 347 bp product from the knock-in mutation.

Western blotting

Brains from P7, P14, P21, P30, P50, and P125 R59X mice and WT littermates were rapidly dissected from the skull. Tissue was flash-frozen in chilled ethanol and stored at −80°C until homogenization. Whole cell protein extraction was performed as described previously (Wenthold et al., 1992; Talos et al., 2006; Rakhade et al., 2012). Halt Protease and Phosphatase Inhibitor Cocktail EDTA-free (Thermo Fisher) and PMSF (Thermo Fisher) were added to inhibit proteases and phosphatases. Total protein concentrations were measured by the Bradford protein assay (Bio-Rad) and samples were diluted to obtain equal amounts of protein for each sample (1μg/ul). Samples were separated by gel electrophoresis on Criterion TGX 4-20% precast gels and transferred to PVDF membranes (Immobilon-FL). Primary antibodies used in this study were CDKL5 (1:1000; Millipore; MABS1132) and β-actin (1:3000; Sigma; A5441). Secondary antibodies used were rabbit IRDye 800CW and mouse IRDye 680LT (Licor). The Odyssey Infrared Imaging System protocols were used for blots and quantification of protein expression

Animal Behavior

All behavioral studies were performed blinded to genotype. Mice were allowed habituate in the testing room at least 30 minutes before each test. All tests were performed at the same time of day. Behavioral tests were performed on male R59X mice and WT littermates at 12-16 weeks of age.

Open-field assay. Home cage-like activity was monitored by beam breaks in a photobeam frame. Mice were placed into a clean environment in a photobeam frame.

The number of beam breaks over 10 minutes was quantified as a measure of locomotor activity, with the first three minutes denoted as the habituation period.

Y maze. Mice were placed at the end of one arm of a Y-shaped apparatus where each arm was labeled. Arm entries were recorded as they occurred. The mouse was considered to enter an arm when all four paws were in the arm. The mouse was allowed to explore the maze for 8 minutes. Percent spontaneous alternation behavior (% SAB) was calculated using the following formula: % SAB= [(number of alternations/total arm entries−2)] ×100.

Three-chambered social approach test. The social approach assay was performed in a three-chambered arena consisting of a center chamber and two end chambers, as previously described (Brodkin, 2007). One end chamber was designated the “social chamber” while the other was designated the “non-social” chamber. Two Plexiglas cylinders with air holes are placed in each end chamber. The test mouse is placed in the arena for a 10-minute habituation phase, during which the amount time spent in each chamber was measured (baseline). For the social phase, a stimulus mouse (adult gonadectomized A/J mouse; Jackson Labs) was placed in the cylinder in the social chamber, and a novel object was placed in the cylinder in the non-social chamber. The test mouse was again allowed to explore the arena for 10 minutes. Time spent in each chamber over the 10-minute test phase was measured.

Context-dependent fear conditioning. In the training phase, mice were placed in conditioning chambers for 3 minutes terminated with a 1.5 mA foot shock. The

uniqueness of the chamber is considered as the conditioned stimulus. Mice were left in the chamber for 1 minute after the foot shock. Mice are returned to the conditioning chamber 24 hours later for a 5-minute test phase. Time spent freezing (no motion except for respiratory movements) during the 5-minute test phase is measured with Freezescan software by Clever Systems.

Accelerating rotarod assay. Adapted from Rothwell et al, Cell 2014. A five station rotarod treadmill (IITC) was modified with a pulley and belt purchased from the vendor to increase the standard of acceleration, allowing the rotarod to attain speeds of up to 80 rpm while maintaining a constant rate of acceleration over a 300 second trial. Mice were placed on the rotarod for 3 trials per day over 4 consecutive days with at least a 15-minute inter-trial interval. On day 1 mice were allowed to acclimate to the stationary rod for 1 minute before beginning the first trial. Days 1 and 2 consisted of 4-40 rpm trials and days 3 and 4 consisted of 8-80 rpm trials. Trials were terminated after a mouse fell off the rod, made one complete revolution while clinging to the rod, or after 300 seconds (maximum speed).

Hindlimb clasping test. Mice were picked up by the base of the tail and lifted clear of all surrounding objects. Hindlimb position was observed for 10 seconds. If the hindlimbs were consistently splayed outward, away from the abdomen, the mouse was assigned a score of 0. If one hindlimb was retracted towards the abdomen for more the 50% of the time, the score was 1. If both hindlimbs were partially retracted for greater than 50% of the time, the score was 2. Finally, if hindlimbs were entirely retracted and touching the abdomen for more than 50% of the time suspended, the mouse received a score of 3.

Olfactory test. Mice were tested to observe whether they could detect and differentiate odors. Mice were exposed to cotton-tipped wooden applicators dipped in water, vanilla, or swiped across the bottom of an unfamiliar social cage. Each applicator was presented for 2 minutes with a 1-minute interval between applicators. Time spent sniffing was defined as when the mouse had its nose within 2 cm of the cotton tip.

PTZ seizure threshold test. 18-week-old male R59X mice and WT littermates were allowed to habituate in the procedure room for 30 minutes. Mice were injected with a sub-threshold dose of PTZ (40 mg/kg) and placed in a Plexiglas grid of 12 individual chambers. Each chamber had fresh bedding. Mice were video-monitored for 2 hours. Videos were scored by blinded observer using a modified Racine scale (Lüttjohann et al., 2009); 0: normal behavior, 1: freezing or immobility for at least 5 seconds, 2: myoclonic jerks, 3: forelimb clonus, 4: rearing, forelimb clonus, 5: tonic-clonic, loss of posture.

Experimental design and statistical analysis

For behavioral tests, we chose sample sizes based on previously published results in the CDD literature. The number of mice used in each experiment was predetermined before the start of the experiment and based on prior behavioral work in CDKL5 KO mice (Wang et al., 2012).

Stastical analysis was completed using GraphPad Prism. All datasets were analyzed using the D'Agostino–Pearson test for normality. Datasets with normal distributions were analyzed for significance using unpaired Student's two-tailed t test. Two-way repeated-

measures ANOVA was conducted for comparing mean differences between groups that have been split on two independent variables with Holm–Sidak's multiple-comparison test.

Figures

Figure 2-1

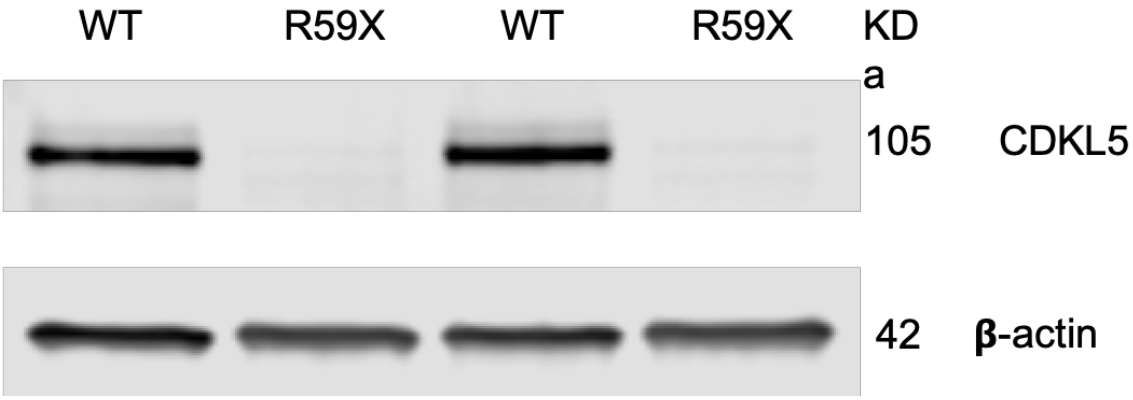

Figure 2-1: Western blot showing absence of CDKL5 protein in R59X whole brain lysates. β-actin is the loading control.

Figure 2-2

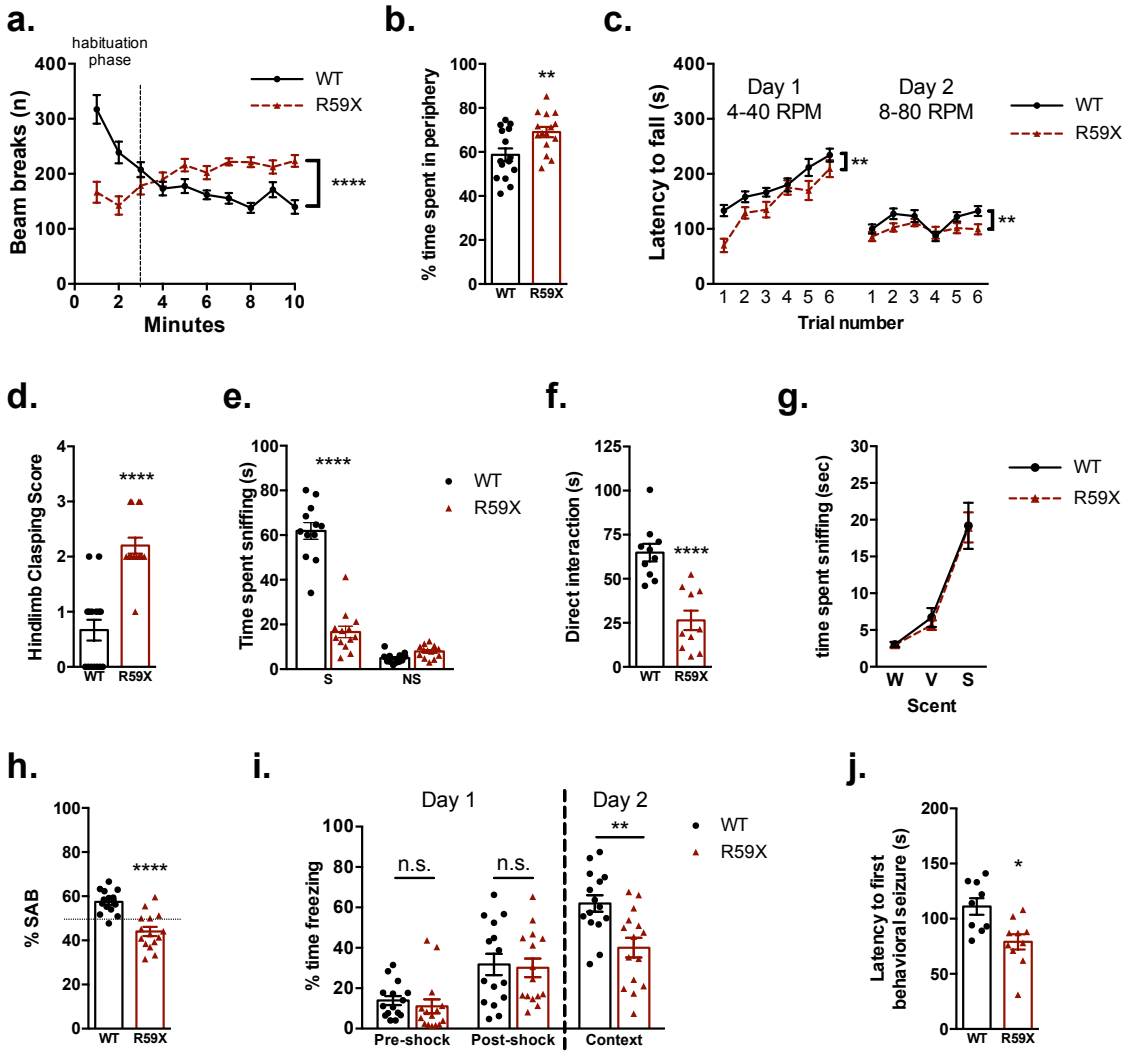

Figure 2-2: R59X mice display behavioral deficits consistent with mouse models of autism and intellectual disability, and lowered seizure threshold. a. Ten-minute open field locomotion test measuring number of infrared beam breaks over time. R59X mice exhibit increased activity compared to WT littermates, after a 3-minute habituation period. Two-way ANOVA, $p<0.0001$ (interaction). **b.** R59X spend significantly more time

in periphery of the open field arena, indicating elevated anxiety compared to WT. Unpaired t test, p=0.0095. **c.** Accelerating rotarod assay measuring latency to fall. R59X mice show comparable motor learning but decreased motor coordination compared to WT mice. Two-way ANOVA, p<0.0001 (main effect of genotype). **d.** Five second hindlimb clasping test assessing motor neuron function with a score of 0 representing no hindlimb clasping and a score of 4 representing both hindlimbs clasped in the middle during the entire trial period. R59X mice display increased clasping compared to WT littermates. Unpaired t test, p<0.0001. **e.** Three-chambered social choice assay measuring social interaction. WT and R59X mice spend comparable amounts of time sniffing the non-social object (NS), but R59X mice spend significantly less time sniffing the stimulus mouse (S). Two-way ANOVA with Sidak correction for multiple comparisons, p<0.0001 (interaction), p<0.0001. **f.** Five-minute direct interaction period with freely moving stimulus mouse. R59X mice spend less time interacting with stimulus mouse than WT littermates. Unpaired t test, p<0.0001. **g.** Olfactory test measuring time spent sniffing neutral, vanilla, and social scents. R59X mice and WT controls spend comparable amounts of time sniffing each scent. Two-way ANOVA, p=0.9499. **h.** Y maze assay testing working memory by measuring spontaneous alternation behavior (% SAB). R59X mice alternate arms of the Y maze significantly less than WT controls, suggesting impaired working memory. Unpaired t test, p<0.0001. **i.** Context-dependent fear conditioning assay measuring freezing behavior. R59X mice freeze similar amounts after a mild foot shock compared to WT mice (post-shock) but show decreased freezing upon returning to the testing chamber 24 hours later (context). Two-way ANOVA with Sidak correction for multiple comparisons, p=0.0309 (interaction). (N=15 for all groups in

a-i.) **j.** Seizure threshold test measuring latency to first behavioral seizure after PTZ injection. R59X (N=10) reach the first behavioral seizure significantly faster than WT littermates (N=10). Unpaired t test, p=0.0117. *p<0.05, **p<0.01, ****p<0.0001

CHAPTER 3 – Glutamate receptor and chloride channel analysis in R59X mice and two human cases of CDD

Introduction

Given the behavioral deficits and hyperexcitability observed in R59X mice, we hypothesized that mutant mice would exhibit underlying alterations in proteins involved in regulating the excitatory:inhibitory balance. Glutamate receptors, which include α-amino-3-hydroxy-5-methyl-4-isoxazolepropionic acid receptors (AMPAR), N-methyl-D-aspartate receptors (NMDAR) and kainate receptors, are heterotetrameric structures that mediate excitatory neurotransmission in the brain. NMDARs are composed of the obligate GluN1 subunit and a combination of two GluN2 or GluN3 subunits of which there are GluN2A-D, GluN3A, and GluN3B (Paoletti et al, 2013). AMPARs are are composed of GluA1-4 subunits (Greger et al., 2017). Expression and localization of receptor subunits are dynamically regulated throughout development by activity-dependent, transcriptional, and translational mechanisms (Paoletti et al., 2013; Greger et al., 2017), and altering receptor composition and biophysical properties to regulate the excitatory-inhibitory (E-I) balance throughout the lifetime (Luján et al., 2005; Rakhade and Jensen, 2009). Dysregulated glutamate receptor subunit expression is often associated with epilepsy, autism, and ID (Loddenkemper et al., 2014; Mignogna et al., 2015; Lippman-Bell et al., 2016).

Importantly, modest changes in the tightly regulated GluA2 AMPAR subunit can have a profound effect on excitability and signal transduction due to the distinct properties of GluA2 (Lippman-Bell et al., 2013; Uzunova et al., 2014; Stephenson et al., 2017). Most notably, GluA2-lacking AMPARs are Ca^{2+}-permeable and play a significant role in

regulating dendritic spine enlargement as well as downstream signaling and gene transcription (Plant et al., 2006; Isaac et al., 2007; Fortin et al., 2010; Henley and Wilkinson, 2016). Indeed, we have previously observed decreased GluA2 expression following neonatal hypoxic seizures in wild-type rats, which contributes to social interaction deficits, elevated activity-dependent Ca^{2+} influx, altered downstream signaling, and increased epileptogenesis (Sanchez et al., 2001; Rakhade et al., 2008; Lippman-Bell et al., 2013, 2016; Rosenberg et al., 2018). Finally, altered GluA2 subunit expression has been observed in several neurodevelopmental disorders such as Rett syndrome, Fragile X syndrome, tuberous sclerosis, and RAB39B-associated mental retardation (Talos et al., 2008; Mignogna et al., 2015; Li et al., 2016; Achuta et al., 2018), pointing to a critical role of GluA2 in neurodevelopmental disease pathophysiology.

Given that elevated GluA2-lacking AMPARs have been previously linked to neurobehavioral deficits and *Cdkl5* knock-down causes dysregulated GluA2 in neurons *in vitro* (Tramarin et al., 2018), we investigated levels of AMPAR subunits GluA1 and GluA2 in the novel R59X mouse model of CDD. However, we also included NMDAR subunits GluN2A and GluN2B, as well as chloride transporter NKCC1 and KCC2 in our protein analysis. NMDARs and chloride transporters also play a huge role during development in regulating the E:I balance (Luján et al., 2005; Rakhade and Jensen, 2009), and have been found to be dysregulated in epilepsy and various neurodevelopmental disorders such as Fragile X Syndrome and autism (Dzhala et al., 2005; Uzunova et al., 2014). Furthermore, glutamate receptors and chloride channels

can be activated and blocked by various pharmacological agents, making them attractive therapeutic targets in autism and epilepsy (Puskarjov et al., 2014; Barker-Haliski and White, 2015; Fung and Hardan, 2015).

Results

Decreased membrane-bound GluA2:GluA1 protein in R59X hippocampus

Given that previous studies support a role for CDKL5 in stabilizing excitatory synaptic scaffolding proteins that are involved in anchoring of neurotransmitter receptors and regulatory proteins at the membrane (Ricciardi et al., 2012; Della Sala et al., 2016) , we hypothesized that R59X mice may have molecular and functional alterations in NMDAR or AMPAR subunits associated with the aforementioned behavioral deficits and seizure susceptibility. We performed Western blot analysis across a developmental range from early postnatal (P7) to adult (P50) in cortical and hippocampal membrane-prepped tissue of NMDAR subunits GluN2A and GluN2B, and AMPAR subunits GluA1 and GluA2, the predominant AMPAR subunits in the brain (Lu et al., 2009; Reimers et al., 2011). Although levels of GluA1 in R59X mice were unaltered compared to WT littermates at all time points (Fig. 3-1a), R59X mice showed significant decreases in hippocampal membrane-bound GluA2 at P30 and P50 (Fig. 3-1b. Multiple t test, P30: $p=0.0089$; P50: $p=0.0053$). We wanted to see whether this decrease persisted throughout adulthood and extended our Western blot analysis in hippocampal tissue to P125. Indeed, decreased GluA2 was observed at this time point as well (Fig. 3-1b. Multiple t tests, P125: $p=0.0193$), indicating a persistent decrease of membrane-bound

GluA2 in the hippocampus. Importantly, when considering the ratio of subunits GluA2:GluA1, which is a measure of GluA2-lacking AMPARs, R59X mice had significantly decreased GluA2:GluA1 in the hippocampus at P30, P50, and P125 (Fig. 3-1c. Multiple t tests, P30: p=0.0180; P50: p=0.0002; P125: p=0.0048), suggesting reduced GluA2-containing AMPARs, or in other words increased hippocampal GluA2-lacking AMPARs. Decreased GluA2 was specific to the hippocampus; no significant changes in GluA1 and GluA2 expression were observed across the lifespan in the cortex of R59X mice (Fig. 3-1h-k). GluA2-lacking AMPARs are Ca^{2+}-permeable and are key regulators of synaptic function and plasticity that are particularly implicated in neurodevelopmental disease pathophysiology (Isaac et al., 2007; Uzunova et al., 2014; Lippman-Bell et al., 2016; Rosenberg et al., 2018). Therefore, decreased GluA2:GluA1 in R59X hippocampus may contribute to hyperexcitability and hippocampal-dependent learning and memory observed in the whole animal.

Levels of NMDAR subunits and chloride transporters are not altered in the hippocampus or cortex in R59X mice

Interestingly, no significant alterations were observed in membrane-bound GluN2A, GluN2B, and the ratio of GluN2B:GluN2A at any developmental time point in the hippocampus of R59X mice compared to controls (Fig. 3-2a-c), contrary to a recent study showing elevated GluN2B at CA1 synapses in CDKL5 KO mice (Okuda et al., 2017). There were no observed alterations in NMDAR subunits in R59X cortex (Fig. 3-2e-g). We also investigated the levels of the developmentally regulated chloride channels NKCC1 and KCC2 which have been found to be dysregulated in Tuberous sclerosis (Talos et al., 2012). Levels of NKCC1 and KCC2 were not altered in either

hippocampus or cortex of R59X mice at any time point (Fig. 3-3a-g). These data suggest that neither NMDARs nor chloride transporters contribute to lowered seizure threshold or behavioral abnormalities in R59X mice.

Fraction of synapses containing GluA2 is significantly decreased in CA1 and dentate gyrus hilus

To determine whether the decreases in membrane-associated GluA2 was occurring at intact synapses, we performed immunohistochemistry of surface GluA2 or GluA1 staining colocalized with presynaptic marker synapsin. The fraction of synapsin puncta that colocalized with surface GluA2 was calculated using the Manders coefficient (Manders et al., 1993). The Manders coefficient has previously been used to quantify association of $GABA_A$ subunits with inhibitory synaptic anchoring protein gephyrin (Gao and Heldt, 2016). We found that the fraction of synapses containing GluA2 was significantly decreased in R59X CA1 s. radiatum (Fig. 3-4a,b. Multiple t tests, $p<0.05$) whereas the fraction of CA1 synapses containing GluA1 was unaltered compared to WT littermates (Fig. 3-4c,d). Similarly, R59X dentate gyrus hilar neurons showed significantly less GluA2-containing synapses (Fig. 3-5a,b. Multiple t tests, $p<0.01$) while GluA1-containing synapses were not altered (Fig. 3-5c,d). Interestingly, this pattern of decreased GluA2-containing synapses was not observed in CA3 s. radiatum (Fig. 3-6a,b) and fraction of GluA1-containing synapses was not altered either (Fig. 3-6c,d). Finally, we investigated cortex layer II/III for alterations in GluA2 and GluA1-containing synapses. Although our Western blot analysis showed no change in the cortex for GluA2 and GluA1, we were curious to see whether we could observe layer II/III-specific changes particularly because long-term potentiation (LTP) has been reported to be

decreased in layer II/III in CDKL5 KO mice (Della Sala et al., 2015) and GluA2-lacking AMPARs are involved with LTP induction (Plant et al., 2006). However, there were no alterations in GluA2- or GluA1-containing synapses in layer II/III in R59X mice (Fig. 3-7).

Expression and whole cell levels of GluA1 and GluA2 are not altered in R59X hippocampus

Prior reports suggest that CDKL5 shuttles from the cytoplasm to the nucleus where it may affect gene regulation (Rusconi et al., 2008), and the observed changes in GluA2 protein expression may be secondary to transcriptional changes. Therefore, we next used RT-qPCR to measure the relative mRNA transcript levels of *Gria1* or *Gria2* (for GluA1 and GluA2 respectively) in hippocampal tissue from P50 R59X mice and WT littermates. We found that R59X mice do not have significantly altered mRNA transcript levels of *Gria1* or *Gria2* (Table 1). Furthermore, in whole cell hippocampal homogenates there were no changes in total protein levels of GluA1 or GluA2 in R59X mice compared to controls (Table 1). These data suggest that decreased membrane-bound GluA2 in the R59X hippocampus is more likely due to alterations in membrane trafficking or localization than altered expression of the subunits themselves.

Investigation of GluA2 trafficking proteins in R59X hippocampus

Given the decrease in membrane-associated GluA2 without a concomitant decrease in transcription or total protein levels, we next investigated whether altered post-translational phosphorylation of GluA2 at Ser880 ($GluA2^{S880}$), which normally causes internalization of GluA2, could be responsible for the observed differences. However, we observed no change in $GluA2^{S880}$ in the R59X hippocampus (Table 1). We also did not

observe alterations in levels of PICK1, CaMKII, or RAB39B (Table 1), proteins that are involved in GluA2 trafficking from the endoplasmic reticulum to the membrane (Lu et al., 2014; Mignogna et al., 2015; Lorgen et al., 2017). However, trafficking of GluA2 may be dysregulated at numerous other pathways that we did not have the chance to investigate.

Exploring human tissue to validate neurotransmitter receptor expression changes in postmortem hippocampal tissue from CDD patients

We obtained postmortem brain tissue samples from two patients with CDD and sought to determine if a similar trend of decreased GluA2:GluA1 could be observed in the human hippocampus, adding some clinical relevance to the results we obtained in the R59X model. Indeed, although statistical analysis could not be performed with just two cases, we see a trend towards decreased GluA2:GluA1 in CDD hippocampus (Figure 3-8a.). This is an intriguing finding given the varied ages of the cases (5 and 30 years old) and the likelihood that they were on different anti-epileptic drug regimens that could differentially affect levels of neurotransmitter receptors. The differences in NMDAR subunits and chloride channels are not as consistent (Figure 3-8b,c), which makes it difficult to interpret whether there could be differences in those proteins in patients with CDD. However, the GluA2:GluA1 data suggests that our findings in the mouse may indeed be clinically relevant, though further investigation is necessary.

Discussion

Here we observed a specific decrease in GluA2 and GluA2:GluA1 in the hippocampus, but not cortex, of R59X mice beginning at P30 and persisting throughout adulthood. No

significant alterations in GluA1, GluN2A, GluN2B, NKCC1 or KCC2 were found in the hippocampus or cortex of R59X mice. Our Western blot results are supported by surface GluA1 and GluA2 staining colocalized with presynaptic marker synapsin in hippocampal slices, which showed a significant decrease in GluA2-containing synapses in CA1 s. radiatum as well as DG hilus. Interestingly, we did not observe a significant decrease in GluA2 in CA3 s. radiatum. It is challenging to fully understand these region-specific changes without further knowledge of the cell types involved and the function of CDKL5 within those cell types. However, our immunohistochemistry analysis was not comprehensive in looking at the entire hippocampus and it is possible that we missed GluA2 changes occurring in other areas within CA3. Finally, we observed a trend towards decreased GluA2:GluA1 in two post-mortem cases of CDD and no strong trends in NMDAR subunits or Cl^- channels, indicating that our findings may be clinically relevant in the CDD patient population.

Decreased GluA2:GluA1 suggests an increase in GluA2-lacking AMPARs at the membrane. The GluA2 subunit is critical in determining biophysical properties of AMPARs including rectification, single channel conductance, and Ca^{2+} permeability (Kumar et al., 2002; Isaac et al., 2007; Migues et al., 2007). Furthermore, decreased surface GluA2 has been observed to contribute to hyperexcitability, altered plasticity, and intellectual disability, implicating GluA2-lacking AMPARs as a critical player in neuronal function and disease (Gardner et al., 2005; Mignogna et al., 2015; Lorgen et al., 2017). Thus, increased GluA2-lacking AMPARs in R59X hippocampus CA1 and DG

may be contributing to the behavioral deficits and hyperexcitability observed at the whole animal level.

Our lab has previously observed increased GluA2-lacking AMPARs in a rat model of early-life epilepsy 48 hours after hypoxic seizures (Sanchez et al., 2001; Rakhade et al., 2012; Lippman-Bell et al., 2016). Furthermore, blocking AMPAR activity with NBQX immediately after seizures in this model prevented later-life epileptic seizures and autistic-like social deficits (Lippman-Bell et al., 2013), suggesting that early intervention of elevated GluA2-lacking AMPAR activity may inhibit development of hyperexcitable and autistic-like phenotypes. GluA2 dysregulation has additionally been observed in Fragile X Syndrome and Rett Syndrome (Li et al., 2016; Achuta et al., 2018).

Recently, glutamate receptor subunit levels have been investigated in two other models of CDD. Interestingly, decreased surface GluA2:GluA1 was also observed in a cell culture model of CDD where Cdkl5 was silenced in primary hippocampal cultures using shRNA (Tramarin et al., 2018). However, our data conflicts with a study in a knock-out mouse model of CDD where investigators observed a significant increase in GluN2B subunits in the hippocampus, which they show also contributes to hyperexcitability at the whole animal level (Okuda et al., 2017). The difference in results of GluN2B may be due to the disparate genetic backgrounds of the mouse models used by each study as well as the techniques used to measure glutamate receptor subunit expression. The GluN2B differences in the knock-out model were observed in the PSD-1T fraction of tissue and by immunogold labeling of CA1 stratum radiatum rather than membrane prepped tissue and standard immunohistochemistry performed here. Further experiments must be

performed in R59X tissue to determine whether increased GluN2B may be observed with more precise techniques.

Although membrane-bound GluA2:GluA1 is significantly decreased in adult R59X mice, we did not observe a similar trend in relative mRNA expression of *Gria1* and *Gria2*, suggesting that loss of CDKL5 results in disrupted trafficking or localization of GluA2 to the membrane. These findings mirror those of the primary hippocampal cell culture model of CDD where they found no change in mRNA levels (Tramarin et al., 2018). However, contrary to our results, the cell culture model exhibited significantly decreased total GluA2, which was accompanied by increased GluA2^{S880} suggesting increased internalization of the subunit. The differences in these results may be due to the heterogenous cell population of tissue samples used for our Western blotting experiments versus the pure neuronal cell population studied in the cell culture model. The mixed cell population in our experiments may also be diluting any potential differences in the trafficking proteins PICK1 or RAB39B that may be contributing to decreased membrane-bound GluA2. However, another mechanism for impaired synaptic localization of GluA2 may be through dysregulation of PSD95, a molecule involved in clustering of AMPARs through interaction with scaffolding protein stargazin/TARP (Coley and Gao, 2017). A reduction of PSD-95 puncta has been observed in neurons after CDKL5 knock-down (Ricciardi et al., 2012; Tramarin et al., 2018), suggesting that anchoring and stability of glutamate receptors at the synapse may be compromised in this disorder. Interestingly, palmitoylation of PSD-95 recruits CDKL5 to synapses (Zhu et al., 2013) and has also been found to increase surface GluA2 levels (Jeyifous et al.,

2016), suggesting a possible link between CDKL5 function and GluA2 localization at the synapse. A deeper understanding of CDKL5 interacting partners and phosphorylation substrates is necessary to identify the primary cause of dysregulated synaptic GluA2 and its functional consequences.

Materials and Methods

Western Blotting

To compare developmental expression patterns of AMPA receptor subunits GluA1 and GluA2, R59X and WT littermates were sacrificed at P7, P14, P21, P30, P50, and P125. Brains were rapidly dissected from the skull, and hippocampal and cortical regions were separated. Tissue was flash-frozen in chilled ethanol and stored at −80°C until homogenization. Membrane and whole cell protein extraction from the anterior two-thirds of the cortex and the entire hippocampal tissue was performed as described previously (Wenthold et al., 1992; Talos et al., 2006; Rakhade et al., 2012). Halt Protease and Phosphatase Inhibitor Cocktail EDTA-free (Thermo Fisher) and PMSF (Thermo Fisher) were added to inhibit proteases and phosphatases. Total protein concentrations were measured by the Bradford protein assay (Bio-Rad) and samples were diluted to obtain equal amounts of protein for each sample (1μg/ul). Samples were separated by gel electrophoresis on Criterion TGX 4-20% precast gels and transferred to PVDF membranes (Immobilon-FL). Primary antibodies used in this study were GluA2 (1:1000; Millipore; MAB397), GluA1 (1:1000; Abcam; ab31232), NR2A (1:1000, Sigma; M264), NR2B (1:1000, Thermo-Fisher; MA1-2014), NKCC1 (1:1000, Millipore), KCC2 (1:1000, Abcam) and β-actin (1:3000; Sigma; A5441). Secondary antibodies used were rabbit

IRDye 800CW and mouse IRDye 680LT (Licor). The Odyssey Infrared Imaging System protocols were used for blots and quantification of protein expression. Protein levels were normalized to the P50 time point.

Immunohistochemistry

P50 WT and R59X mice were perfused transcardially with 4% paraformaldehyde. Brains were dissected from the skull and post-fixed for 1 hour at room temperature before being transferred to 30% sucrose. Once saturated with sucrose, the brains were embedded in OCT and frozen. 16 μm sections were collected using a cryostat and mounted on slides. Sections containing the middle 1/3 of the hippocampus were blocked with 10% normal goat serum in PBS and incubated with either anti-GluA2 (extracellular, 1:500, Millipore) or anti-GluA1 (extracellular, 1:500, NeuroMab) overnight, then incubated with AlexaFluor secondary (1:1000, Invitrogen) for 1 hour at room temperature. Sections were then permeabilized with 0.2% Triton X-100 in PBS for 5 minutes and then blocked with 10% normal goat serum (NGS) with 0.1% Triton in PBS for 1 hour. Finally, the sections were incubated with anti-synapsin (1:1000, Millipore) diluted in 0.1% NGS and 0.1% Triton in PBS overnight at 4°C, washed with PBS, and incubated with AlexaFluor secondary (1:1000, Invitrogen) for 1 hour at room temperature. Fluoromount with Dapi was used to mount the sections with a coverslip. Sections incubated without primary and only with secondary antibody were imaged to verify antibody specificity. We have previously confirmed the surface specificity of the GluA2 antibody used here in permeabilized and non-permeabilized sections incubated with an antibody to MAP2 (1:1000, Millipore) in addition to GluA2 (Lippman-Bell et al., 2016). Blinded sections were placed on a Zeiss

LSM710 confocal microscope with an oil-immersion 63x1.7 NA objective. Z-stacks for all images were 0.25 μm.

Analysis of z-stacks was performed blindly using Image-J software. To avoid a thresholding artifact, colocalization was first measured at the maximum threshold incorporating all GluA2 puncta, then the GluA2 channel was thresholded at multiple intervals of the max threshold (95, 90, 85, 80, 75, and 70%), and colocalization was determined again at each threshold (Nie et al., 2010; Zhou et al., 2011). After thresholding each channel, the overlap of GluA2 with synapsin puncta was quantified using the plugin coloc2 to determine the Manders coefficient (Manders et al., 1993).

RT-qPCR

P50 mice were sacrificed and whole hippocampus was collected. RNA was isolated using Qiagen RNeasy kit and then converted to cDNA with Invitrogen SuperScript III First-Strand Synthesis System. RT-qPCR was run using TaqMan optimized primer probe sets—for GRIA1, GRIA2, ACTB (β-actin), and HPRT—and TaqMan Master Mix.

Experimental design and statistical analysis

We determined sample size and power for Western blots and immunohistochemistry based on previously published work in our laboratory (Rakhade et al., 2012; Lippman-Bell et al., 2016). The number of mice used in each experiment was predetermined before the start of the experiment.

Stastical analysis was completed using GraphPad Prism. All datasets were analyzed using the D'Agostino–Pearson test for normality. Datasets with normal distributions were

analyzed for significance using unpaired Student's two-tailed t test. Two-way repeated-measures ANOVA was conducted for comparing mean differences between groups that have been split on two independent variables with Holm–Sidak's multiple-comparison test.

Figures

Figure 3-1

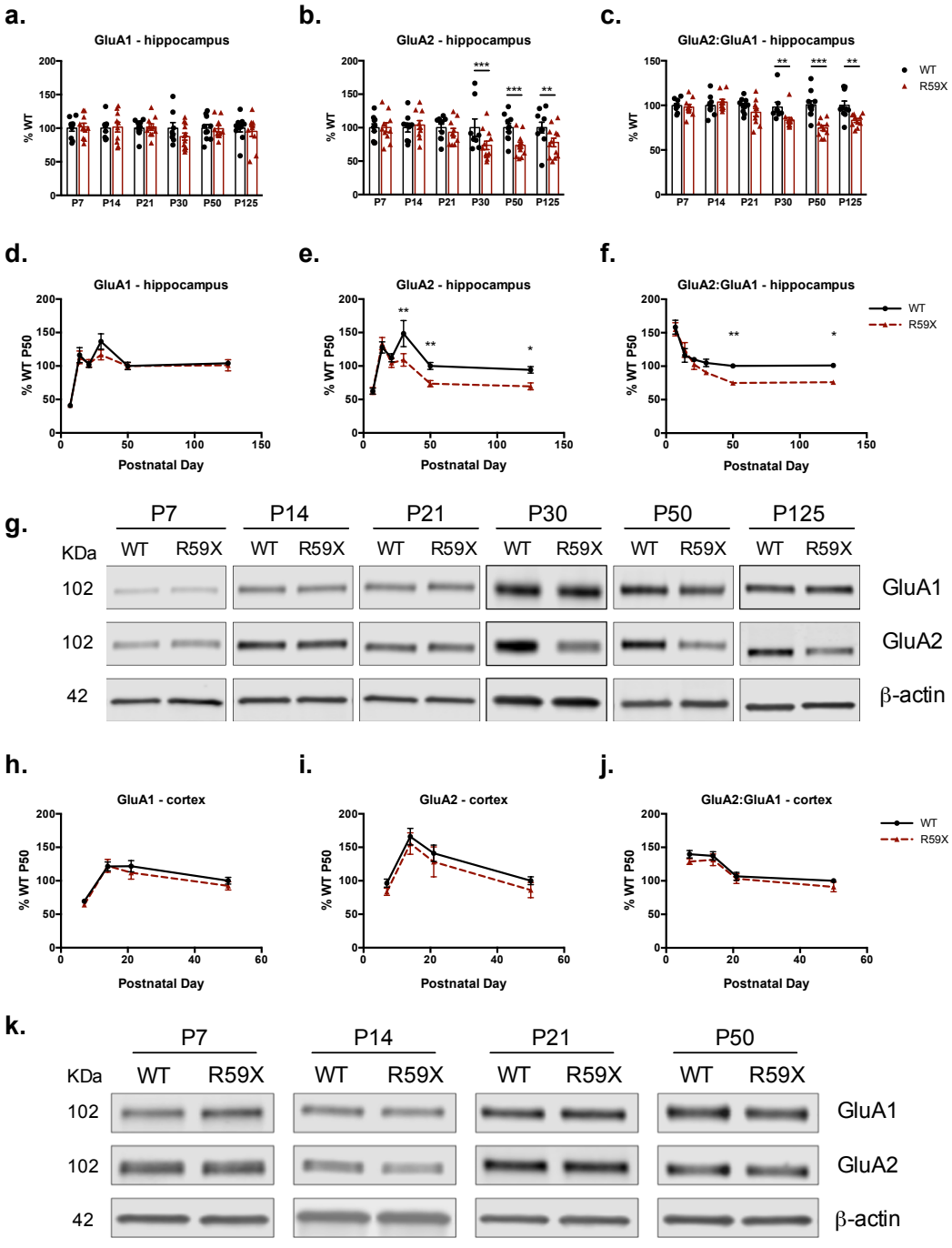

Figure 3-1. AMPAR subunit GluA2 and ratio of subunits GluA2:GluA1 are significantly decreased at developmental time points P30, P50 and P125 in R59X hippocampus. a. Levels of GluA1 are not significantly altered at any time point. Multiple t tests. **b.** Levels of GluA2 are significantly decreased at P30, P50, and P125. Multiple t tests, P30: p=0.0089, P50: p=0.0053, P125: p=0.0193 **c.** Levels of GluA2:GluA1 are significantly decreased at P30, P50, and P125. Multiple t tests, P30: p=0.0180, P50: p=0.0002, P125: p=0.0048 **d-f.** Developmental curve of GluA1. Two-way ANOVA, p=0.99. **e.** Developmental curve of GluA2. Two-way ANOVA with Sidak's multiple comparisons, interaction p=0.0250. **f.** Developmental curve of GluA2:GluA1. Two-way ANOVA with Sidak's multiple comparisons, interaction p=0.0440. **d.** Representative Western blots of GluA1 and GluA2 compared to actin loading control. **e-g.** No change in AMPAR subunits in R59X cortex. Two-way ANOVA, GluA1: p=0.891, GluA2: p=0.999, GluA2:GluA1: p=0.928. **h.** Representative Western blots of AMPAR subunits compared to actin loading control. N=8-12 for all time points. All time points in a-c normalized to age-matched WT controls All time points in d-j normalized to WT P50. *p<0.05, **p<0.01, ***p<0.001

Figure 3-2

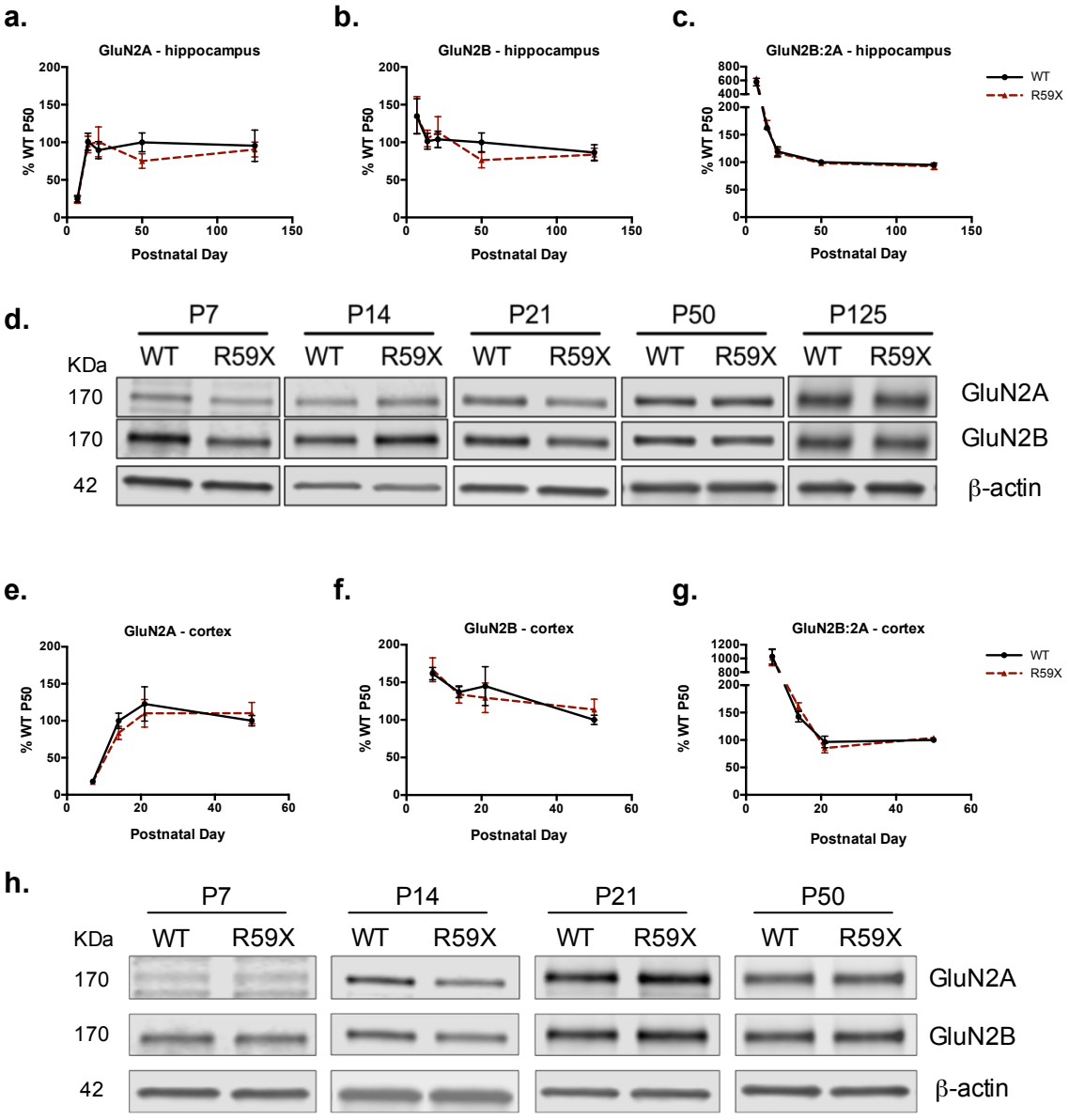

Figure 3-2: No alterations in NMDAR subunit levels in R59X cortex and hippocampus over development. a-c. Developmental expression of GluN2A, GluN2B, or GluN2B:2A is not altered in R59X hippocampus. Two-way ANOVA, GluN2A: p=0.672, GluN2B:

p=0.852, GluN2B:N2A: p=0.696. **d.** Representative Western blots of GluN2A and GluN2B compared to actin loading control. **e-g.** No change in NMDAR subunits in R59X cortex. Two-way ANOVA, GluN2A: p=0.703, GluN2B: p=0.780, GluN2B:2A p=0.991 **h.** Representative Western blots of NMDAR subunits compared to actin loading control. N=8-12 for all time points. All time points normalized to WT P50.

Figure 3-3

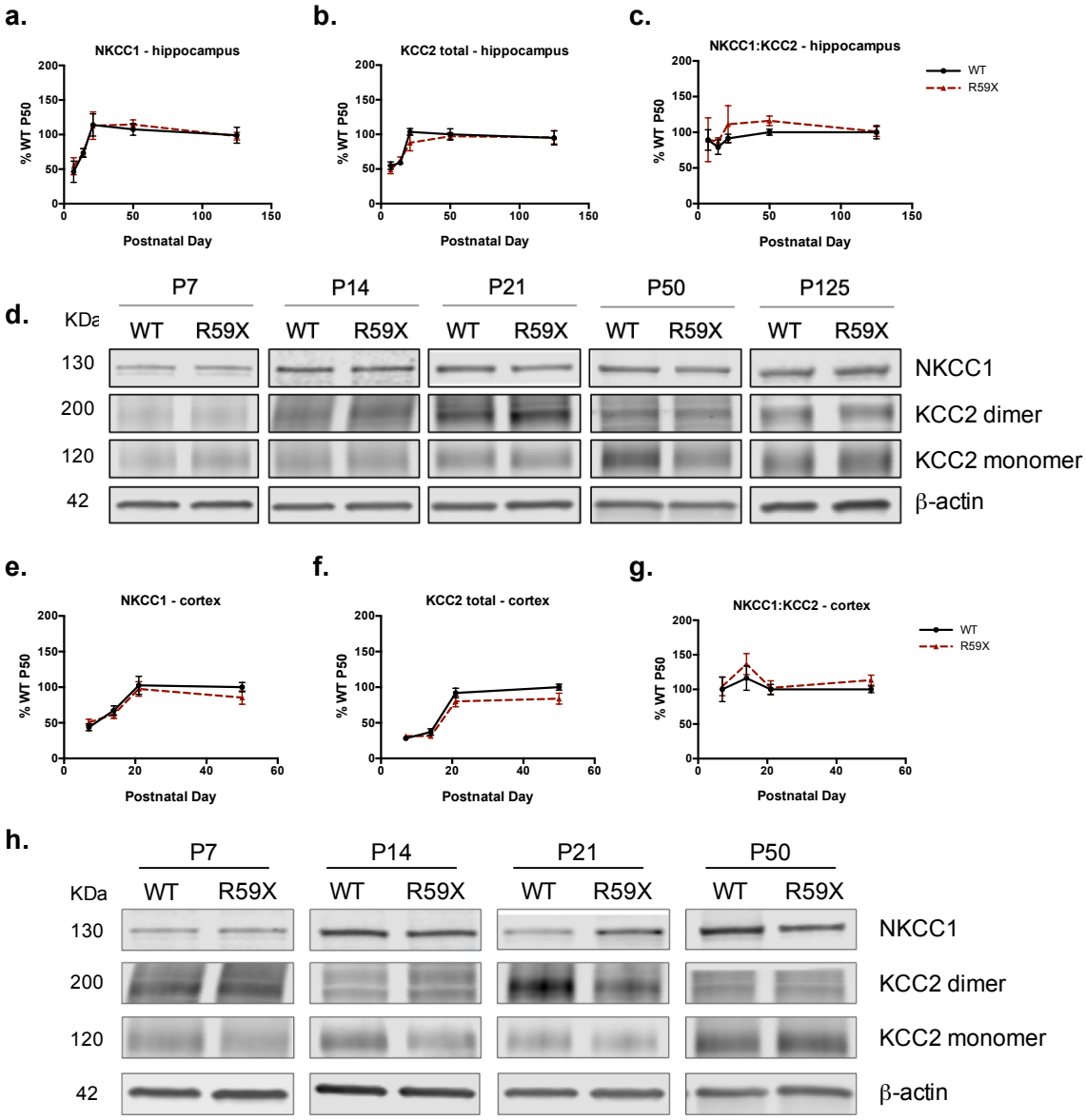

Figure 3-3: No alterations in chloride transporters NKCC1 or KCC2 levels in R59X cortex or hippocampus over development. a-c. Developmental expression of NKCC1 and KCC2 is not altered in R59X hippocampus. Two-way ANOVA, NKCC1: p=0.992, KCC2 (total): p=0.799, NKCC1:KCC2: p=0.908. **d.** Representative Western blots of NKCC1 and KCC2

(monomer and dimer bands) in hippocampus compared to actin loading control. **e-g.** No change in chloride channels NKCC1 or KCC2 over development in R59X cortex. Two-way ANOVA, NKCC1: p=0.644, KCC2: p=0.519, NKCC1:KCC2: p=0.833. **h.** Representative Western blots of NKCC1 and KCC2 (monomer and dimer bands) in cortex compared to actin loading control. N=8-12 for all time points. All time points normalized to WT P50.

Figure 3-4

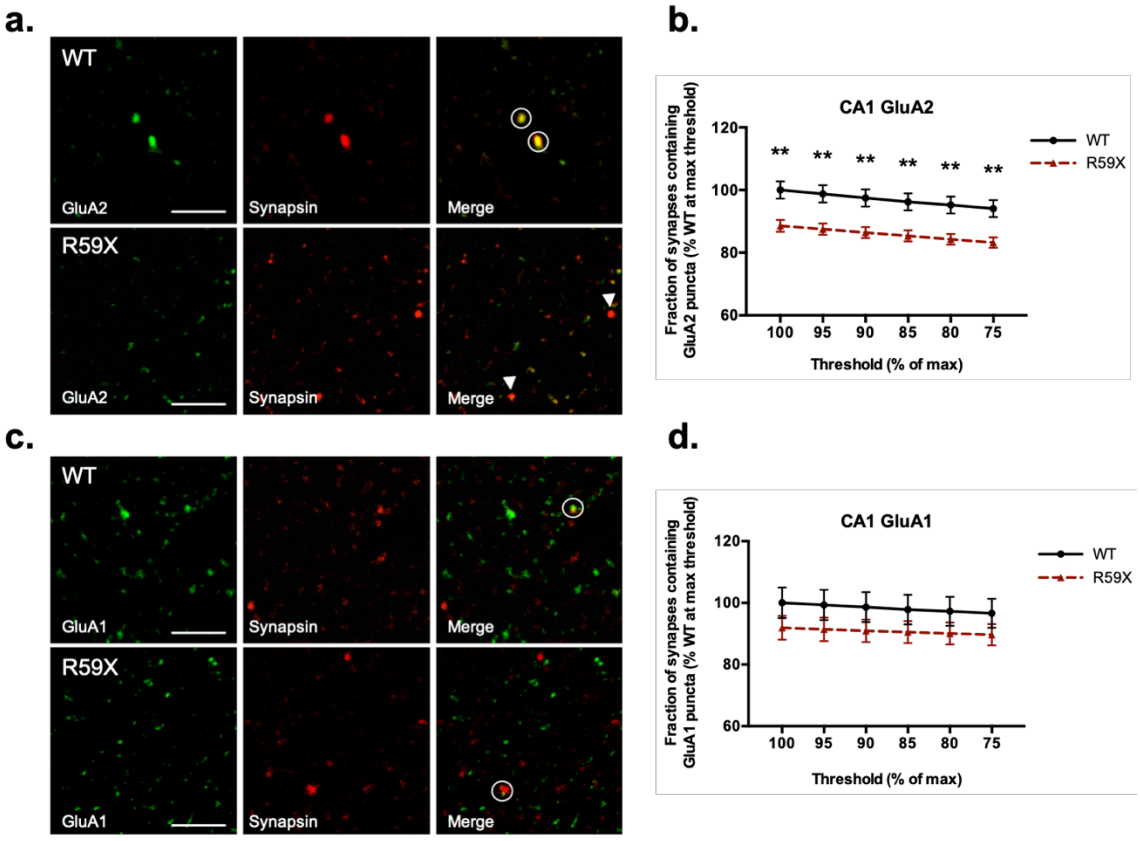

Figure 3-4: Fraction of GluA2-containing synapses is significantly decreased in CA1. a. Immunohistochemistry of surface GluA2 (green) and presynaptic marker synapsin (red) in CA1. **b.** Quantification shows a significant decrease in the fraction of synapsin puncta that colocalize with GluA2, representative of decreased synaptic GluA2 in CA1. Unpaired t test, p=0.003. **c,d.** Synaptic GluA1 is not significantly altered in R59X CA1 s. radiatum. Unpaired t test, p=0.24. Circles highlight colocalization and arrowheads mark synapsin without GluA2. N=10 fields from 5 mice for all groups. ** p<0.01.

Figure 3-5

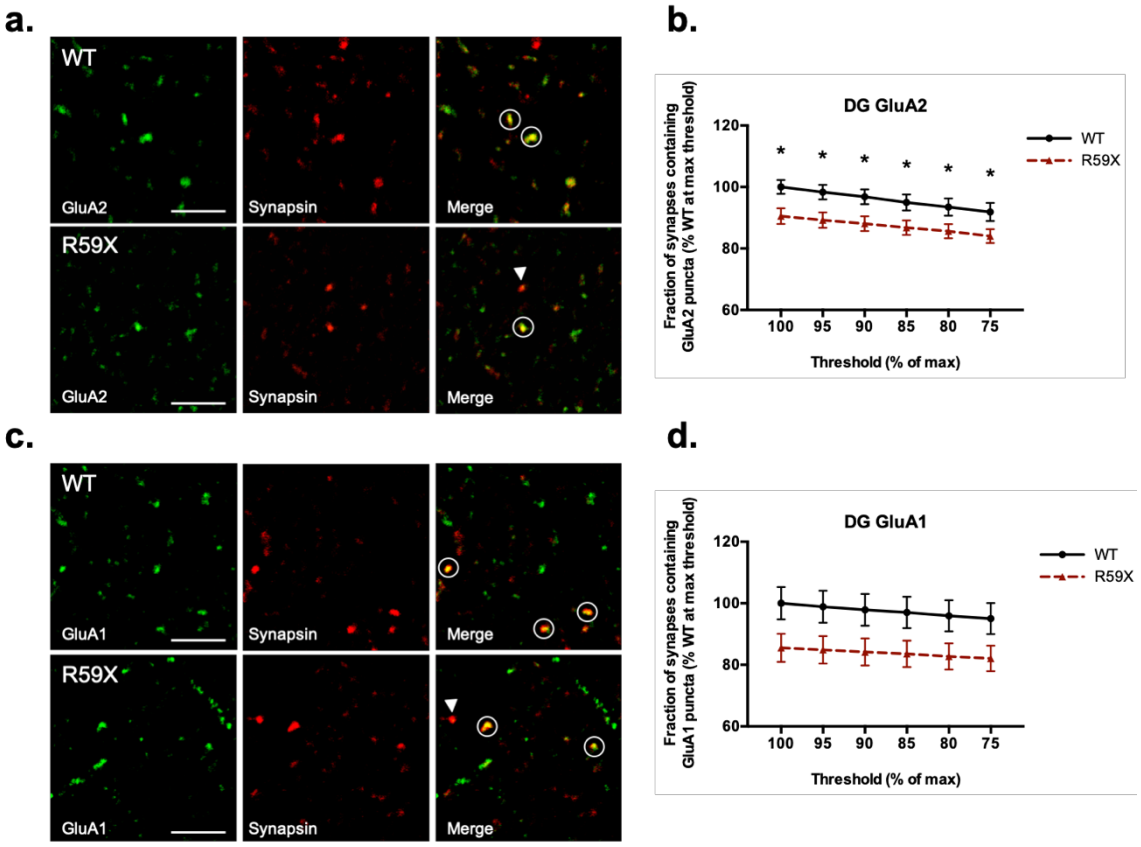

Figure 3-5: Fraction of synapses containing GluA2 is significantly decreased in DG. a. Immunohistochemistry of surface GluA2 (green) and presynaptic marker synapsin (red) in DG. **b.** Quantification shows a significant decrease in the fraction of synapsin puncta that overlap with GluA2, representative of decreased synaptic GluA2 in DG hilus. Unpaired t test, p=0.01. **c,d.** Synaptic GluA1 is not significantly altered in DG hilus. Unpaired t test, p=0.06. Circles highlight colocalization and arrowheads mark synapsin without GluA2. N=10 fields from 5 mice for all groups. * p<0.05.

Figure 3-6

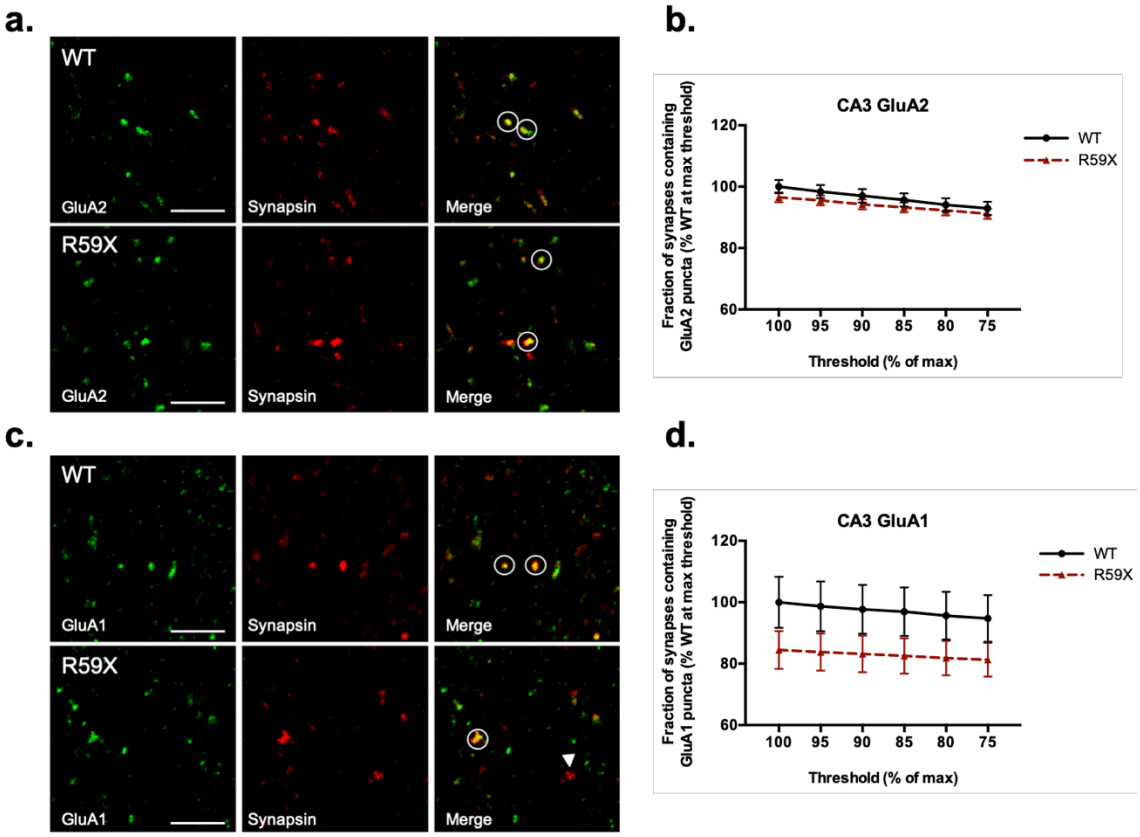

Figure 3-6: No change in fraction of synapses containing GluA2 or GluA1 in CA3. **a,b.** Synaptic GluA2 is not significantly altered in CA3. Unpaired t test, p=0.22. **c,d.** Synaptic GluA1 is not significantly altered in CA3. Unpaired t test, p=0.16. Circles highlight colocalization and arrowheads mark synapsin without GluA2. N=10 fields from 5 mice for all groups.

Figure 3-7

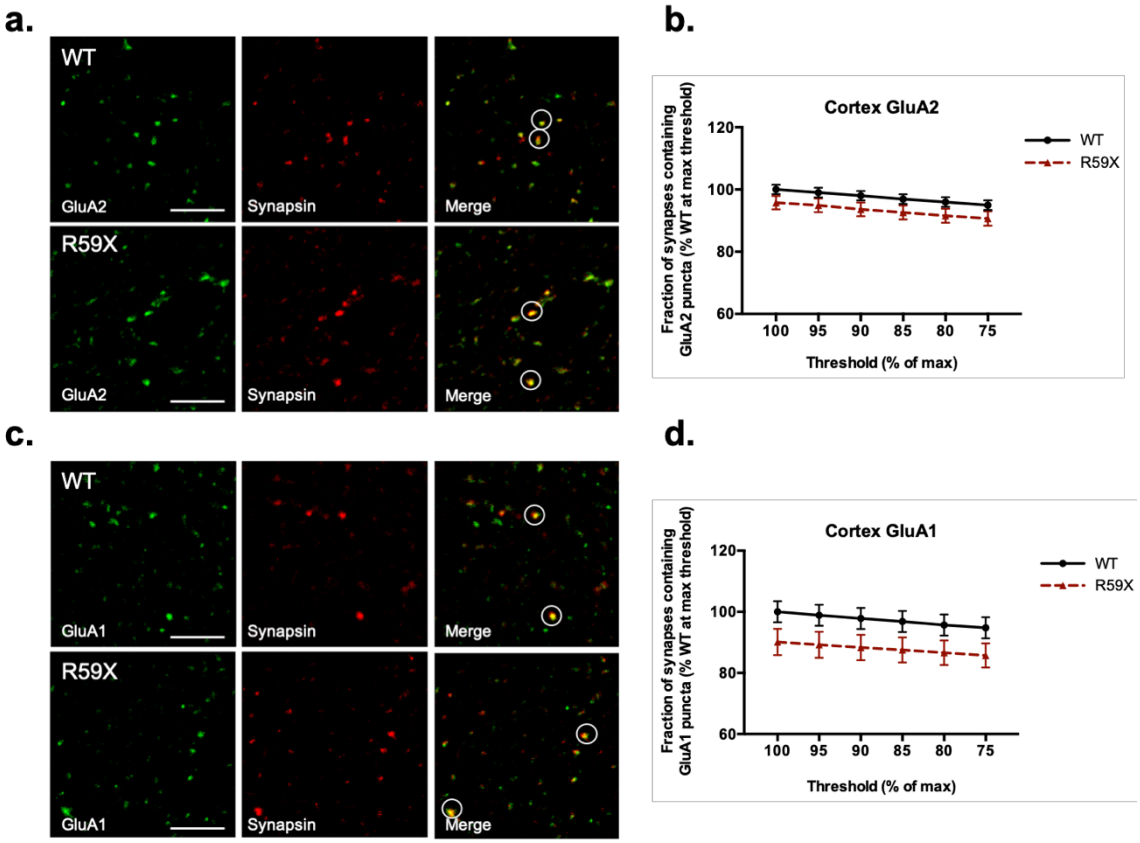

Figure 3-7: No change in fraction of synapses containing GluA2 or GluA1 in cortex layer II/III. a,b. Synaptic GluA2 is not significantly altered in layer II/III. Unpaired t test, p=0.12. **c,d.** Synaptic GluA1 is not significantly altered in II/III. Unpaired t test, p=0.10. Circles highlight colocalization and arrowheads mark synapsin without GluA2. N=10 fields from 5 mice for all groups.

Figure 3-8

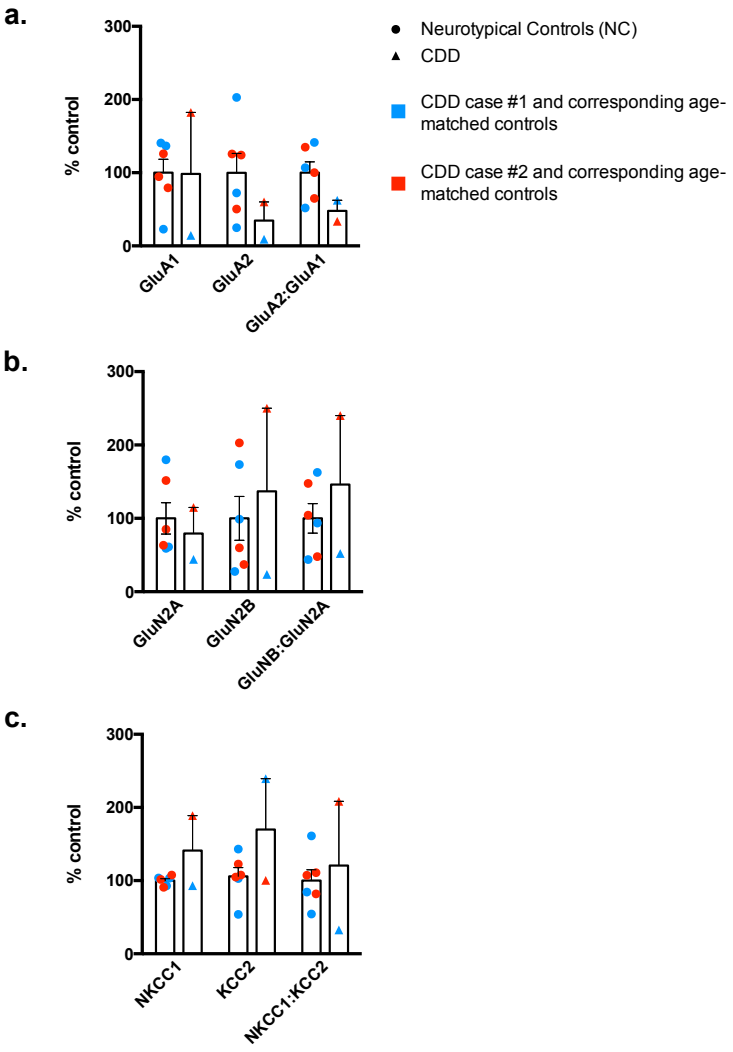

Figure 3-8. Western blot analysis in post-mortem hippocampal tissue from patients with CDD. a. Trend towards decreased GluA2 and GluA2:GluA1 in both post mortem disease cases. **b.** No observable trend in NMDAR subunits or subunit ratio. **c.** No observable trend in levels or ratio of chloride transporters.

Tables

Table 3-1

mRNA or protein	WT	R59X	n	P value
Gria1	1.00 ± 0.046	1.03 ± 0.069	8	0.788
Gria2	1.00 ± 0.054	1.07 ± 0.087	8	0.587
GluA1 (total)	100.000 ± 8.46	98.74 ± 8.48	8	0.918
GluA2 (total)	100.000 ± 9.22	97.27 ± 8.37	8	0.830
GluA2:GluA1	100.000 ± 2.13	99.13 ± 2.66	8	0.803
$GluA2^{S880}$/total	100.000 ± 3.41	98.49 ± 7.71	14	0.935
PICK1	100.000 ± 6.55	103.00 ± 6.73	8	0.754
RAB39B	100.000 ± 9.16	105.59 ± 9.75	8	0.685
CaMKII	100.0 ± 6.027	99.85 ± 5.607	13	0.985

Table 3-1: Normalized mRNA and protein levels of GluA1, GluA2 and associated trafficking proteins in whole cell hippocampal lysate. No significant changes were found in GluA1 or GluA2 mRNA levels (*Gria1* and *Gria2* respectively) in R59X mice. Whole cell levels of GluA1 and GluA2 and were also not altered in R59X hippocampus. We thus investigated levels of phosphorylated GluA2 at Ser880 ($GluA2^{S880}$), which sequesters GluA2 in intracellular pools, and several proteins involved in GluA2 trafficking: PICK1, RAB39B, and CaMKII. No significant alterations were found in $GluA2^{S880}$/total or the GluA2 trafficking proteins in R59X hippocampus.

Table 3-2

	CDD cases compared to age-matched neurotypical controls	
Protein	**Temporal**	**Hipp**
GluN2A	-	0
GluN2B	- -	0
GluN2B:2A	-	0
GluA1	- -	0
GluA2	- -	- -
GluA2:GluA1	-	- -
NKCC1	+	+
KCC2	-	+
NKCC1:KCC2	+	0
$GABA_A$ α1	0	0
$GABA_A$ α3	0	0
$GABA_A$ α3:α1	0	0

Table 3-2: Temporal and hippocampal tissue from two human CDD cases. Cases were aged 5 and 30, and were compared to three age-matched neurotypical controls each and probed for NMDAR receptor subunits GluN2A and GluN2B, AMPAR subunits GluA1 and GluA2, chloride channels NKCC1 and KCC2, and $GABA_A$ subunits α1 and α3. Trends are denoted with "+" or "-" to symbolize an increase or decrease respectively with larger magnitude of the increase or decrease represented by increasing number of symbols. Proteins with no discernible trend are marked with "0".

CHAPTER 4 – Functional analysis in hippocampal slices

Introduction

Our Western blot and immunohistochemical data suggests increased levels of membrane-associated GluA2-lacking AMPARs at hippocampal CA1 synapses in R59X mice, so we sought to verify whether the molecular changes are accompanied by functional alterations through extracellular and whole-cell patch clamp recordings in hippocampal slices.

Electrophysiology explores the electrical activity of living neurons, either in cell culture or brain slices, and is an excellent technique to understand neuronal circuitry and underlying mechanisms of plasticity such as long-term potentiation (LTP) and long-term depression (LTD). For extracellular recordings, field excitatory post synaptic potentials (fEPSPs) are generated from the activity of a group of neurons and recorded using a glass electrode placed directly onto the slice. Synaptic activity is evoked by delivering a pulse of current with a stimulating electrode placed a short distance away from the recording electrode. Extracellular recordings are useful for studying network dynamics and plasticity. For example, the input-output (I-O) curve is used to measure the basal network excitability of a slice and is obtained by simulating the slice with increasing current intensities and measuring the slope or amplitude of fEPSPs at each current. I-O function is then used to determine the intensity of current used for other paradigms such as the paired pulse ratio (PPR), LTP, and LTD. Typically, 50-60% of the current intensity that elicits the max response in the I-O curve is used. To determine PPR, a conventional measure of presynaptic function, pulses are delivered at various inter-stimulus intervals

(ISIs), ranging from 5 to 500 ms, and the ratio of the 2^{nd}:1^{st} fEPSP is plotted against the ISIs. Paired pulse facilitation is commonly observed, where the second fEPSP will be greater than the first due to a higher neurotransmitter release probability due to the Ca^{2+} accumulation in presynaptic terminals (Fioravante and Regehr, 2011). Thus, if there are variations in PPR it is attributed to altered presynaptic function. Extracellular recordings may also be used to probe activity-dependent forms of synaptic plasticity such as LTP and LTD by delivering patterned stimulation to the slice.

In whole-cell voltage patch-clamp recordings, current is recorded from an individual cell in the slice rather than fEPSPs from a collection of cells. A glass pipette filled with solution that mimics intracellular environment is used to break the membrane of a cell, which allows electrical access to the interior of the cell and changes in current are measured by holding the membrane at various voltages. Whole-cell patch clamp recordings allow for analysis of isolated AMPAR or NMDAR-mediated currents over different holding potentials by pharmacologically inhibiting one or the other, along with GABA receptors. The AMPAR-mediated current-voltage (*I-V*) plot is used to verify functional surface populations of GluA2-lacking AMPARs due to their characteristic inward rectification at high voltage potentials. GluA2-lacking AMPARs are subject to intracellular spermine block at high voltages resulting in decreased current to flow through the channel and inward rectification (Isaac et al., 2007), which can be blocked with GluA2-lacking specific blocker IEM-1460 (Buldakova et al., 2007).

Given that increased GluA2-lacking AMPARs are typically accompanied with electrophysiological alterations (Jia et al., 1996; Lippman-Bell et al., 2016), we

investigated whether decreased GluA2 in R59X mice results in functional alterations in I-O curve, PPR, LTD, and LTP at Schaffer collateral-CA1 synapses in the hippocampus. All electrophysiology experiments were performed by Rachel White, PhD with experimental design input by Madhu Yennawar and Frances Jensen.

Results

Extracellular recordings reveal normal I-O function, PPR, and LTD, but elevated LTP in R59X mice

Given the hippocampal-associated memory deficits and molecular changes in R59X mice, we aimed to determine whether R59X mice exhibit alterations in synaptic plasticity by performing extracellular field recordings in *ex vivo* hippocampal slices. We chose the P30 time point for electrophysiological experiments because it was the earliest time point that significant GluA2 deficits were observed in the Western blot. First, we observed no change in input-output (I-O) function (Fig. 4-1a) or PPR (Fig. 4-1b), suggesting that both basal synaptic function and presynaptic function are unaltered at Schaffer collateral-CA1 synapses. Next, we tested synaptic plasticity by evaluating LTD and LTP. LTD was induced using low-frequency stimulation (LFS) and found to be unaltered in R59X mice (Fig 4-1c). In the LTP paradigm, however, R59X mice responded significantly differently to high frequency stimulation (HFS) compared to controls (Fig 4-1d. Two-way ANOVA, main effect of genotype, $p<0.0001$); mutant mice displayed significantly elevated early-phase potentiation 15 min post-HFS (Unpaired t test, R59X: 188.7 ± 14.88, vs WT: 136.8 ± 9.911, $p=0.0125$) followed by a steeper decay slope (Linear regression, R59X: -1.192 ± 0.1071 vs WT: -0.1192 ± 0.08017 $p<0.0001$), resulting in R59X activity approximately reaching WT levels of potentiation by 60 min post-HFS.

Whole-cell patch clamp recordings show inward rectification of AMPAR-mediated currents

To more directly examine the functional consequence of GluA2 deficiency in R59X mice, we performed whole-cell patch clamp recordings in CA1 pyramidal neurons to observe whether the responses in the AMPAR *I-V* relationship in R59X mice showed inward rectification, a hallmark characteristic of an increased population of GluA2-lacking AMPARs (Kamboj et al., 1995; Washburn et al., 1997; Lippman-Bell et al., 2016). Cells were held at potentials from -80 to +40 mV and the observed current at each holding potential was recorded. R59X mice displayed significantly greater inward rectification in the *I-V* plot at +20 and +40 mV holding potentials (Fig. 4-2a. Two-way ANOVA, $F_{6,105}$=7.074, interaction p<0.000, Sidak's multiple comparison test: +20 mV, R59X: 0.176 $\pm$ 0.03 vs WT: 0.367 $\pm$ 0.029; +40 mV, R59X: 0.299 $\pm$ 0.025 vs WT: 0.614 $\pm$ 0.058) and a significantly greater rectification ratio (-60/+40 mV) of AMPAR-mediated EPSCs in slices from mutant mice compared to controls (Fig. 4-2b. Unpaired t test, R59X: 2.55 $\pm$ 0.194 vs WT: 1.46 $\pm$ 0.136). Input resistance was not altered between R59X mice and WT littermates (data not shown), suggesting that cell size does not vary significantly between genotypes. Taken together with the elevated early-phase LTP, these data demonstrate a physiologically relevant increase in hippocampal GluA2-lacking AMPARs in R59X mice.

Discussion

Our whole cell patch recordings reveal significant inward rectification of AMPAR currents in R59X mice at higher voltages, which is a hallmark characteristic of GluA2-lacking AMPARs due to their susceptibility to voltage-dependent spermine block (Isaac et al., 2007; Liu and Zukin, 2007). Inward rectification in the *I-V* plot supports our Western blot

results that suggest increased GluA2-lacking AMPARs in the hippocampus of R59X mice due to decreased ratio of GluA2:GluA1 subunits. Furthermore, the *I-V* data suggests that the increased population of GluA2-lacking AMPARs is functionally relevant in CA1 and thus may contribute to the altered plasticity observed in extracellular recordings.

Our extracellular recordings showed that mutant mice exhibit significantly elevated early-phase LTP at Schaffer collateral-CA1 synapses. Previous reports by others have shown impaired LTP, induced by theta-burst stimulation, in cortex layer II-III in CDKL5 KO mice (Della Sala et al., 2016). We did not investigate LTP in this region as our molecular and functional analyses focused on hippocampal alterations. However, is possible that loss of CDKL5 affects LTP differentially in the cortex and hippocampus due to variations in cell populations and circuit dynamics. Indeed, more recently in a different CDKL5 KO mouse, LTP induced by tetanic stimulation was observed to be significantly elevated in the hippocampus. Interestingly, in contrast to our results where elevated early-phase potentiation declined to WT levels 60 minutes post-HFS, elevated potentiation in CDKL5 KO mice was sustained throughout the 60 minutes post-tetanus. One reason for this may be that the induction paradigms between these results differs slightly; in our experiment LTP was induced by 4 trains of 100 Hz stimulation for 1 second, 20 seconds apart and in the CDKL5 KO mice LTP was induced with one 100 Hz burst for 1 second. Although these two stimulation paradigms have not been directly compared in the literature, it has been observed that different stimulation paradigms such as high frequency stimulation and theta burst stimulation can result in varied magnitudes of

potentiation as well as activation of distinct intracellular signaling pathways, contributing to differences in results (Hernandez et al., 2005; Larson and Munkácsy, 2015; Zhu et al., 2015). GluA2 KO mice also display elevated LTP that is sustained throughout the recording period (Jia et al., 1996), perhaps due to the even greater levels of GluA2-lacking AMPARs that are present in GluA2 KO mice compared to R59X mice.

Indeed, GluA2-lacking AMPARs are normally crucial for LTP induction and are inserted into the synaptic membrane immediately following HFS. They are gradually replaced by GluA2-containing AMPARs at the synapse during the consolidation phase of LTP (40-60 min post-HFS; Plant et al., 2006; Jaafari et al., 2012; Hanley, 2014). Thus, the elevated potentiated response in R59X mice 15 min-post HFS is likely a result of 1) elevated basal levels of GluA2-lacking AMPARs at the synapse and 2) additional insertion of GluA2-lacking AMPARs that normally occurs during the induction phase of LTP.

Data from our extracellular recordings in R59X hippocampal slices indicate that mutant mice have normal I-O function and PPR compared to slices from WT controls. Observing normal baseline network activity in mutant mice is not surprising, as at the whole animal level R59X mice did not exhibit visible spontaneous seizures and required provocation with pentylenetetrazol to demonstrate hyperexcitability. Furthermore, a recent study in CDKL5 KO mice also did not report altered I-O function in hippocampal slices (Okuda et al., 2017). Our PPR data showing normal presynaptic function in R59X hippocampus was also expected, as the majority of the literature describing cell culture and animal models of CDD indicate that loss of CDKL5 results in post-synaptic deficits such as decreased PSD-95 and spine and dendritic abnormalities (Zhu et al., 2013; Amendola

et al., 2014; Fuchs et al., 2014; Della Sala et al., 2016), although we ourselves have not yet investigated presynaptic proteins in R59X mice. Finally, a GluA2 KO mouse model also exhibited normal I-O function and PPR in the hippocampus (Jia et al., 1996), corroborating our results.

Finally, although GluA2 is important for LTD (Chater and Goda, 2014) we did not observe abnormal LTD in R59X mice, similar to other models with GluA2 deficits (Jia et al., 1996; Meng et al., 2003) suggesting that GluA2 may not be required for LTD in all cases. Additionally, PICK1-mediated AMPAR endocytosis is reported to be involved with LTD expression (Rocca et al., 2013), and PICK1 levels are not significantly altered in R59X hippocampus (see Chapter 3, Table 1), indicating that this step of LTD induction is likely normal in R59X mice.

Materials and Methods

Hippocampal slice preparation

P28-32 R59X and WT animals were decapitated and brains rapidly dissected from the skull and placed for section in ice-cooled cutting solution containing the following (in mM) 220 sucrose, 3 KCl, 1.25 NaH_2PO_4, 0.5 $CaCl_2$, 1 $MgCl_2$, 26.19 NaHCO3, and 10 D-glucose, pH 7.4, 295-305mOsm bubbled with 95%O_2/5%CO_2 at 4°C. Coronal hippocampal slices (350 μm thickness) were sectioned from the middle third of hippocampus with a vibratome (Leica VT1000S) in cutting solution. Slices were incubated for 30 min at 32 degrees C followed by at least 30 min at room temperature in oxygenated artificial cerebrospinal fluid (ACSF), containing the following (in mM): 130 NaCl, 3 KCl, 1.25 NaH_2PO_4, 1 $MgCl_2$, 2 $CaCl_2$, 26 $NaHO_2$, 10 D-glucose, pH 7.4, 295-305mOsm, bubbled with 95%O_2/5%CO_2.

Extracellular field recordings

Slices were transferred to the recording chamber with ACSF heated to 32 degrees C and Schaffer collaterals from CA3 to CA1 were stimulated at 30 sec intervals to obtain input-output curves. Stimulus intensity (0.1 msec in duration) that evoked 60-70% maximal slope response was used for paired pulse ratio and LTD and LTP induction. Paired-pulse stimuli were delivered at interstimulus intervals ranging from 5 to 500 ms, and the degree of paired-pulse inhibition or facilitation was calculated for each interval. For paired-pulse analysis, a ratio of the second response amplitude to that of the first was used. At a given interstimulus interval, a ratio >1 indicated paired-pulse facilitation and a ratio <1 indicated paired-pulse inhibition. Finally, baseline responses were

recorded every 30 s for 10–20 min. After a stable baseline of ≥10 min, either LTD or LTP was induced. LTP was induced by high frequency stimulation (4 stimuli at 100-Hz, 1-s duration, repeated 20 s apart) (Jensen et al., 1998). After tetanus, single half-maximal stimuli were applied every 30 s for 60 min in all slices. The percent change in fEPSP 10-90% slope was calculated after tetanus compared with pre-tetanus baseline. To induce LTD low-frequency (LFS) stimuli protocol consisted of 1800 shocks at 2Hz for 15mins (Lippman-Bell et al., 2016).

Whole-cell patch-clamp

Whole-cell patch-clamp recordings from hippocampal CA1 pyramidal neurons in brain slices using infrared- differential interference contrast microscope as described previously (Rakhade et al., 2008). The patch-pipette internal solution contained the following (in mM): 110 Cs-methanesulfonate, 10 TEA-Cl, 4 NaCl, 2 MgCl2, 10 EGTA, 10 HEPES, 4 ATP-Mg, and 0.3 GTP, pH 7.25, 5 QX-314, 7 phosphocreatine, creatine phosphokinase (17 unit/ml) and 0.1 spermine, 280-290mOsm. Filled electrodes had resistances of 2–5 MΩ. Evoked (e) EPSCs were elicited at 10 s intervals. Picrotoxin (100μM) or AP5 (50μM) were added to block GABA receptors or NMDA receptors respectively for the *I-V* recordings. To collect evoked AMPA receptor currents for *I-V* curves cells were held from -80mV to +40mV and evoked by stimulating the Schaffer collaterals. The data were obtained from the average max amplitude from 3-4 recordings per holding voltage (Vh). Data were collected using an Axopatch200B amplifier (Molecular Devices Inc., Union City, CA, USA) and Clampex 9.2 software (Molecular Devices Inc., Union City, CA, USA) with compensation for series resistance (70%) and

cell capacitance, filtered at 2 kHz, and digitized at 20 kHz using a Digidata 1320A analog to digital converter (Molecular Devices Inc., Union City, CA, USA).

Experimental design and statistical analysis

For electrophysiology, we chose sample sizes based on previously published results from our lab (Zhou et al., 2011; Lippman-Bell et al., 2016)

Stastical analysis was completed using GraphPad Prism. All datasets were analyzed using the D'Agostino–Pearson test for normality. Datasets with normal distributions were analyzed for significance using unpaired Student's two-tailed t test. Two-way repeated-measures ANOVA was conducted for the appropriate datasets with Holm–Sidak's multiple-comparison test. Linear regression analysis was used to determine decay slopes in the LTP experiments.

Figures

Figure 4-1

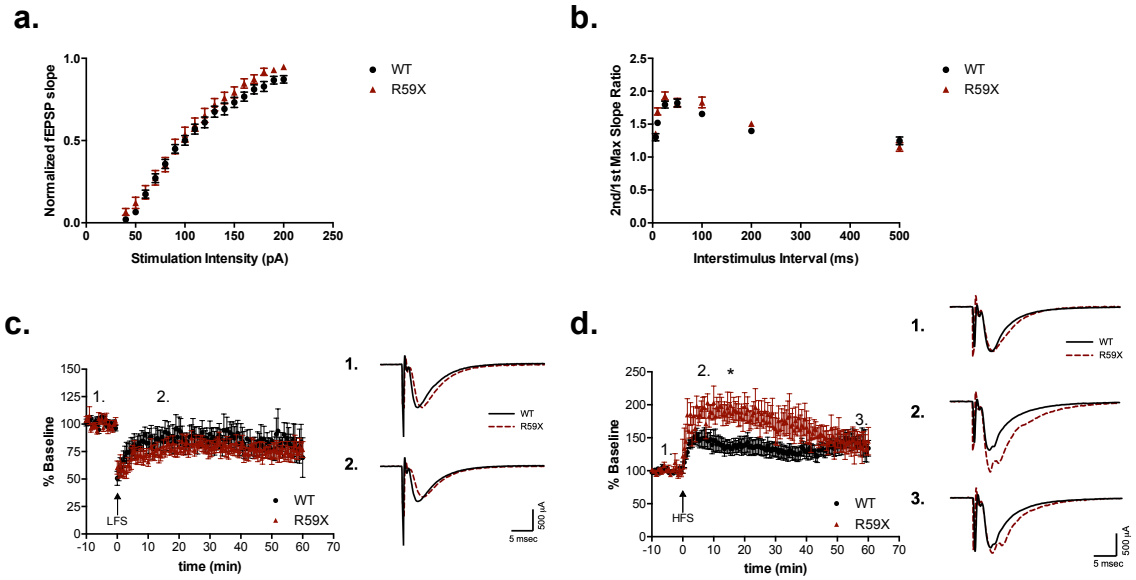

Figure 1. Extracellular recordings in R59X mice show no change in IO function, paired-pulse ratio, or LTD but elevated early-phase LTP. a. R59X mice have normal input-output function (N=16). **b.** Paired-pulse ratio, a conventional measure of presynaptic function, is not altered in R59X mice (N=22-27). **c.** LTD is normal in R59X mice (N=10). **d.** R59X display abnormal LTP. Two-way ANOVA, main effect of genotype, $p<0.0001$, with significantly elevated potentiation at 15 min post-HFS and steeper decay slope. Unpaired t test,* $p<0.05$, and linear regression, $p<0.0001$. N=6-7

Figure 4-2

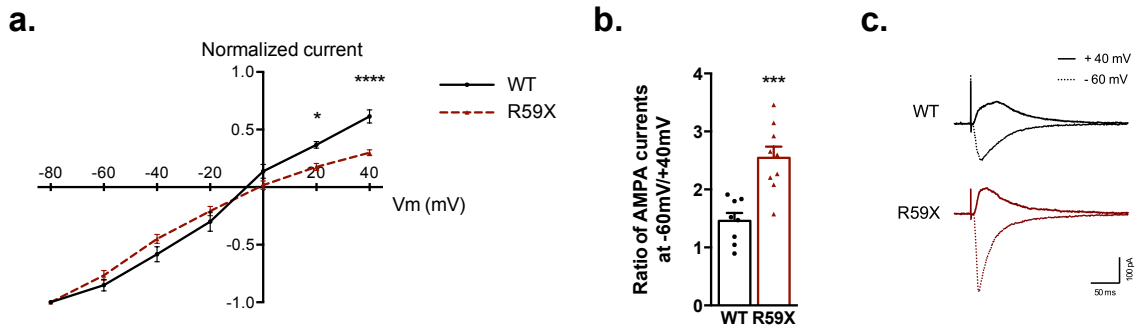

Figure 2. Whole-cell electrophysiology recordings verify increased population of GluA2-lacking AMPARs at CA1 synapses. a. CA1 pyramidal neurons in R59X mice exhibit significant inward rectification at +20 and +40 mV, characteristic of GluA2-lacking AMPARs. Two-way ANOVA with Sidak's multiple comparisons, interaction $p<0.0001$ **b.** Rectification ratio is significantly elevated in R59X mice. Unpaired t-test, $p<0.001$ **c.** Representative traces at -60 and +40 mV. N=8-9, *$p<0.05$, ***$p<0.001$, ****$p<0.0001$

CHAPTER 5 – Therapeutic effects of GluA2-lacking AMPAR blocker IEM-1460 in R59X mice

Introduction

There is currently no therapy to slow or halt disease progression in patients with CDD. Furthermore, seizures in CDD are largely refractory to traditional anti-epileptic drugs, although valproate and vigabatrin are typically administered for infantile spasms and levetiracetam and topiramate are often used in later stages of myoclonic and multifocal epilepsy (Bahi-Buisson and Bienvenu, 2012). These drugs are commonly used in infantile and pediatric patients with epilepsy, and are not targeted to CDD-specific protein dysregulation.

Because our molecular and functional analysis identified increased GluA2-lacking AMPARs in the hippocampus in R59X mice, we decided to test whether specifically blocking this receptor subtype with GluA2-lacking AMPAR blocker IEM-1460 (Samoilova et al., 1999) would have therapeutic effects on behavioral deficits and lowered seizure threshold in mutant mice. IEM-1460 has been observed to exert anti-epileptic effects in rats but has not been tested in behavioral assays evaluating social behavior or learning and memory. However, we have previously showed that blocking AMPARs immediately post-seizure in a rat model of early-life epilepsy prevented development of later-life social deficits and epileptogenesis (Lippman-Bell et al., 2013), suggesting that blocking AMPARs may be therapeutic in mouse models of autism and hyperexcitability. AMPAR blockers are not currently used to treat patients with CDD.

Few studies have evaluated therapeutic intervention on behavioral phenotypes in mouse models of CDD. Chronic administration of two GSK3β inhibitors, SB216763 and FDA-approved Tideglusib, exhibits efficacy in rescuing working and spatial memory deficits respectively in CDKL5 KO mice (Fuchs et al., 2015, 2018). Another group found that ifenprodil reduced NMDA-induced seizure severity in CDKL5 KO mice (Okuda et al., 2017) but did not evaluate the effects on ifenprodil on behavioral deficits in their model.

We show that acute treatment of IEM-1460 results in significant therapeutic effects on social behavior, short-term memory, and hyperexcitability in R59X mice. These results suggest that increased GluA2-lacking AMPARs found in R59X hippocampus could be contributing to altered behavioral phenotypes in R59X mice. Furthermore, the data suggest that blocking GluA2-lacking AMPARs may be a novel therapeutic strategy in CDD not only for hyperexcitability, but for impairments in behavior and social interaction as well.

Results

IEM-1460 rescues social behavior deficits and working memory in R59X mice

Because GluA2-lacking AMPARs are implicated in autism and intellectual disability (Isaac et al., 2007; Mignogna et al., 2015; Lippman-Bell et al., 2016), we sought to determine if specifically blocking GluA2-lacking AMPARs attenuates behavioral deficits and memory in R59X mice. Mutant mice and WT littermates were treated with GluA2-lacking AMPAR-specific blocker IEM-1460 (10 mg/kg, i.p.) one hour before behavioral tests (Magazanik et al., 1997; Szczurowska and Mareš, 2015). IEM-1460 caused both WT and R59X animals to be mildly hypoactive during the first 8 minutes of the open field

test (data not shown, Two-way ANOVA with Sidak's multiple comparisons, $F_{27, 310}$ = 3.441, interaction p<0.0001). However, by minutes 9 and 10 there were no significant differences in number of beam breaks between treatment groups. In the social choice assay, drug treatment rescued R59X duration of time sniffing to saline treated WT levels (Fig. 5-1a, Two-way ANOVA $F_{3,76}$= 8.947, interaction p<0.0001), while also increasing the time spent directly interacting with the novel mouse (Fig. 5-1b, One-way ANOVA, $F_{3,38}$ = 10.71, p<0.0001). In the Y maze, IEM-1460 rescued % SAB in R59X mice to WT levels (Fig. 5-1d. One-way ANOVA, $F_{3,33}$=14.06, interaction p<0.0001) suggesting that blocking GluA2-lacking AMPARs acutely has therapeutic effects on short-term working memory deficits. There were no significant differences between number of arm entries between groups. While IEM-1460 slightly improved context-dependent fear memory mutant mice, the effect was not significant enough to rescue it to WT-saline levels (Fig. 5-1e. Two-way ANOVA, $F_{6,129}$=2.819, interaction p=0.013). Although we did not observe a significant improvement in long-term fear memory in this study, it is possible that the effects of IEM-1460 on long-term memory will be more pronounced with a chronic treatment paradigm.

IEM-1460 rescues latency to behavioral seizures after PTZ administration in R59X mice

Finally, IEM-1460 rescued latency to seizure in mutant mice to WT saline levels, indicating that targeting GluA2-lacking AMPARs in CDD may attenuate hyperexcitability in the brain (Fig. 5-1f. One-way ANOVA, $F_{3,36}$=4.621, p=0.0078). These data provide evidence to support the role of elevated GluA2-lacking AMPARs underlying deficits in memory, social behavior, and hyperexcitability in R59X mice.

Discussion

Our treatment results indicate that the R59X model exhibits robust behavioral readouts in response to drug administration and could be used for future studies evaluating various treatment paradigms for CDD. Furthermore, they provide evidence for the therapeutic potential of both IEM-1460 and CBD in attenuating social and memory deficits as well as hyperexcitability in CDD.

IEM-1460 significantly increased social interaction and attenuated working memory deficits and lowered seizure threshold in R59X mice. We have previously shown that administration of AMPAR blocker NBQX immediately following early-life seizures decreases development of social interaction deficits in rats. Although disturbances in GluA2 levels have been observed in autism and intellectual disability (Mignogna et al., 2015; Achuta et al., 2018), this is the first time that a GluA2-lacking AMPAR-specific blocker has shown efficacy for deficits in social behavior and short-term memory. IEM-1460 was not as effective in rescuing long-term contextual fear memory deficits in R59X mice—it increased % time freezing enough to be not significantly different than the WT vehicle treated mice but not significantly more than the R59X vehicle group. This suggests that perhaps a more chronic treatment paradigm with IEM-1460 would be effective in rescuing long-term memory deficits.

Finally, IEM-1460 rescued latency to seizure in R59X mice to WT vehicle levels. To date no clinical trials have been conducted specifically with GluA2-lacking AMPAR blockers in patients with epilepsy, although perampanel, a general non-competitive AMPAR blocker,

has been approved to treat patients with epilepsy older than 12 years of age. IEM-1460 is not currently an FDA approved drug, but has previously shown efficacy for reducing seizure severity in rodents (Gmiro et al., 2008; Szczurowska and Mareš, 2015). Our data adds to the sizeable literature reporting GluA2-lacking AMPAR dysregulation in autism (Lippman-Bell et al., 2013), intellectual disability (Mignogna et al. 2015; Achuta et al., 2018), and epilepsy (Grooms et al., 2000; Lippman-Bell et al., 2016), and supports development of GluA2-lacking AMPAR specific blockers for clinical trials.

Materials and Methods

Effect of IEM-1460 on memory and social interaction

12-16 week old mice were administered 10 mg/kg IEM-1460 (Tocris Biosciences) in 0.9% saline or vehicle. Mice were tested 1 hour later for each behavioral test.

Effect of IEM-1460 on seizure threshold

18 week-old mice were administered 10 mg/kg IEM-1460 or vehicle followed one hour later by 40 mg/kg PTZ. Mice were placed in Plexiglass grid for video-monitoring. Videos were scored by blinded observer using a modified Racine scale as before (Lüttjohann et al., 2009).

Experimental design and statistical analysis

For behavioral tests, the number of mice used in each experiment was predetermined before the start of the experiment and based on prior behavioral work in CDKL5 KO mice (Wang et al., 2012).

Stastical analysis was completed using GraphPad Prism. All datasets were analyzed using the D'Agostino–Pearson test for normality. Datasets with normal distributions were analyzed for significance using unpaired Student's two-tailed t test. One-way ANOVA and Two-way repeated-measures ANOVA were conducted for the appropriate datasets with Holm–Sidak's multiple-comparison test.

Figures

Figure 5-1

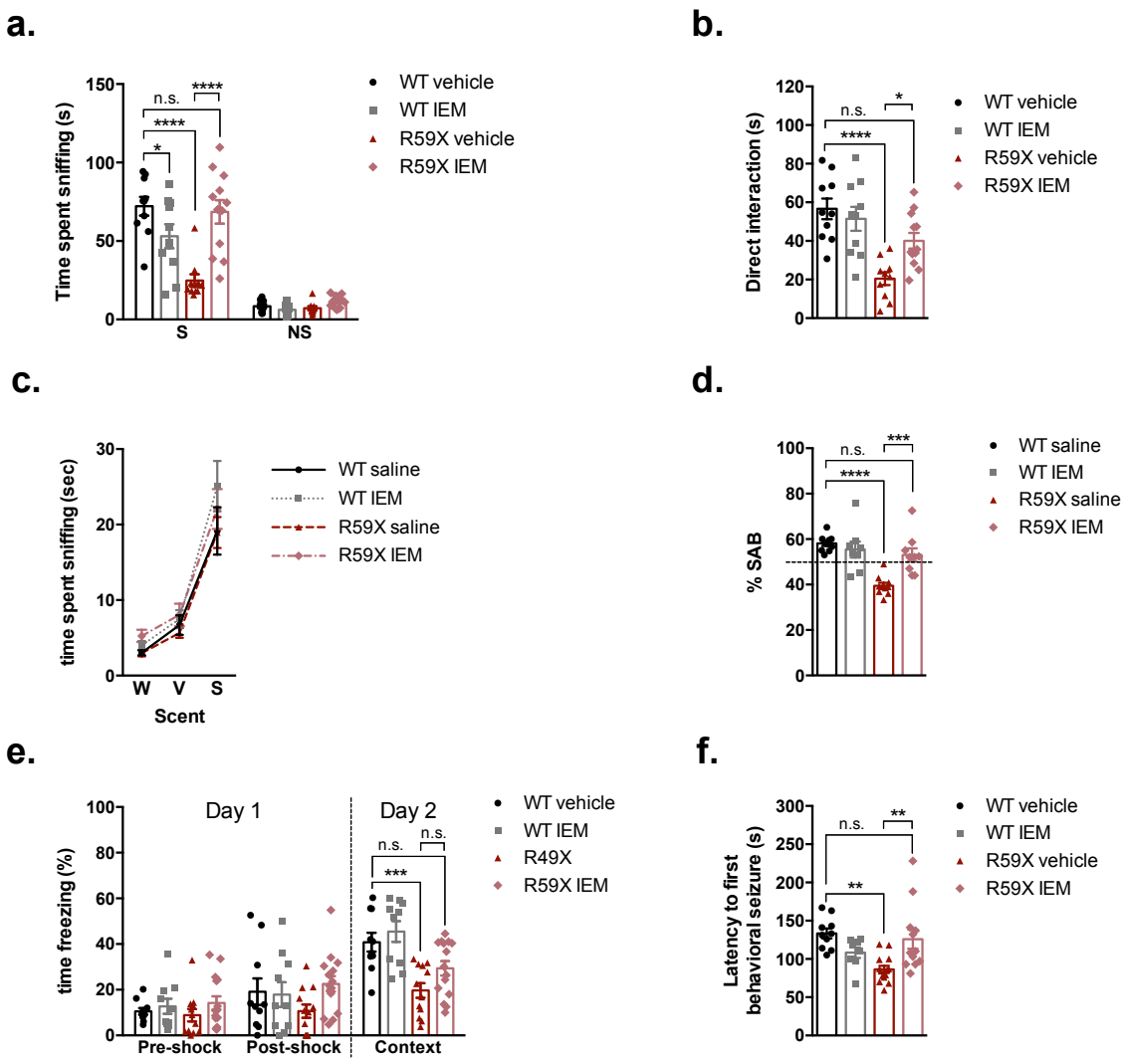

Figure 5-1. Effect of GluA2-lacking AMPAR-specific blocker IEM-1460 on behavioral deficits in R59X mice. a, b. IEM-1460 rescues social behavior deficits in

CDKL5 R59X mice and increases direct interaction time. Two-way ANOVA with Sidak's multiple comparisons test, interaction, $p<0.0001$ and ordinary one-way ANOVA with Sidak's multiple comparisons test c. Olfactory function is not altered in CDKL5 R59X mice treated with IEM-1460. Two-way ANOVA, $p=0.806$ d. IEM-1460 rescues % SAB in CDKL5 R59X mice to WT levels. Ordinary one-way ANOVA with Sidak's multiple comparisons test, $p<0.0001$ e. Drug treatment partially attenuates deficits in long-term fear memory. Two-way ANOVA with Sidak's multiple comparisons test, interaction, $p=0.013$ f. Latency to first behavioral seizure after PTZ injection is rescued with pretreatment of IEM-1460. Ordinary one-way ANOVA, with Sidak's multiple comparison's test, $p=0.0078$. N=8-14 for all groups. *$p<0.05$, **$p<0.01$, ***$p<0.001$, ****$p<0.0001$.

CHAPTER 6 – Therapeutic effects of cannabidiol in R59X mice

Introduction

Several patient groups for treatment-resistant early-life epilepsies have begun to treat pediatric patients with the natural compound cannabidiol (CBD), the major non-psychoactive component of marijuana. Recently, this resulted in the first randomized, double-blind clinical trials showing efficacy in reducing seizures in several patient groups including those with Dravet Syndrome, Lennox-Gastaut Syndrome, and CDD (Devinsky et al., 2018a, 2018b; Thiele et al., 2018). Beyond seizures, CBD has been reported to improve quality of life scores, which encompass improvements in sociability, memory, cognition, and other behavior (Rosenberg et al., 2017).

The mechanism of action of cannabidiol in the brain is poorly understood. It has antagonist activity at G-protein coupled receptor 55 (GPR55) (Ryberg et al., 2007), which is predicted to mediate some of the anti-excitatory effects of CBD (Kaplan et al., 2017; Gaston and Szaflarski, 2018).

We hypothesized that CBD would have significant therapeutic effects in R59X mice similar to the human patients in CDD patients. Secondly, we predicted that GPR55 would be upregulated in R59X mice given the difference in regulation of GluA2 in R59X mice. We also show that acute treatment of CBD results in significant therapeutic effects on social interaction, short-term memory, long-term memory and hyperexcitability in R59X mice. These intriguing findings suggest that CBD may be beneficial in improving patient quality of life not only because of its effects on hyperexcitability, but on other behaviors that affect patients' day to day lives.

Results

CBD attenuates memory and hyperexcitability deficits in R59X mice

Given that CBD is currently being used to treat patients of CDD and other early-life epilepsy disorders (Devinsky et al., 2018a, 2018b; Thiele et al., 2018), we sought to examine whether CBD has therapeutic effects on behavior and seizure threshold in R59X mice. Dosing for behavioral tests was based on experiments performed in Dravet mice, which showed that the optimal dose in the social choice assay was 20 mg/kg and the optimal dose for reducing seizure severity was 100 mg/kg (Kaplan et al., 2017). Thus, we chose to use 20 mg/kg for all behavioral tests except for the seizure threshold assay where we administered 100 mg/kg. In the social choice assay, R59X mice treated with CBD spent significantly more time sniffing and investigating the novel mouse than vehicle-treated mutant mice, but it was still significantly less time compared to the WT vehicle group (Fig 6-1a., Two-way ANOVA, $F_{3, 66}$= 14.04, interaction p<0.0001; R59X CBD vs R59X vehicle, p<0.01; R59X CBD vs WT vehicle, p<0.0001). There was no difference in direct interaction time between R59X CBD and R59X vehicle groups (Fig 6-1b., One-way ANOVA with Sidak's multiple comparisons, $F_{3, 31}$= 17.51, p<0.0001; R59X CBD vs R59X vehicle, p=0.684). Interestingly, CBD significantly decreased the amount of time WT mice spent investigating the novel mouse in the cylinder (Fig 6-1a., WT CBD vs WT vehicle, p<0.01) as well as when the mouse was freely moving during the direct interaction portion (Fig 6-1b., WT CBD vs WT vehicle, p<0.05). Olfactory function was not altered between treatment groups (Fig 6-2c., Two-way ANOVA, interaction p=0.891). In the Y maze assay, CBD significantly improved % SAB in both WT and R59X mice (Fig. 6-2d. One-way ANOVA with Sidak's multiple comparisons, $F_{3, 33}$= 33.39, p<0.0001;

WT CBD vs WT vehicle, p<0.05; R59X CBD vs R59X vehicle, p<0.0001; R59X CBD vs WT vehicle, p=0.580), suggesting that it improves short-term working memory. Interestingly, in the context-dependent fear conditioning paradigm, CBD significantly improved fear memory on Day 2 only in R59X mice (Fig. 6-2e. Two-way ANOVA with Sidak's multiple comparisons, $F_{3, 102}$ = 4.738, main effect of treatment group, p=0.0039; R59X CBD vs R59X vehicle, p<0.05), providing evidence that CBD may have beneficial effects on both short and long-term memory in CDD. Finally, latency to seizure in R59X mice treated with CBD was rescued to WT vehicle levels (Fig. 6-2f. One-way ANOVA with Sidak's multiple comparisons, $F_{3, 33}$ = 8.998, p=0.0002; R59X CBD vs R59X vehicle, p<0.001) suggesting that CBD may also have therapeutic effects on hyperexcitability in CDD.

Expression of GPR55, a target of CBD, is not altered in R59X mice or in CDD patient samples

CBD is reported to act as an antagonist at GPR55 (Ryberg et al., 2007), a G-protein coupled receptor that regulates intracellular calcium and neurotransmitter release (Sylantyev et al., 2013). Given the significant therapeutic effects of CBD in R59X mice, we investigated whether expression of GPR55 is increased in R59X and CDD patient samples. Expression of GPR55 is not significantly altered in cortex or hippocampus of R59X at any developmental time point or in CDD patient samples (Figure 6-2a-c). However, expression of GPR55 is regulated over development in the cortex and hippocampus of neurotypical controls, peaking in expression at approximately 10 years of age in the cortex and approximately 35 years of age in the hippocampus (Figure 6-2d).

Discussion

CBD significantly rescued latency to seizure in R59X mice to WT vehicle levels. Recently, preclinical and clinical studies have consistently reported therapeutic effects of CBD for seizures in treatment-resistant early life epilepsy (Kaplan et al., 2017; Devinsky et al., 2018a, 2018b; Thiele et al., 2018). Furthermore, one trial reported significantly decreased seizure events in patients with CDD (Devinsky et al., 2018). Patients stayed on previously prescribed anti-epileptic drugs during this trial, so some of the effects may be due to drug-drug interactions. Further preclinical studies are necessary to determine beneficial and adverse drug interactions with CBD, as well as optimal dosing strategies.

Therapeutic effects of CBD in R59X mice extended beyond the lowered seizure threshold to deficits in memory and social interaction. CBD significantly improved social interaction in R59X mice, but not enough to rescue the deficit to WT vehicle levels. It also improved hippocampal-dependent short and long-term memory deficits in R59X mice. Children with autism treated with CBD were reported to have improved communication and behavior, which has led to several clinical and preclinical studies (Poleg et al., 2018). Indeed, CBD has previously shown efficacy for social deficits in a mouse model of Dravet syndrome (Kaplan et al., 2017). Furthermore, in a transgenic mouse model of Alzheimer's Disease, CBD prevented development of social recognition memory deficits (Cheng et al., 2014). Finally, parent-reported observations on quality of life after CBD treatment in their children suggest that CBD may improve quality of life measures such as energy and fatigue, social interaction, memory, cognitive functions, and other behavior (Rosenberg et al., 2017). Our data showing social and memory

improvements in R59X mice provides additional evidence that CBD may be a successful therapeutic in cases of autism and intellectual disability.

Expression of GPR55, a target of CBD, was not elevated in R59X tissue or CDD patient samples but it still may mediate therapeutic effects of CBD in CDD. CBD has been shown to increase inhibitory neurotransmission through antagonism of GPR55, and antagonists of GPR55 mimicked and occluded these effects of CBD on inhibitory neurotransmission *in vitro* (Kaplan et al., 2017). However, CBD has also been observed to have activity at several other proteins involved in neuronal excitability, including TRPV1 (Bisogno et al., 2001), T-type Ca^{2+} channels (Ross et al., 2008), and mutant sodium channels (Patel et al., 2016). Additionally, CBD is reported to modulate adenosine receptors, voltage-dependent anion selective channel protein (VDAC1), and release of tumor necrosis factor alpha (TNFα) (Devinsky et al., 2014). Given the number of purported targets of CBD and potential indirect effects on the endocannabinoid system itself via TRPV1 (Marzo and Petrocellis, 2012), it is difficult to speculate the exact mechanism by which CBD exerts therapeutic effects on seizures, memory, and social behavior in R59X mice. Furthermore, the relationship between CBD and GluA2-lacking AMPARs has not been investigated and would be interesting to pursue.

Materials and Methods

Effect of CBD on memory and social interaction

12-16 week old mice were administered 20 mg/kg cannabidiol (Tocris) in 1:1:18 ethanol:cremophore:saline or vehicle. Mice were tested 1 hour later for each behavioral test.

Effect of CBD on seizure threshold

18 week-old mice were administered 100 mg/kg cannabidiol (Tocris) in 1:1:18 ethanol:cremophore:saline or vehicle followed one hour later by 40 mg/kg PTZ. Mice were placed in Plexiglass grid for video-monitoring. Videos were scored by blinded observer using a modified Racine scale as before (Lüttjohann et al., 2009).

Experimental design and statistical analysis

For behavioral tests, the number of mice used in each experiment was predetermined before the start of the experiment and based on prior behavioral work in CDKL5 KO mice (Wang et al., 2012).

Stastical analysis was completed using GraphPad Prism. All datasets were analyzed using the D'Agostino–Pearson test for normality. Datasets with normal distributions were analyzed for significance using unpaired Student's two-tailed t test. One-way ANOVA and Two-way repeated-measures ANOVA were conducted for the appropriate datasets with Holm–Sidak's multiple-comparison test.

Figures

Figure 6-1

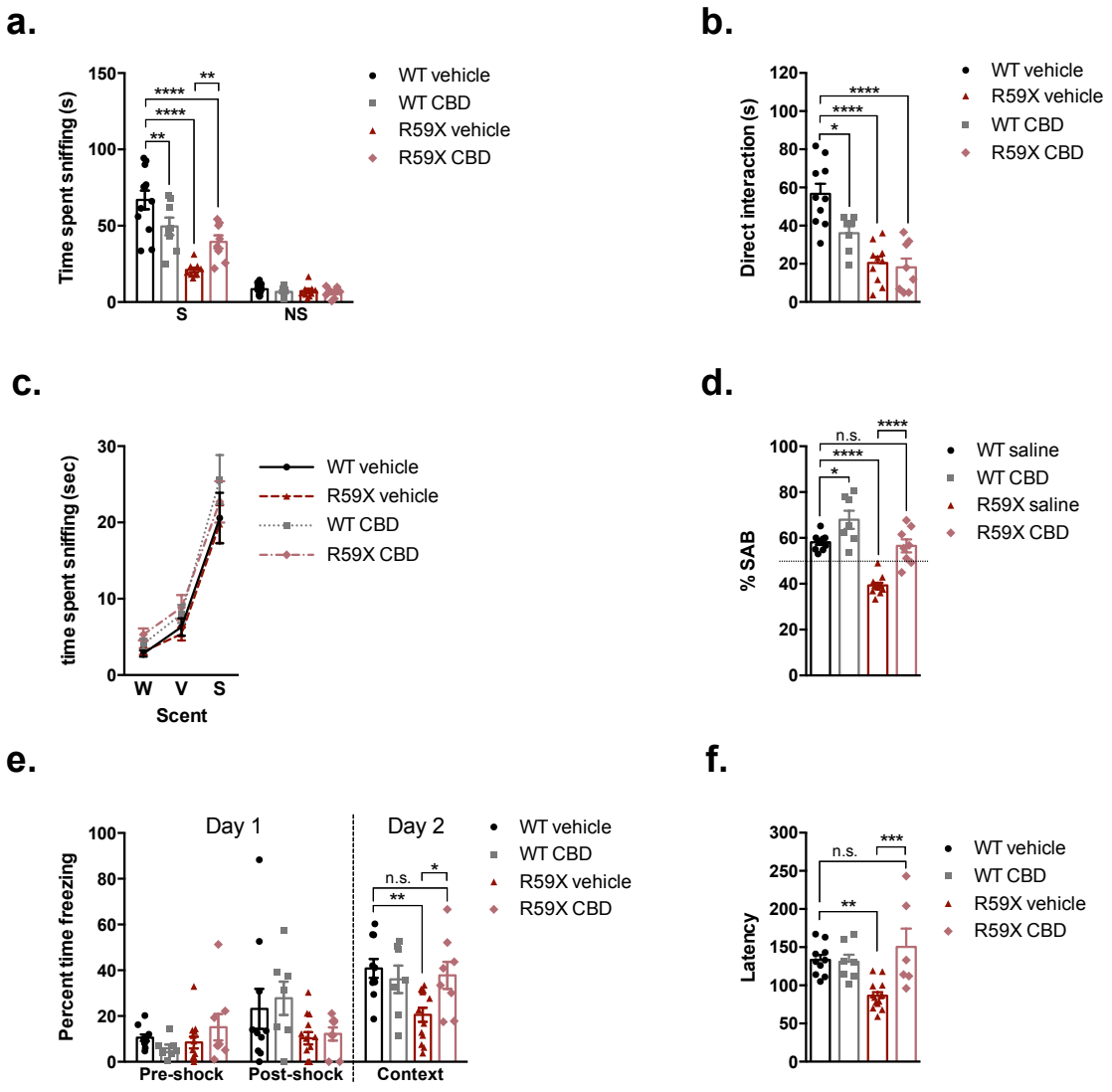

Figure 6-1. Effect of experimental therapeutic CBD on behavioral deficits in R59X mice. a. R59X mice treated with CBD (20 mg/kg) display significantly more time interacting with the novel mouse than vehicle-treated R59X group, but are still

significantly less social than the WT vehicle group. Two-way ANOVA with Sidak's multiple comparisons test, interaction, $p<0.0001$ **b.** CBD (20 mg/kg) does not rescue deficits in direct interaction in R59X mice, and significantly reduces the time WT mice spend interacting with novel mice. Ordinary one-way ANOVA with Sidak's multiple comparisons test, $p<0.0001$ **c.** Olfactory function is not altered in R59X mice treated with CBD (20 mg/kg). Two-way ANOVA, $p=0.891$ **d.** CBD (20 mg/kg) increases % SAB in R59X mice to WT vehicle levels and significantly increases % SAB in WT mice. Ordinary one-way ANOVA with Sidak's multiple comparisons test, $p<0.0001$ **e.** Acute CBD treatment (20 mg/kg) one hour before training and testing rescues deficits in long-term fear memory. Two-way ANOVA with Sidak's multiple comparisons test, main effect of treatment group, $p=0.0039$ **f.** CBD (100 mg/kg) rescues latency to first behavioral seizure after PTZ injection in R59X mice. Ordinary one-way ANOVA, with Sidak's multiple comparison's test, $p=0.0002$. N=6-14 for all groups. *$p<0.05$, **$p<0.01$, ***$p<0.001$, ****$p<0.0001$.

Figure 6-2

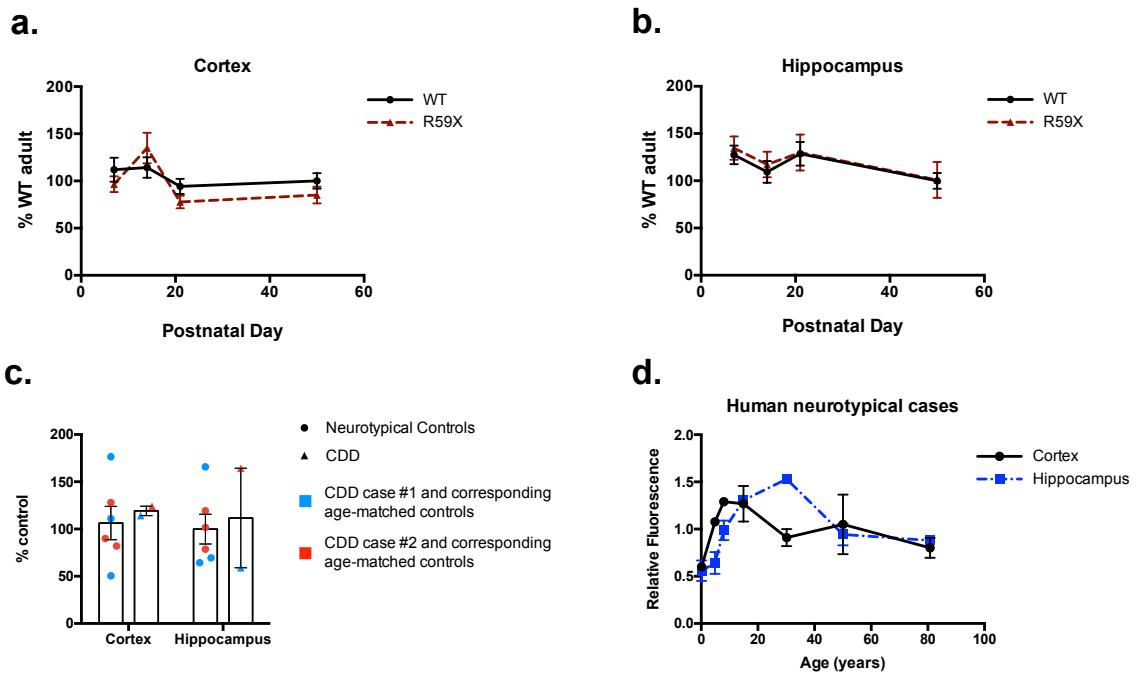

Figure 6-2: Developmental expression of GPR55 in R59X and WT mice and human CDD and neurotypical cases. a. Expression of GPR55 is not significantly altered in R59X cortex at P7, P14, P21, or P50. N=6-10 for each time point. **b.** Expression of GPR55 is not significantly different in R59X hippocampus at P7, P14, P21, or P50. N=10 for each time point. **c.** Expression of GPR55 does not appear to be dramatically altered in two CDD cases compared to age-matched neurotypical controls. N=2-3. **d.** Expression of GPR55 increases over human development and peaks at approximately 10 years of age in the cortex and approximately 35 years of age in the hippocampus. N=2 per age.

CHAPTER 7 – Discussion

Autism, intellectual disability, and seizures are key features of CDD and frequently co-occur in neurodevelopmental disorders, suggesting common disease mechanisms of dysregulated synaptic structure and function (Eichler and Meier, 2008; Zoghbi and Bear, 2012). There is currently no therapy that targets the core symptoms of CDD, which drove us to ask whether there are targetable synaptic alterations in the novel R59X mouse model of CDD that may contribute to disease pathogenesis. Here we found a specific dysregulation of membrane-bound GluA2-lacking AMPARs in R59X mice, and that targeting the activity of these receptors using IEM-1460, a specific antagonist of GluA2-lacking AMPARs, was effective in rescuing several core CDD phenotypes.

Our results elucidate a critical molecular mechanism underlying hippocampal-associated learning and memory impairment and lowered seizure threshold in R59X mice. Mutant mice exhibit hyperactivity, impaired motor function and autistic-like deficits in social interaction, as well as impaired hippocampal-dependent learning and memory and lowered seizure threshold. In our molecular and functional analyses, we found evidence of increased synaptic GluA2-lacking AMPARs in the R59X hippocampus that was accompanied by elevated early-phase LTP. Finally, working memory and seizure threshold were rescued in the R59X mice by acute administration of a GluA2-lacking AMPAR open channel blocker, IEM1460. Together, these data reveal a GluA2-lacking AMPAR-specific mechanism of neurobehavioral deficits in R59X mice and may represent a potential therapeutic strategy for CDD.

NMDAR and AMPAR subunits are tightly regulated to mediate synaptic excitability and plasticity during critical periods of neuronal network formation in the brain. In particular, regulation of AMPAR subunit ratio GluA2:GluA1 determines levels of GluA2-lacking AMPARs at the synapse and resulting Ca^{2+} influx (Jonas and Neuron, 1995), which has long-lasting effects on synaptic plasticity, neuronal growth, and gene transcription (Anggono and Huganir, 2012; Chater and Goda, 2014). During normal brain development, GluA2-lacking AMPARs are present postnatally during the critical period but decrease by adulthood. In contrast, the R59X mice exhibited unexpected persistence of GluA2-lacking AMPARs from P50 onwards. GluA2-lacking AMPAR dysregulation has been implicated in numerous disorders of E-I imbalance and autism (Lippman-Bell et al., 2013; Mignogna et al., 2015; Achuta et al., 2018), and indeed the GluA2 deficits in R59X mice were accompanied by neurobehavioral deficits, elevated LTP, and seizure susceptibility. Furthermore, decreased GluA2:GluA1 was observed in two human cases of CDD, highlighting the potential clinical validity of Western blot results.

Our whole cell patch clamp recordings levels expand upon our Western blot data and indicate that there is a physiologically relevant, increased population of GluA2-lacking AMPARs at hippocampal synapses. Inward rectification in the *I-V* plot, as observed in the R59X mice, is a hallmark characteristic of increased GluA2-lacking AMPARs due to their susceptibility to intracellular spermine block at high voltages (Rozov et al., 2012). GluA2-lacking AMPARs are also Ca^{2+}-permeable (CP), unlike GluA2-containing AMPARs (Geiger et al., 1995), and elevated GluA2-lacking CP-AMPARs may cause hyperexcitability through elevated Ca^{2+} influx as well as increased NMDAR activation.

Additionally, increased Ca^{2+} influx through dysregulated GluA2-lacking AMPARs likely underlies enhanced early-phase LTP in R59X mice observed in our extracellular electrophysiology recordings.

GluA2-lacking AMPARs are normally crucial for LTP induction and are inserted into the synaptic membrane immediately following HFS. Upon Ca^{2+} influx through GluA2-lacking AMPARs, GluA2 is released from intracellular stores by PICK1 and translocates to the synaptic membrane to form GluA2-containing AMPARs, which gradually replace GluA2-lacking AMPARs at the synapse during the consolidation phase of LTP (40-60 min post-HFS) (Plant et al., 2006; Jaafari et al., 2012; Hanley, 2014). The elevated potentiated response in R59X mice 15 min-post HFS is likely a result of increased Ca^{2+} influx due to 1) elevated basal levels of GluA2-lacking CP-AMPARs at the synapse and 2) additional insertion of GluA2-lacking AMPARs that normally occurs during the induction phase of LTP.

Furthermore, given that our earlier data suggests impaired transport of GluA2 to the membrane in R59X mice, it is possible that GluA2-containing AMPARs are hindered from being inserted into the membrane during the late-phase of LTP, causing the observed decay in the response. Our data from extracellular field recordings align with studies performed in hippocampal slices from GluA2 knock-out mice, showing that mice lacking the GluA2 subunit exhibited normal input-output function, PPR, and LTD along with elevated LTP (Jia et al., 1996)

The behavioral effects observed in the R59X mice are similar to the CDKL5 KO mouse model that also exhibited hyperexcitability, deficits in motor coordination and social interaction, and impaired working and long-term memory (Wang et al., 2012). Furthermore hippocampal-dependent learning and memory impairments were observed in conditional knock-out mice where CDKL5 was selectively knocked out of forebrain excitatory neurons, emphasizing the importance of normal function of CDKL5 in excitatory hippocampal neurons (Tang et al., 2017). Our observed increase in GluA2-lacking AMPARs at hippocampal synapses combined with the functional and plasticity alterations at hippocampal synapses in R59X mice suggest an underlying mechanism for altered behavior at the whole animal level. Indeed, changes in GluA2 subunit levels and signaling have previously been linked to social interaction deficits (Lippman-Bell et al., 2013) and learning and memory impairments (Wang et al., 2018; Zhou et al., 2018). Additionally, our lab has observed increased phosphorylation of calcium calmodulin-dependent protein kinase II (CaMKII) at Thr286 and downstream genome-wide transcription factor methyl CPG binding protein 2 (MeCP2) at Ser421 as a result of Ca^{2+} influx through GluA2-lacking AMPARs (Rosenberg et al., 2018). Although there is no change in total MeCP2 protein levels in mouse models of CDD (Amendola et al., 2014), elevated phosphorylation of CaMKII and MeCP2 may be a downstream signaling mechanism by which increased GluA2-lacking AMPARs result in behavioral deficits and hyperexcitability observed in R59X mice. Indeed, CaMKII has been implicated in fear conditioning and spatial memory (Wang et al., 2017) and increased CaMKII Thr286 phosphorylation has been observed to cause seizures and ID in humans (Akita et al., 2018). Furthermore, mutations in MeCP2 are known to cause autism and Rett syndrome

(Amir et al., 1999) and MeCP2 Ser421 phosphorylation controls ability of MeCP2 to regulate dendritic growth and spine maturation (Zhou et al., 2006). In R59X mice, these effector molecules may be causing chronic alterations in plasticity, excitability, and gene transcription due to increased Ca^{2+} influx through GluA2-lacking AMPARs. In future experiments, we aim to investigate alterations in gene expression and signaling pathways that may be downstream of elevated GluA2-lacking AMPARs in R59X mice.

The GluA2-lacking AMPAR blocker IEM-1460 has previously been reported to increase latency to seizure after PTZ injection in rats at multiple ages. IEM-1460 also had age-specific effects on seizure severity according to when expression levels of GluA2-lacking AMPARs were greatest in the brain (Szczurowska and Mareš, 2015), as well as preventing seizure-induced phosphorylation of CAMKII and MeCP2 in immature rodents (Rosenberg et al., 2018). Our findings expand upon the therapeutic potential of IEM-1460, demonstrating that selectively blocking GluA2-lacking AMPARs not only has beneficial effects on seizure threshold, but also on social interaction deficits and working memory. Our findings align with the lab's previous work showing that AMPAR antagonist NBQX attenuates deficits in social preference following seizure-induced elevation of GluA2-lacking AMPARs in rats (Lippman-Bell et al., 2013). Notably, the Jensen lab also showed a significant increase in synaptic GluA2-lacking AMPARs 48 hours post hypoxic seizures in rats that resulted in enhanced epileptogenesis later in life (Sanchez et al., 2001; Rakhade et al., 2008; Lippman-Bell et al., 2013), suggesting that increased hippocampal GluA2-lacking AMPARs in R59X mice may be a targetable contributor to hyperexcitable circuit formation and behavioral alterations even in the absence of visible

seizures, and that blocking GluA2-lacking AMPARs with IEM-1460 may mitigate this process.

Interestingly, acute administration of CBD also attenuated social deficits and rescued short and long-term memory in R59X mice to WT saline levels. Additionally, it increased latency to seizure behavior to WT levels. The mechanism of action of CBD is poorly understood, though it is reported to interact with GPR55, a protein implicated metabolism, motor coordination, cognitive functions, mediating sensory information, and activity of neurons and glia (Marichal-Cancinoa et al., 2017). GPR55 appears to mediate these effects through regulating intracellular Ca^{2+} influx (Laukner et al., 2008), though its activity is not fully understood. Recent data suggests that CBD antagonist activity at GPR55 increases inhibitory neurotransmission (Kaplan et al., 2018). However, CBD is also reported to interact with numerous other neuronal targets (Morales et al., 2017), which makes it challenging to postulate which pathways it may be affecting in R59X mice.

Our experimental design focused on acute administration of both IEM-1460 and CBD to determine whether one dose was effective at providing therapeutic benefits. In future studies, it would be interesting to test both varying doses and chronic treatment paradigms, as well as whether early treatment results in later-life rescue of behavioral deficits. Our data supports further investigation of IEM-1460 and CBD in patients with CDD, not only for decreasing hyperexcitability but attenuating autistic behaviors and memory deficits as well.

BIBLIOGRAPHY

Achuta VS, Möykkynen T, Peteri U-KK, Turconi G, Rivera C, Keinänen K, Castrén ML (2018) Functional changes of AMPA responses in human induced pluripotent stem cell-derived neural progenitors in fragile X syndrome. Sci Signal 11.

Akita T et al. (2018) De novo variants in CAMK2A and CAMK2B cause neurodevelopmental disorders. Ann Clin Transl Neurol 5:280–296.

Amendola E, Zhan Y, Mattucci C, Castroflorio E, Calcagno E, Fuchs C, Lonetti G, Silingardi D, Vyssotski AL, Farley D, Ciani E, Pizzorusso T, Giustetto M, Gross CT (2014) Mapping pathological phenotypes in a mouse model of CDKL5 disorder. PLoS ONE 9:e91613.

Amir RE, Van den Veyver IB, Wan M, Tran CQ, Francke U, Zoghbi HY (1999) Rett syndrome is caused by mutations in X-linked MECP2, encoding methyl-CpG-binding protein 2. Nat Genet 23:185–188.

Anggono V, Huganir RL (2012) Regulation of AMPA receptor trafficking and synaptic plasticity. Curr Opin Neurobiol 22:461–469.

Bahi-Buisson N, Bienvenu T (2012) CDKL5-Related Disorders: From Clinical Description to Molecular Genetics. Mol Syndromol 2:137–152.

Bahi-Buisson N, Kaminska A, Boddaert N, Rio M, Afenjar A, Gérard M, Giuliano F, Motte J, Héron D, Morel MA, Plouin P, Richelme C, des Portes V, Dulac O, Philippe C, Chiron C, Nabbout R, Bienvenu T (2008a) The three stages of epilepsy in patients with CDKL5 mutations. Epilepsia 49:1027–1037.

Bahi-Buisson N, Nectoux J, Rosas-Vargas H, Milh M, Boddaert N, Girard B, Cances C, Ville D, Afenjar A, Rio M, Héron D, N'guyen Morel MA, Arzimanoglou A, Philippe C, Jonveaux P, Chelly J, Bienvenu T (2008b) Key clinical features to identify girls with CDKL5 mutations. Brain 131:2647–2661.

Baltussen LL, Negraes PD, Silvestre M, Claxton S, Moeskops M, Christodoulou E, Flynn HR, Snijders AP, Muotri AR, Ultanir SK (2018) Chemical genetic identification of CDKL5 substrates reveals its role in neuronal microtubule dynamics. EMBO J.

Barbiero I, Peroni D, Tramarin M, Chandola C, Rusconi L, Landsberger N, Kilstrup-Nielsen C (2017) The neurosteroid pregnenolone reverts microtubule derangement induced by the loss of a functional CDKL5-IQGAP1 complex. Hum Mol Genet 26:3520–3530.

Barker-Haliski M, White SH (2015) Glutamatergic Mechanisms Associated with Seizures and Epilepsy. Csh Perspect Med 5:a022863.

Ben-Ari Y (2002) Excitatory actions of gaba during development: the nature of the nurture. Nat Rev Neurosci 3:728–739.

Bisogno T, Hanuš L, Petrocellis L, Tchilibon S, Ponde DE, Brandi I, Moriello A, Davis JB, Mechoulam R, Marzo V (2001) Molecular targets for cannabidiol and its synthetic analogues: effect on vanilloid VR1 receptors and on the cellular uptake and enzymatic hydrolysis of anandamide. Brit J Pharmacol 134:845–852.

Brodkin ES (2007) BALB/c mice: low sociability and other phenotypes that may be relevant to autism. Behav Brain Res 176:53–65.

Brown MW, Aggleton JP (2001) Recognition memory: What are the roles of the perirhinal cortex and hippocampus? Nat Rev Neurosci 2:51–61.

Buldakova SL, Kim KK, Tikhonov DB, Magazanik LG (2007) Selective blockade of Ca2+ permeable AMPA receptors in CA1 area of rat hippocampus. Neuroscience 144:88–99.

Chahrour M, Jung SY, Shaw C, Zhou X, Wong ST, Qin J, Zoghbi HY (2008) MeCP2, a key contributor to neurological disease, activates and represses transcription. Science 320:1224–1229.

Chater TE, Goda Y (2014) The role of AMPA receptors in postsynaptic mechanisms of synaptic plasticity. Front Cell Neurosci 8:401.

Chawla S, Vanhoutte P, Arnold FJ, Huang CL, Bading H (2003) Neuronal activity-dependent nucleocytoplasmic shuttling of HDAC4 and HDAC5. J Neurochem 85:151–159.

Chen Q, Zhu Y-CC, Yu J, Miao S, Zheng J, Xu L, Zhou Y, Li D, Zhang C, Tao J, Xiong Z-QQ (2010) CDKL5, a protein associated with rett syndrome, regulates neuronal morphogenesis via Rac1 signaling. J Neurosci 30:12777–12786.

Chen X, Levy JM, Hou A, Winters C, Azzam R, Sousa AA, Leapman RD, Nicoll RA, Reese TS (2015) PSD-95 family MAGUKs are essential for anchoring AMPA and NMDA receptor complexes at the postsynaptic density. Proc Natl Acad Sci USA 112:E6983–92.

Chen X, Nelson CD, Li X, Winters CA, Azzam R, Sousa AA, Leapman RD, Gainer H, Sheng M, Reese TS (2011) PSD-95 is required to sustain the molecular organization of the postsynaptic density. J Neurosci 31:6329–6338.

Cheng D, Spiro AS, Jenner AM, Garner B, Karl T (2014) Long-term cannabidiol treatment prevents the development of social recognition memory deficits in Alzheimer's disease transgenic mice. J Alzheimers Dis 42:1383–1396.

Citri A, Malenka RC (2007) Synaptic Plasticity: Multiple Forms, Functions, and Mechanisms. Neuropsychopharmacol 33:1301559.

Coley AA, Gao W-J (2017) PSD95: A synaptic protein implicated in schizophrenia or autism? Progress in Neuro-Psychopharmacology and Biological Psychiatry.

Corroon J, Kight R (2018) Regulatory Status of Cannabidiol in the United States: A Perspective. Cannabis Cannabinoid Res 3:190–194.

Crawley J (2004) Designing mouse behavioral tasks relevant to autistic-like behaviors. Ment Retard Dev D R 10:248–258.

Crawley J (2007) Mouse Behavioral Assays Relevant to the Symptoms of Autism*. Brain Pathol 17:448–459.

Daenen EW, Van der Heyden JA, Kruse CG, Wolterink G, Van Ree JM (2001) Adaptation and habituation to an open field and responses to various stressful events in animals with neonatal lesions in the amygdala or ventral hippocampus. Brain Res 918:153–165.

Della Sala G, Putignano E, Chelini G, Melani R, Calcagno E, Michele Ratto G, Amendola E, Gross CT, Giustetto M, Pizzorusso T (2016) Dendritic Spine Instability in a Mouse Model of CDKL5 Disorder Is Rescued by Insulin-like Growth Factor 1. Biol Psychiatry 80:302–311.

Devinsky O, Cilio M, Cross H, Fernandez-Ruiz J, French J, Hill C, Katz R, Marzo V, Jutras-Aswad D, Notcutt W, Martinez-Orgado J, Robson PJ, Rohrback BG, Thiele E, Whalley B, Friedman D (2014) Cannabidiol: Pharmacology and potential therapeutic role in epilepsy and other neuropsychiatric disorders. Epilepsia 55:791–802.

Devinsky O, Patel AD, Thiele EA, Wong MH, Appleton R, Harden CL, Greenwood S, Morrison G, Sommerville K (2018a) Randomized, dose-ranging safety trial of cannabidiol in Dravet syndrome. Neurology 90:e1204–e1211.

Devinsky O, Verducci C, Thiele EA, Laux LC, Patel AD, Filloux F, Szaflarski JP, Wilfong A, Clark GD, Park YD, Seltzer LE, Bebin EM, Flamini R, Wechsler RT, Friedman D (2018b) Open-label use of highly purified CBD (Epidiolex®) in patients with CDKL5 deficiency disorder and Aicardi, Dup15q, and Doose syndromes. Epilepsy Behav 86:131–137.

Dewey D, Cantell M, Crawford SG (2007) Motor and gestural performance in children with autism spectrum disorders, developmental coordination disorder, and/or attention deficit hyperactivity disorder. J Int Neuropsych Soc 13:246–256.

Do Val-da Silva RA, Peixoto-Santos JE, Kandratavicius L, De Ross JB, Esteves I, De Martinis BS, Alves MN, Scandiuzzi RC, Hallak JE, Zuardi AW, Crippa JA, Leite JP (2017) Protective Effects of Cannabidiol against Seizures and Neuronal Death in a Rat Model of Mesial Temporal Lobe Epilepsy. Front Pharmacol 8:131.

Dzhala VI, Talos DM, Sdrulla DA, Brumback AC, Mathews GC, Benke TA, Delpire E, Jensen FE, Staley KJ (2005) NKCC1 transporter facilitates seizures in the developing brain. Nat Med 11:1205–1213.

Eichler SA, Meier JC (2008) E-I balance and human diseases - from molecules to networking. Front Mol Neurosci 1:2.

El-Husseini AE-D el-D, Schnell E, Dakoji S, Sweeney N, Zhou Q, Prange O, Gauthier-Campbell C, Aguilera-Moreno A, Nicoll RA, Bredt DS (2002) Synaptic strength regulated by palmitate cycling on PSD-95. Cell 108:849–863.

Fehr S, Downs J, Ho G, de Klerk N, Forbes D, Christodoulou J, Williams S, Leonard H (2016) Functional abilities in children and adults with the CDKL5 disorder. Am J Med Genet A 170:2860–2869.

Fehr S, Leonard H, Ho G, Williams S, de Klerk N, Forbes D, Christodoulou J, Downs J (2015) There is variability in the attainment of developmental milestones in the CDKL5 disorder. J Neurodev Disord 7:2.

Fioravante D, Regehr WG (2011) Short-term forms of presynaptic plasticity. Curr Opin Neurobiol 21:269–274.

Fortin DA, Davare MA, Srivastava T, Brady JD, Nygaard S, Derkach VA, Soderling TR (2010) Long-term potentiation-dependent spine enlargement requires synaptic Ca2+-permeable AMPA receptors recruited by CaM-kinase I. J Neurosci 30:11565–11575.

Fuchs C, Fustini N, Trazzi S, Gennaccaro L, Rimondini R, Ciani E (2018) Treatment with the GSK3-beta inhibitor Tideglusib improves hippocampal development and memory performance in juvenile, but not adult, Cdkl5 knockout mice. Eur J Neurosci 47:1054-1066.

Fuchs C, Rimondini R, Viggiano R, Trazzi S, De Franceschi M, Bartesaghi R, Ciani E (2015) Inhibition of GSK3β rescues hippocampal development and learning in a mouse model of CDKL5 disorder. Neurobiol Dis 82:298–310.

Fuchs C, Trazzi S, Torricella R, Viggiano R, De Franceschi M, Amendola E, Gross C, Calzà L, Bartesaghi R, Ciani E (2014) Loss of CDKL5 impairs survival and dendritic growth of newborn neurons by altering AKT/GSK-3β signaling. Neurobiol Dis 70:53–68.

Fung LK, Hardan AY (2015) Developing Medications Targeting Glutamatergic Dysfunction in Autism: Progress to Date. Cns Drugs 29:453–463.

Gao Y, Heldt SA (2016) Enrichment of GABAA Receptor α-Subunits on the Axonal Initial Segment Shows Regional Differences. Front Cell Neurosci 10:39.

Gardner SM, Takamiya K, Xia J, Suh J-GG, Johnson R, Yu S, Huganir RL (2005) Calcium-permeable AMPA receptor plasticity is mediated by subunit-specific interactions with PICK1 and NSF. Neuron 45:903–915.

Gaston TE, Szaflarski JP (2018) Cannabis for the Treatment of Epilepsy: an Update. Curr Neurol Neurosci 18:73.

Geiger JR, Melcher T, Koh DS, Sakmann B, Seeburg PH, Jonas P, Monyer H (1995) Relative abundance of subunit mRNAs determines gating and Ca2+ permeability of AMPA receptors in principal neurons and interneurons in rat CNS. Neuron 15:193–204.

Gmiro VE, Serdyuk SE, Efremov OM (2008) Peripheral and central routes of administration of quaternary ammonium compound IEM-1460 are equally potent in reducing the severity of nicotine-induced seizures in mice. Bull Exp Biol Med 146:18–21.

Goodlett CR, Thomas JD, West JR (1991) Long-term deficits in cerebellar growth and rotarod performance of rats following “binge-like” alcohol exposure during the neonatal brain growth spurt. Neurotoxicol Teratol 13:69–74.

Greger IH, Watson JF, Cull-Candy SG (2017) Structural and Functional Architecture of AMPA-Type Glutamate Receptors and Their Auxiliary Proteins. Neuron 94:713–730.

Grooms SY, Opitz T, Bennett MV, Zukin RS (2000) Status epilepticus decreases glutamate receptor 2 mRNA and protein expression in hippocampal pyramidal cells before neuronal death. Proc Natl Acad Sci USA 97:3631–3636.

Guire ES, Oh MC, Soderling TR, Derkach VA (2008) Recruitment of calcium-permeable AMPA receptors during synaptic potentiation is regulated by CaM-kinase I. Journal of Neuroscience 28:6000–6009.

Guy J, Hendrich B, Holmes M, Martin JE, Bird A (2001) A mouse Mecp2-null mutation causes neurological symptoms that mimic Rett syndrome. Nat Genet 27:322–326.

Hanley JG (2014) Subunit-specific trafficking mechanisms regulating the synaptic expression of Ca(2+)-permeable AMPA receptors. Semin Cell Dev Biol 27:14–22.

Hector RD, Dando O, Landsberger N, Kilstrup-Nielsen C, Kind PC, Bailey ME, Cobb SR (2016) Characterisation of CDKL5 Transcript Isoforms in Human and Mouse. PLoS ONE 11:e0157758.

Hector RD, Kalscheuer VM, Hennig F, Leonard H, Downs J, Clarke A, Benke TA, Armstrong J, Pineda M, Bailey MESE, Cobb SR (2017) CDKL5 variants: Improving our understanding of a rare neurologic disorder. Neurol Genet 3:e200.

Henley JM, Wilkinson KA (2016) Synaptic AMPA receptor composition in development, plasticity and disease. Nat Rev Neurosci 17:337–350.

Hernandez RV, Navarro MM, Rodriguez WA, Martinez JL, LeBaron RG (2005) Differences in the magnitude of long-term potentiation produced by theta burst and high frequency stimulation protocols matched in stimulus number. Brain Res Brain Res Protoc 15:6–13.

Irwin RE, Pentieva K, Cassidy T, Lees-Murdock DJ, McLaughlin M, Prasad G, McNulty H, Walsh CP (2016) The interplay between DNA methylation, folate and neurocognitive development. Epigenomics 8:863–879.

Isaac JT, Ashby MC, McBain CJ (2007) The role of the GluR2 subunit in AMPA receptor function and synaptic plasticity. Neuron 54:859–871.

Jaafari N, Henley JM, Hanley JG (2012) PICK1 mediates transient synaptic expression of GluA2-lacking AMPA receptors during glycine-induced AMPA receptor trafficking. Journal of Neuroscience Available at: http://www.jneurosci.org/content/32/34/11618.short.

Jensen FE, Wang C, Stafstrom CE, Liu Z, Geary C, Stevens MC (1998) Acute and chronic increases in excitability in rat hippocampal slices after perinatal hypoxia In vivo. J Neurophysiol 79:73–81.

Jeyifous O, Lin EI, Chen X, Antinone SE, Mastro R, Drisdel R, Reese TS, Green WN (2016) Palmitoylation regulates glutamate receptor distributions in postsynaptic densities through control of PSD95 conformation and orientation. Proc Natl Acad Sci USA 113:E8482–E8491.

Jhang C-LL, Huang T-NN, Hsueh Y-PP, Liao W (2017) Mice lacking cyclin-dependent kinase-like 5 manifest autistic and ADHD-like behaviors. Hum Mol Genet 26:3922–3934.

Jia Z, Agopyan N, Miu P, Xiong Z, Henderson J, Gerlai R, Taverna FA, Velumian A, MacDonald J, Carlen P (1996) Enhanced LTP in mice deficient in the AMPA receptor GluR2. Neuron 17:945–956 Available at: http://www.sciencedirect.com/science/article/pii/S0896627300802251.

Jin Y, Sui HJ, Dong Y, Ding Q, Qu WH, Yu SX, Jin YX (2012) Atorvastatin enhances neurite outgrowth in cortical neurons in vitro via up-regulating the Akt/mTOR and Akt/GSK-3β signaling pathways. Acta Pharmacol Sin 33:861–872.

Jonas P, Neuron B-N (1995) Molecular mechanisms controlling calcium entry through AMPA-type glutamate receptor channels. Neuron Available at: https://www.cell.com/neuron/pdf/0896-6273(95)90087-X.pdf.

Jonas P, Racca C, Sakmann B, Seeburg PH, Neuron M-H (1994) Differences in Ca2+ permeability of AMPA-type glutamate receptor channels in neocortical neurons caused by differential GluR-B subunit expression. Neuron Available at: https://www.sciencedirect.com/science/article/pii/0896627394904448.

Kaizuka T, Takumi T (2018) Postsynaptic density proteins and their involvement in neurodevelopmental disorders. J Biochem 163:447–455.

Kalscheuer VM, Tao J, Donnelly A, Hollway G, Schwinger E, Kübart S, Menzel C, Hoeltzenbein M, Tommerup N, Eyre H, Harbord M, Haan E, Sutherland GR, Ropers H-HH, Gécz J (2003) Disruption of the serine/threonine kinase 9 gene causes severe X-linked infantile spasms and mental retardation. Am J Hum Genet 72:1401–1411.

Kamboj SK, Swanson GT, Cull-Candy SG (1995) Intracellular spermine confers rectification on rat calcium-permeable AMPA and kainate receptors. J Physiol (Lond) 486 (Pt 2):297–303.

Kameshita I, Sekiguchi M, Hamasaki D, Sugiyama Y, Hatano N, Suetake I, Tajima S, Sueyoshi N (2008) Cyclin-dependent kinase-like 5 binds and phosphorylates DNA methyltransferase 1. Biochem Biophys Res Commun 377:1162–1167.

Kaplan JS, Stella N, Catterall WA, Westenbroek RE (2017) Cannabidiol attenuates seizures and social deficits in a mouse model of Dravet syndrome. Proc Natl Acad Sci USA 114:11229–11234.

Kaushik R, Grochowska KM, Butnaru I, Kreutz MR (2014) Protein trafficking from synapse to nucleus in control of activity-dependent gene expression. Neuroscience 280:340–350.

Kazdoba TM, Leach PT, Silverman JL, Crawley JN (2014) Modeling fragile X syndrome in the Fmr1 knockout mouse. Intractable Rare Dis Res 3:118–133.

Keller R, Basta R, Salerno L, Elia M (2017) Autism, epilepsy, and synaptopathies: a not rare association. Neurol Sci 38:1353–1361.

Khan S, Baradie R (2012) Epileptic Encephalopathies: An Overview. Epilepsy Res Treat 2012:403592.

Kilstrup-Nielsen C, Rusconi L, Montanara P, Ciceri D, Bergo A, Bedogni F, Landsberger N (2012) What We Know and Would Like to Know about CDKL5 and Its Involvement in Epileptic Encephalopathy. Neural Plast 2012:728267.

Kim S, Burette A, Chung HS, Kwon S-KK, Woo J, Lee HW, Kim K, Kim H, Weinberg RJ, Kim E (2006) NGL family PSD-95-interacting adhesion molecules regulate excitatory synapse formation. Nat Neurosci 9:1294–1301.

Kumar SS, Bacci A, Kharazia V, Huguenard JR (2002) A developmental switch of AMPA receptor subunits in neocortical pyramidal neurons. J Neurosci 22:3005–3015.

Kumar V, Zhang M-XX, Swank MW, Kunz J, Wu G-YY (2005) Regulation of dendritic morphogenesis by Ras-PI3K-Akt-mTOR and Ras-MAPK signaling pathways. J Neurosci 25:11288–11299.

La Montanara P, Rusconi L, Locarno A, Forti L, Barbiero I, Tramarin M, Chandola C, Kilstrup-Nielsen C, Landsberger N (2015) Synaptic synthesis, dephosphorylation, and degradation: a novel paradigm for an activity-dependent neuronal control of CDKL5. J Biol Chem 290:4512–4527.

Larson J, Munkácsy E (2015) Theta-burst LTP. Brain Res 1621:38–50.

Lasser M, Tiber J, Lowery LA (2018) The Role of the Microtubule Cytoskeleton in Neurodevelopmental Disorders. Front Cell Neurosci 12:165.

Lauckner JE, Jensen JB, Chen H-YY, Lu H-CC, Hille B, Mackie K (2008) GPR55 is a cannabinoid receptor that increases intracellular calcium and inhibits M current. Proc Natl Acad Sci USA 105:2699–2704.

Lee S (2014) Old versus New: Why Do We Need New Antiepileptic Drugs? J Epilepsy Res 4:39–44.

Li W, Xu X, Pozzo-Miller L (2016) Excitatory synapses are stronger in the hippocampus of Rett syndrome mice due to altered synaptic trafficking of AMPA-type glutamate receptors. Proc Natl Acad Sci USA 113:E1575–84.

Lin C, Franco B, Rosner MR (2005) CDKL5/Stk9 kinase inactivation is associated with neuronal developmental disorders. Hum Mol Genet 14:3775–3786.

Lin K-LL, Lin J-JJ, Chou M-LL, Hung P-CC, Hsieh M-YY, Chou I-JJ, Lim S-NN, Wu T, Wang H-SS (2018) Efficacy and tolerability of perampanel in children and adolescents with pharmacoresistant epilepsy: The first real-world evaluation in Asian pediatric neurology clinics. Epilepsy Behav 85:188–194.

Lippman-Bell JJ, Rakhade SN, Klein PM, Obeid M, Jackson MC, Joseph A, Jensen FE (2013) AMPA receptor antagonist NBQX attenuates later-life epileptic seizures and autistic-like social deficits following neonatal seizures. Epilepsia 54:1922–1932.

Lippman-Bell JJ, Zhou C, Sun H, Feske JS, Jensen FE (2016) Early-life seizures alter synaptic calcium-permeable AMPA receptor function and plasticity. Mol Cell Neurosci 76:11–20.

Lipton JO, Sahin M (2014) The neurology of mTOR. Neuron 84:275–291.

Liu SJ, Zukin RS (2007) Ca2+-permeable AMPA receptors in synaptic plasticity and neuronal death. Trends Neurosci 30:126–134.

Loddenkemper T, Talos DM, Cleary RT, Joseph A, Sánchez Fernández I, Alexopoulos A, Kotagal P, Najm I, Jensen FE (2014) Subunit composition of glutamate and gamma-aminobutyric acid receptors in status epilepticus. Epilepsy Res 108:605–615.

Lorgen J-ØØ, Egbenya DL, Hammer J, Davanger S (2017) PICK1 facilitates lasting reduction in GluA2 concentration in the hippocampus during chronic epilepsy. Epilepsy Res 137:25–32.

Lu W, Khatri L, Ziff EB (2014) Trafficking of α-amino-3-hydroxy-5-methyl-4-isoxazolepropionic acid receptor (AMPA) receptor subunit GluA2 from the endoplasmic reticulum is stimulated by a complex containing Ca2+/calmodulin-activated kinase II (CaMKII) and PICK1 protein and by release of Ca2+ from internal stores. J Biol Chem 289:19218–19230.

Lu W, Shi Y, Jackson AC, Bjorgan K, During MJ, Sprengel R, Seeburg PH, Nicoll RA (2009) Subunit composition of synaptic AMPA receptors revealed by a single-cell genetic approach. Neuron 62:254–268.

Luján R, Shigemoto R, López-Bendito G (2005) Glutamate and GABA receptor signalling in the developing brain. Neuroscience 130:567–580.

Lüttjohann A, Fabene PF, van Luijtelaar G (2009) A revised Racine's scale for PTZ-induced seizures in rats. Physiol Behav 98:579–586.

Magazanik LG, Buldakova SL, Samoilova MV, Gmiro VE, Mellor IR, Usherwood PN (1997) Block of open channels of recombinant AMPA receptors and native AMPA/kainate receptors by adamantane derivatives. J Physiol (Lond) 505 (Pt 3):655–663.

Man H-YY (2011) GluA2-lacking, calcium-permeable AMPA receptors--inducers of plasticity? Curr Opin Neurobiol 21:291–298.

Manders E, Verbeek F, Aten J (1993) Measurement of co-localization of objects in dual-colour confocal images. J Microsc-oxford 169:375–382.

Mansour M, Nagarajan N, Nehring RB, Clements JD, Rosenmund C (2001) Heteromeric AMPA receptors assemble with a preferred subunit stoichiometry and spatial arrangement. Neuron 32:841–853.

Mari F et al. (2005) CDKL5 belongs to the same molecular pathway of MeCP2 and it is responsible for the early-onset seizure variant of Rett syndrome. Hum Mol Genet 14:1935–1946.

Martínez-Cerdeño V (2017) Dendrite and spine modifications in autism and related neurodevelopmental disorders in patients and animal models. Dev Neurobiol 77:393–404.

Marzo V, Petrocellis L (2012) Why do cannabinoid receptors have more than one endogenous ligand? Philosophical Transactions Royal Soc B Biological Sci 367:3216–3228.

Maussion G et al. (2017) Implication of LRRC4C and DPP6 in neurodevelopmental disorders. Am J Med Genet A 173:395–406.

McClain MB, Hasty Mills AM, Murphy LE (2017) Inattention and hyperactivity/impulsivity among children with attention-deficit/hyperactivity-disorder, autism spectrum disorder, and intellectual disability. Res Dev Disabil 70:175–184.

Meng Y, Zhang Y, Jia Z (2003) Synaptic Transmission and Plasticity in the Absence of AMPA Glutamate Receptor GluR2 and GluR3. Neuron 39:163–176.

Mignogna ML, Giannandrea M, Gurgone A, Fanelli F, Raimondi F, Mapelli L, Bassani S, Fang H, Van Anken E, Alessio M, Passafaro M, Gatti S, Esteban JAA, Huganir R, D'Adamo P (2015) The intellectual disability protein RAB39B selectively regulates GluA2 trafficking to determine synaptic AMPAR composition. Nature communications 6:6504.

Migues PV, Cammarota M, Kavanagh J, Atkinson R, Powis DA, Rostas JA (2007) Maturational changes in the subunit composition of AMPA receptors and the functional consequences of their activation in chicken forebrain. Dev Neurosci 29:232–240.

Montini E, Andolfi G, Caruso A, Buchner G, Walpole SM, Mariani M, Consalez G, Trump D, Ballabio A, Franco B (1998) Identification and characterization of a novel serine-threonine kinase gene from the Xp22 region. Genomics 51:427–433.

Monyer H, Seeburg PH, Wisden W (1991) Glutamate-operated channels: developmentally early and mature forms arise by alternative splicing. Neuron 6:799–810.

Moretti P, Bouwknecht JA, Teague R, Paylor R, Zoghbi HY (2005) Abnormalities of social interactions and home-cage behavior in a mouse model of Rett syndrome. Hum Mol Genet 14:205–220.

Moy SS, Nadler JJ, Poe MD, Nonneman RJ, Young NB, Koller BH, Crawley JN, Duncan GE, Bodfish JW (2008) Development of a mouse test for repetitive, restricted behaviors: relevance to autism. Behav Brain Res 188:178–194.

Muñoz IM, Morgan ME, Peltier J, Weiland F, Gregorczyk M, Brown FC, Macartney T, Toth R, Trost M, Rouse J (2018) Phosphoproteomic screening identifies physiological substrates of the CDKL5 kinase. EMBO J.

Murray TK, Ridley RM (1999) The effect of excitotoxic hippocampal lesions on simple and conditional discrimination learning in the rat. Behav Brain Res 99:103–113.

Musumeci SA, Calabrese G, Bonaccorso CM, D'Antoni S, Brouwer JR, Bakker CE, Elia M, Ferri R, Nelson DL, Oostra BA, Catania MV (2007) Audiogenic seizure susceptibility is reduced in fragile X knockout mice after introduction of FMR1 transgenes. Exp Neurol 203:233–240.

Nawaz MS, Giarda E, Bedogni F, La Montanara P, Ricciardi S, Ciceri D, Alberio T, Landsberger N, Rusconi L, Kilstrup-Nielsen C (2016) CDKL5 and Shootin1 Interact and Concur in Regulating Neuronal Polarization. PLoS ONE 11:e0148634.

Oi A, Katayama S, Hatano N, Sugiyama Y, Kameshita I, Sueyoshi N (2017) Subcellular distribution of cyclin-dependent kinase-like 5 (CDKL5) is regulated through phosphorylation by dual specificity tyrosine-phosphorylation-regulated kinase 1A (DYRK1A). Biochem Biophys Res Commun 482:239–245.

Okabe S (2007) Molecular anatomy of the postsynaptic density. Mol Cell Neurosci 34:503–518.

Okuda K, Kobayashi S, Fukaya M, Watanabe A, Murakami T, Hagiwara M, Sato T, Ueno H, Ogonuki N, Komano-Inoue S, Manabe H, Yamaguchi M, Ogura A, Asahara H, Sakagami H, Mizuguchi M, Manabe T, Tanaka T (2017) CDKL5 controls postsynaptic localization of GluN2B-containing NMDA receptors in the hippocampus and regulates seizure susceptibility. Neurobiol Dis 106:158–170.

Okuda K, Takao K, Watanabe A, Miyakawa T, Mizuguchi M, Tanaka T (2018) Comprehensive behavioral analysis of the Cdkl5 knockout mice revealed significant enhancement in anxiety- and fear-related behaviors and impairment in both acquisition and long-term retention of spatial reference memory. PLoS ONE 13:e0196587.

Okuno H (2011) Regulation and function of immediate-early genes in the brain: Beyond neuronal activity markers. Neurosci Res 69:175–186.

Owens DF, Kriegstein AR (2002) Is there more to gaba than synaptic inhibition? Nat Rev Neurosci 3:715–727.

Pandey SP, Rai R, Gaur P, Prasad S (2015) Development-and age-related alterations in the expression of AMPA receptor subunit GluR2 and its trafficking proteins in the hippocampus of male mouse brain. Biogerontology 16:317–328.

Paoletti P, Bellone C, Neuroscience Z-Q (2013) NMDA receptor subunit diversity: impact on receptor properties, synaptic plasticity and disease. Nature Reviews Neuroscience Available at: https://www.nature.com/articles/nrn3504.

Park P, Sanderson TM, Amici M, Choi S-LL, Bortolotto ZA, Zhuo M, Kaang B-KK, Collingridge GL (2016) Calcium-Permeable AMPA Receptors Mediate the Induction of the Protein Kinase A-Dependent Component of Long-Term Potentiation in the Hippocampus. J Neurosci 36:622–631.

Patel RR, Barbosa C, Brustovetsky T, Brustovetsky N, Cummins TR (2016) Aberrant epilepsy-associated mutant Nav1.6 sodium channel activity can be targeted with cannabidiol. Brain J Neurology 139:2164–2181.

Pavone P, Striano P, Falsaperla R, Pavone L, Ruggieri M (2014) Infantile spasms syndrome, West syndrome and related phenotypes: What we know in 2013. Brain Dev 36:739–751.

Paylor R, Hirotsune S, Gambello MJ, Yuva-Paylor L, Crawley JN, Wynshaw-Boris A (1999) Impaired learning and motor behavior in heterozygous Pafah1b1 (Lis1) mutant mice. Learn Mem 6:521–537.

Phillips RG, LeDoux JE (1992) Differential contribution of amygdala and hippocampus to cued and contextual fear conditioning. Behav Neurosci 106:274–285.

Pisanti S, Malfitano AM, Ciaglia E, Lamberti A, Ranieri R, Cuomo G, Abate M, Faggiana G, Proto MC, Fiore D, Laezza C, Bifulco M (2017) Cannabidiol: State of the art and new challenges for therapeutic applications. Pharmacol Ther 175:133–150.

Pinheiro PS, Mulle C (2008) Presynaptic glutamate receptors: physiological functions and mechanisms of action. Nat Rev Neurosci 9:423–436.

Plant K, Pelkey KA, Bortolotto ZA, Morita D, Terashima A, McBain CJ, Collingridge GL, Isaac JT (2006) Transient incorporation of native GluR2-lacking AMPA receptors during hippocampal long-term potentiation. Nat Neurosci 9:602–604.

Poleg S, Golubchik P, Offen D, Weizman A (2018) Cannabidiol as a suggested candidate for treatment of autism spectrum disorder. Prog Neuropsychopharmacol Biol Psychiatry 89:90–96.

Porter BE, Jacobson C (2013) Report of a parent survey of cannabidiol-enriched cannabis use in pediatric treatment-resistant epilepsy. Epilepsy Behav 29:574–577.

Puskarjov M, Kahle KT, Ruusuvuori E, Kaila K (2014) Pharmacotherapeutic targeting of cation-chloride cotransporters in neonatal seizures. Epilepsia 55:806–818.

Raam T, McAvoy KM, Besnard A, Veenema AH, Sahay A (2017) Hippocampal oxytocin receptors are necessary for discrimination of social stimuli. Nat Commun 8:2001.

Rakhade SN, Fitzgerald EF, Klein PM, Zhou C, Sun H, Huganir RL, Hunganir RL, Jensen FE (2012) Glutamate receptor 1 phosphorylation at serine 831 and 845 modulates seizure susceptibility and hippocampal hyperexcitability after early life seizures. J Neurosci 32:17800–17812.

Rakhade SN, Jensen FE (2009) Epileptogenesis in the immature brain: emerging mechanisms. Nat Rev Neurol 5:380–391.

Rakhade SN, Zhou C, Aujla PK, Fishman R, Sucher NJ, Jensen FE (2008) Early alterations of AMPA receptors mediate synaptic potentiation induced by neonatal seizures. J Neurosci 28:7979–7990.

Reimers JM, Milovanovic M, Wolf ME (2011) Quantitative analysis of AMPA receptor subunit composition in addiction-related brain regions. Brain Res 1367:223–233.

Ricciardi S, Kilstrup-Nielsen C, Bienvenu T, Jacquette A, Landsberger N, Broccoli V (2009) CDKL5 influences RNA splicing activity by its association to the nuclear speckle molecular machinery. Hum Mol Genet 18:4590–4602.

Ricciardi S, Ungaro F, Hambrock M, Rademacher N, Stefanelli G, Brambilla D, Sessa A, Magagnotti C, Bachi A, Giarda E, Verpelli C, Kilstrup-Nielsen C, Sala C, Kalscheuer VM, Broccoli V (2012) CDKL5 ensures excitatory synapse stability by reinforcing NGL-1-PSD95 interaction in the postsynaptic compartment and is impaired in patient iPSC-derived neurons. Nat Cell Biol 14:911–923.

Rojas DC (2014) The role of glutamate and its receptors in autism and the use of glutamate receptor antagonists in treatment. J Neural Transm 121:891–905.

Rosenberg EC, Louik J, Conway E, Devinsky O, Friedman D (2017) Quality of Life in Childhood Epilepsy in pediatric patients enrolled in a prospective, open-label clinical study with cannabidiol. Epilepsia 58:e96–e100.

Rosenberg EC, Lippman-Bell JJ, Handy M, Soldan SS, Rakhade S, Hilario-Gomez C, Folweiler K, Jacobs L, Jensen FE (2018) Regulation of seizure-induced MeCP2 Ser421 phosphorylation in the developing brain. Neurobiol Dis 116:120–130.

Ross H, Napier I, Connor M (2008) Inhibition of Recombinant Human T-type Calcium Channels by Δ9-Tetrahydrocannabinol and Cannabidiol. J Biol Chem 283:16124–16134.

Rozov A, Sprengel R, Seeburg PH (2012) GluA2-lacking AMPA receptors in hippocampal CA1 cell synapses: evidence from gene-targeted mice. Front Mol Neurosci 5:22.

Rusconi L, Salvatoni L, Giudici L, Bertani I, Kilstrup-Nielsen C, Broccoli V, Landsberger N (2008) CDKL5 expression is modulated during neuronal development and its subcellular distribution is tightly regulated by the C-terminal tail. J Biol Chem 283:30101–30111.

Ryberg E, Larsson N, Sjögren S, Hjorth S, Hermansson N, Leonova J, Elebring T, Nilsson K, Drmota T, Greasley P (2007) The orphan receptor GPR55 is a novel cannabinoid receptor. Brit J Pharmacol 152:1092–1101.

Samoilova MV, Buldakova SL, Vorobjev VS, Sharonova IN, Magazanik LG (1999) The open channel blocking drug, IEM-1460, reveals functionally distinct alpha-amino-3-hydroxy-5-methyl-4-isoxazolepropionate receptors in rat brain neurons. Neuroscience 94:261–268.

Sanchez RM, Koh S, Rio C, Wang C, Lamperti ED, Sharma D, Corfas G, Jensen FE (2001) Decreased glutamate receptor 2 expression and enhanced epileptogenesis in immature rat hippocampus after perinatal hypoxia-induced seizures. J Neurosci 21:8154–8163.

Sanderson JL, Gorski JA, Neuron D-M (2016) NMDA receptor-dependent LTD requires transient synaptic incorporation of Ca2+-permeable AMPARs mediated by AKAP150-anchored PKA and calcineurin. Neuron Available at: https://www.sciencedirect.com/science/article/pii/S0896627316000908.

Sando R, Gounko N, Pieraut S, Liao L, Yates J, Maximov A (2012) HDAC4 governs a transcriptional program essential for synaptic plasticity and memory. Cell 151:821–834.

Saneyoshi T, Hayashi Y (2014) Synapse reorganization-a new partnership revealed. EMBO J 33:1292–1294.

Schroeder E, Yuan L, Seong E, Ligon C, DeKorver N, Gurumurthy CB, Arikkath J (2018) Neuron-Type Specific Loss of CDKL5 Leads to Alterations in mTOR Signaling and Synaptic Markers. Mol Neurobiol.

Sekiguchi M, Katayama S, Hatano N, Shigeri Y, Sueyoshi N, Kameshita I (2013) Identification of amphiphysin 1 as an endogenous substrate for CDKL5, a protein kinase associated with X-linked neurodevelopmental disorder. Arch Biochem Biophys 535:257–267.

Seibenhener ML, Wooten MC (2015) Use of the Open Field Maze to Measure Locomotor and Anxiety-like Behavior in Mice. J Vis Exp:e52434.

Squires RF, Saederup E, Crawley JN, Skolnick P, Paul SM (1984) Convulsant potencies of tetrazoles are highly correlated with actions on GABA/benzodiazepine/picrotoxin receptor complexes in brain. Life Sci 35:1439–1444.

Stearns NA, Schaevitz LR, Bowling H, Nag N, Berger UV, Berger-Sweeney J (2007) Behavioral and anatomical abnormalities in Mecp2 mutant mice: a model for Rett syndrome. Neuroscience 146:907–921.

Stephenson JR, Wang X, Perfitt TL, Parrish WP, Shonesy BC, Marks CR, Mortlock DP, Nakagawa T, Sutcliffe JS, Colbran RJ (2017) A Novel Human CAMK2A Mutation Disrupts Dendritic Morphology and Synaptic Transmission, and Causes ASD-Related Behaviors. J Neurosci 37:2216–2233.

Sun H, Takesian AE, Wang T, Lippman-Bell JJ, Hensch TK, Jensen FE (2018) Early Seizures Prematurely Unsilence Auditory Synapses to Disrupt Thalamocortical Critical Period Plasticity. Cell Reports 23:2533–2540.

Swanson GT, Kamboj SK, Cull-Candy SG (1997) Single-channel properties of recombinant AMPA receptors depend on RNA editing, splice variation, and subunit composition. Journal of Neuroscience 17:58–69.

Sylantyev S, Jensen TP, Ross RA, Rusakov DA (2013) Cannabinoid- and lysophosphatidylinositol-sensitive receptor GPR55 boosts neurotransmitter release at central synapses. Proc National Acad Sci 110:5193–5198.

Szczurowska E, Mareš P (2015) An antagonist of calcium permeable AMPA receptors, IEM1460: Anticonvulsant action in immature rats? Epilepsy Res 109:106–113.

Talos DM, Fishman RE, Park H, Folkerth RD, Follett PL, Volpe JJ, Jensen FE (2006) Developmental regulation of alpha-amino-3-hydroxy-5-methyl-4-isoxazole-propionic acid receptor subunit expression in forebrain and relationship to regional susceptibility to hypoxic/ischemic injury. I. Rodent cerebral white matter and cortex. J Comp Neurol 497:42–60.

Talos DM, Kwiatkowski DJ, Cordero K, Black PM, Jensen FE (2008) Cell-specific alterations of glutamate receptor expression in tuberous sclerosis complex cortical tubers. Ann Neurol 63:454–465.

Talos DM, Sun H, Kosaras B, Joseph A, Folkerth RD, Poduri A, Madsen JR, Black PM, Jensen FE (2012) Altered inhibition in tuberous sclerosis and type IIb cortical dysplasia. Ann Neurol 71:539–551.

Tang S, Wang I-TJ, Yue C, Takano H, Terzic B, Pance K, Lee JY, Cui Y, Coulter DA, Zhou Z (2017) Loss of CDKL5 in Glutamatergic Neurons Disrupts Hippocampal Microcircuitry and Leads to Memory Impairment in Mice. J Neurosci 37:7420–7437.

Thiele EA, Marsh ED, French JA, Mazurkiewicz-Beldzinska M, Benbadis SR, Joshi C, Lyons PD, Taylor A, Roberts C, Sommerville K (2018) Cannabidiol in patients with seizures associated with Lennox-Gastaut syndrome (GWPCARE4): a randomised, double-blind, placebo-controlled phase 3 trial. Lancet 391:1085–1096.

Tramarin M, Rusconi L, Pizzamiglio L, Barbiero I, Peroni D, Scaramuzza L, Guilliams T, Cavalla D, Antonucci F, Kilstrup-Nielsen C (2018) The antidepressant tianeptine reverts synaptic AMPA receptor defects caused by deficiency of CDKL5. Hum Mol Genet.

Trazzi S, De Franceschi M, Fuchs C, Bastianini S, Viggiano R, Lupori L, Mazziotti R, Medici G, Lo Martire V, Ren E, Rimondini R, Zoccoli G, Bartesaghi R, Pizzorusso T, Ciani E (2018) CDKL5 protein substitution therapy rescues neurological phenotypes of a mouse model of CDKL5 disorder. Hum Mol Genet 27:1572–1592.

Trazzi S, Fuchs C, Viggiano R, De Franceschi M, Valli E, Jedynak P, Hansen FK, Perini G, Rimondini R, Kurz T, Bartesaghi R, Ciani E (2016) HDAC4: a key factor underlying brain developmental alterations in CDKL5 disorder. Hum Mol Genet 25:3887–3907.

Uzunova G, Hollander E, Shepherd J (2014) The role of ionotropic glutamate receptors in childhood neurodevelopmental disorders: autism spectrum disorders and fragile x syndrome. Current neuropharmacology 12:71–98.

Verdoorn TA, Burnashev N, … M-H (1991) Structural determinants of ion flow through recombinant glutamate receptor channels. … Available at: http://science.sciencemag.org/content/252/5013/1715.short.

Wang I-TJT, Allen M, Goffin D, Zhu X, Fairless AH, Brodkin ES, Siegel SJ, Marsh ED, Blendy JA, Zhou Z (2012) Loss of CDKL5 disrupts kinome profile and event-related potentials leading to autistic-like phenotypes in mice. Proc Natl Acad Sci USA 109:21516–21521.

Wang P, Mei F, Hu J, Zhu M, Qi H, Chen X, Li R, McNutt MA, Yin Y (2017) PTENα Modulates CaMKII Signaling and Controls Contextual Fear Memory and Spatial Learning. Cell Rep 19:2627–2641.

Wang W, Tan T, Yu Y, Huang Z, Du Y, Han H, Dong Z (2018) Inhibition of AMPAR endocytosis alleviates pentobarbital-induced spatial memory deficits and synaptic depression. Behav Brain Res 339:66–72.

Watanabe M, Inoue Y, Sakimura K, Mishina M (1992) Developmental changes in distribution of NMDA receptor channel subunit mRNAs. Neuroreport 3:1138–1140.

Weaving LS, Christodoulou J, Williamson SL, Friend KL, McKenzie OL, Archer H, Evans J, Clarke A, Pelka GJ, Tam PP, Watson C, Lahooti H, Ellaway CJ, Bennetts B, Leonard

H, Gécz J (2004) Mutations of CDKL5 cause a severe neurodevelopmental disorder with infantile spasms and mental retardation. Am J Hum Genet 75:1079–1093.

Wenthold RJ, Petralia RS, Blahos J II, Niedzielski AS (1996) Evidence for multiple AMPA receptor complexes in hippocampal CA1/CA2 neurons. J Neurosci 16:1982–1989.

Wenthold, Yokotani, Doi, Wada (1992) Immunochemical characterization of the non-NMDA glutamate receptor using subunit-specific antibodies. Evidence for a hetero-oligomeric structure in rat brain. J Biological Chem 267:501–507.

Willard SS, Koochekpour S (2013) Glutamate, Glutamate Receptors, and Downstream Signaling Pathways. Int J Biol Sci 9:948–959.

Woo J, Kwon S-KK, Kim E (2009) The NGL family of leucine-rich repeat-containing synaptic adhesion molecules. Mol Cell Neurosci 42:1–10.

Yamada H, Ohashi E, Abe T, Kusumi N, Li S-AA, Yoshida Y, Watanabe M, Tomizawa K, Kashiwakura Y, Kumon H, Matsui H, Takei K (2007) Amphiphysin 1 is important for actin polymerization during phagocytosis. Mol Biol Cell 18:4669–4680.

Yang Y, Wang X, of the … F-M (2008) Delivery of AMPA receptors to perisynaptic sites precedes the full expression of long-term potentiation. Proceedings of the … Available at: http://www.pnas.org/content/105/32/11388.short.

Yang Y, Wang X-BB, Zhou Q (2010) Perisynaptic GluR2-lacking AMPA receptors control the reversibility of synaptic and spines modifications. Proc Natl Acad Sci USA 107:11999–12004.

Young LJ (2002) The neurobiology of social recognition, approach, and avoidance. Biol Psychiatry 51:18–26.

Zhou Z, Hong EJ, Cohen S, Zhao W-NN, Ho H-YHY, Schmidt L, Chen WG, Lin Y, Savner E, Griffith EC, Hu L, Steen JA, Weitz CJ, Greenberg ME (2006) Brain-specific phosphorylation of MeCP2 regulates activity-dependent Bdnf transcription, dendritic growth, and spine maturation. Neuron 52:255–269.

Zhou Z, Liu A, Xia S, Leung C, Qi J, Meng Y, Xie W, Park P, Collingridge GL, Jia Z (2018) The C-terminal tails of endogenous GluA1 and GluA2 differentially contribute to hippocampal synaptic plasticity and learning. Nat Neurosci 21:50–62.

Zhu G, Liu Y, Wang Y, Bi X, Baudry M (2015) Different patterns of electrical activity lead to long-term potentiation by activating different intracellular pathways. J Neurosci 35:621–633.

Zhu Y-CC, Li D, Wang L, Lu B, Zheng J, Zhao S-LL, Zeng R, Xiong Z-QQ (2013) Palmitoylation-dependent CDKL5-PSD-95 interaction regulates synaptic targeting of CDKL5 and dendritic spine development. Proc Natl Acad Sci USA 110:9118–9123.

Zingerevich C, Greiss-Hess L, Lemons-Chitwood K, Harris SW, Hessl D, Cook K, Hagerman RJ (2009) Motor abilities of children diagnosed with fragile X syndrome with and without autism. J Intellect Disabil Res 53:11–18.

Zoghbi HY, Bear MF (2012) Synaptic dysfunction in neurodevelopmental disorders associated with autism and intellectual disabilities. Cold Spring Harb Perspect Biol 4.

Zhou A, Han S, Zhou Z (2017) Molecular and genetic insights into an infantile epileptic encephalopathy – CDKL5 disorder. Frontiers Biology 12:1–6.